# Age-dependent VAP$^{P58S}$ aggregation in a *Drosophila* model of Amyotrophic Lateral Sclerosis

**A thesis**

**Submitted in partial fulfilment of the requirements**

**Of the degree of**

**Doctor of Philosophy**

**By**

**Aparna Thulasidharan**

**20152002**


**INDIAN INSTITUTE OF SCIENCE EDUCATION AND RESEARCH PUNE**

**2023**

## CERTIFICATE

Certified that the work incorporated in the thesis entitled, "Age-dependent $VAP^{P58S}$ aggregation in a *Drosophila* model of Amyotrophic Lateral Sclerosis ", submitted by Aparna Thulasidharan, was carried out by the candidate, under my supervision. The work presented here or any part of it has not been included in any other thesis submitted previously for the award of any degree or diploma from any other University or institution.

G S Ratnaparkhi

Dr. Girish Ratnaparkhi

Date: 14.03.2023

## Declaration

I declare that this written submission represents my ideas in my own words and where others' ideas and work have been included, I have adequately cited and referenced the original sources. I also declare that I have adhered to all principles of academic honesty and integrity and have not misrepresented or fabricated or falsified any idea/data/fact/source in my submission. I understand that violation of the above will be cause for disciplinary action by the Institute and can also evoke penal action from the sources which have thus not been properly cited or from whom proper permission has not been taken when needed.

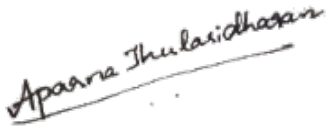

Aparna Thulasidharan

Roll No: 20152002

Date:14.03.2023

# Acknowledgements

I would like to thank Dr. Girish Ratnaparkhi for being a supportive guide and mentor. Girish has gone out of his way to always be available to his students and help out in all possible ways. He has been there for every last minute review of reports that needed to be presented. He has always found time to have simple sit-down talks to motivate me when everything seemed to be going out of hand (which happened often enough). He has truly been the wind in the sails for my work and I am forever grateful for his wise advice, humorous anecdotes and patience.

I would like to express my sincere gratitude to my RAC members, Dr. Raghav Rajan and Dr. Amitabha Majumdar. They have been an integral part of my journey and have always been supportive and generous with their time and advice. I would like to thank Dr. Anuradha Ratnaparkhi for her inputs and advice. I would also like to thank Dr. Richa Rikhy. She has been a very kind and keen supporter of my work and has always offered fresh perspective on the topics during discussions. I am also very grateful for the support and guidance given to me by the biology department, be it in the form of organizing presentations, or group outings and events. I would like to specifically thank Dr. Collins Assisi and Dr. Suhita Nadkarni for being my very first hosts at IISER Pune and introducing me to the wonderful community here.

I am deeply indebted to all the staff at the Institute. The bio-office has extensively supported each and every project in the bio department and I am grateful to them for all their help. The microscopy facility and fly facilty deserves a special mention, as without their help and support, none of the work I did would be possible. Snehal, Yashwant and Ashwini have done a phenomenal job maintaining our fly stocks and ensuring a reliable supply of media, come rain, come COVID. In the microscopy facility, Santosh and Vijay have helped throughout the project, be it through troubleshooting issues in the middle of the night or organizing demonstrations for the latest systems.

I would like to thank all my friends and lab mates in GR lab. I learnt a lot about science and life from my seniors, Bhagyashree, Vallari, Kriti, Prajna, Amar and Shweta. They were always ready to discuss work or offer insight and help troubleshoot when no explanation was in sight. We have also had great times together and these are all moments I cherish. I am

happy to see the baton of work hard and play hard being passed on to Subhradip, Kundan, Lovleen, Namrata, Sanhita, Amrita and Alex. A big thank you to Sushmitha, who has been my go to person during my tenure here. Sushmitha has always been an excellent experimentalist and I have greatly benefitted from her advice.

I wish to thank the Integrated PhD batch of 2015 for their support and love. Aishwarya, Joyeeta, Mrinmayee, Sneha, Pratima, Shikha, Sutirth, Yamini, Susovan, Sasank, Vinayak, Rutwik and Shubham are thanked for being supportive and most importantly an extremely fun group to be with. Meenakshi and Sushmitha have been my partners in identifying new spots to visit and eat out at. In the end, we relied on each other for suggestions, advice and occasional cheering ups, as we grew older (and wiser?) in an exciting city, far from our homes.

I am deeply indebted to my family for supporting me through this journey. My Amma and Achan were the main source of all emotional strength, particularly during challenging times. Indeed a trip home always recharged my scientific batteries and had me look forward to more experiments. My loving Husband, Rahul, for dealing with all the eccentricities that come with being married to a Graduate student and being my rock throughout this journey.

This journey would have not started without the blessings and kind support of my grandparents. They would have rejoiced to see this thesis come to fruition and I am sure they are showering their blessings from above. I dedicate my thesis to them.

-Aparna

# Synopsis

Neurodegenerative Disorders (NDs) are a fast growing, debilitating set of diseases which vastly affect the quality of living and life span. Protein aggregates are a common feature among ND. There are a lot of unanswered questions regarding protein aggregation and their role in disease. For my thesis, I am looking at the regulation of VAP aggregates in an *ALS8* disease model, which would allow me to study disease progression in the context of other specific events such as aging, ER stress and proteasomal dysfunction.

In my first chapter, I give a brief introduction to the problem of neurodegenerative disorders, how they are a cause of concern, and the physiological pathways commonly disrupted in them including pathways responsible for controlling Oxidative Stress, ER stress, autophagy, protein aggregation and aging. I discuss protein aggregation in Alzheimer's disease, Parkinson's disease and Huntington's disease and give a brief account of the therapeutic strategies available currently for neurodegenerative disorders which target protein aggregation. I introduce ALS and the familial forms of ALS, and mention the different loci currently identified. I discuss how the identification of familial ALS loci can provide us clues for identifying aberrations in cellular pathways, and how a large number of loci correspond to components of pathways involved in proteostasis. I also talk about my goals and objectives, namely studying protein aggregation of an ALS locus, *VAPB* in an age dependent context in a *Drosophila* model. My objectives included characterizing a null rescue model, identifying possible modulators of VAP aggregation and generating a *VAP* mutant using CRISPR-Cas9 technology.

In the second chapter, I discuss the characterization of the null rescue line. I developed and standardized a system to quantitatively measure the aggregation of VAP in larval and adult fly brains, using immunohistochemical techniques, confocal imaging and image analysis. We used the *Drosophila* larval ventral nerve cord to validate our techniques by comparing the VAP aggregation in three genotypes where the genetic dosage of VAP was varied. Following the standardization of the technique in the larval system, we characterized VAP aggregation in adults in a dose and age dependent manner, where we observed an increase in aggregation with genetic dosage, but no increase in aggregation with age. Another novel observation we made was that the addition of $VAP^{WT}$ to the $\Delta VAP;;gVAP^{P58S}$ rescue cleared VAP aggregation in an age dependent manner in adults. We also characterized ER stress by means of the ER

marker, BiP. We observed BiP punctae in 15 day old *ΔVAP;;gVAP$^{P58S}$*/+ flies, which was not seen in wild-type flies. A copy of *VAP$^{WT}$* was seen to reduce the BiP puncta density at this age. We also characterized BiP aggregation with age and saw that the aggregation appears to reduce with age, with the addition of *VAP$^{WT}$* further reducing this aggregation.

In the third chapter, I explore the role played by the members of the *Caspar-VAP-Ter94* axis. I talk about Caspar and Ter94 and their association through VAP, which was part of the publication (Tendulkar et al. 2022). Upon overexpression of *Caspar* in either the glia or neurons, we do not observe a change in VAP aggregation, the same is true for a knockdown of *Caspar* as well. BiP aggregation is also not affected by the modulation of *Caspar* levels in the glia. In the case of *Ter94*, we find that the neuronal knockdown of *Ter94* clears VAP aggregates, while the overexpression of the disease mutation *ter94$^{R152H}$* increases the VAP aggregation density, implying a role for *ter94* in modulation of VAP aggregation density.

In the fourth chapter, I talk about my experiments with *SOD1*, a known modulator of VAP aggregation in the larval ventral nerve chord. Our lab has previously demonstrated that *SOD1* is a modulator of VAP aggregation in the larval VNC. I validated this by knocking down *SOD1* neuronally in the larval VNC of the null rescue lines. We wished to understand if and how aggregation was modulated in the adults, and for this, we tried knocking down *SOD1* neuronally and observing VAP aggregation in the adult fly brain. We found out that the *SOD1* knockdown did not appear to change the VAP aggregation density. We also tried *SOD1* wild-type overexpression, this too did not appear to affect the VAP aggregation density. From our results, we understand that the mechanisms regulating VAP aggregation maybe different for the larval and adult nervous systems. We next tried targeting the autophagic pathway by knocking down *ATG1* in a *VAP$^{P58S}$ /VAP$^{WT}$* background. We normally observe a negligible quantity of aggregates in the *VAP$^{P58S}$ /VAP$^{WT}$* background, and knocking down *ATG1* increases the VAP aggregation. Thus we hypothesise that autophagic pathways may be employed in the adult nervous system to carry out VAP aggregation regulation.

In the fifth chapter, I discuss the making of an alternate line for our studies using the CRISPR -Cas9 system. I have introduced the system and spoken about the need and motivation behind the development of a CRISPR mutant for the *VAP$^{P58S}$* mutation. I detail the strategy we have employed to achieve the successful generation of the mutation, including the design, fly crosses, screening and confirmation of the putative mutation. I also carried out a set of experiments to validate the lines we obtained. We found out that these CRISPR mutants show

motor defects and lifespan defects, along with the presence of VAP aggregates in both larval and adult nervous systems. This also validates our findings from the null rescue.

In the appendix 1, I have added a set of experiments we carried out to understand VAP aggregation in the context of motor function. We saw ambiguous results, which I wanted to document as there may be better and more sensitive assays which would give us more resolute answers.

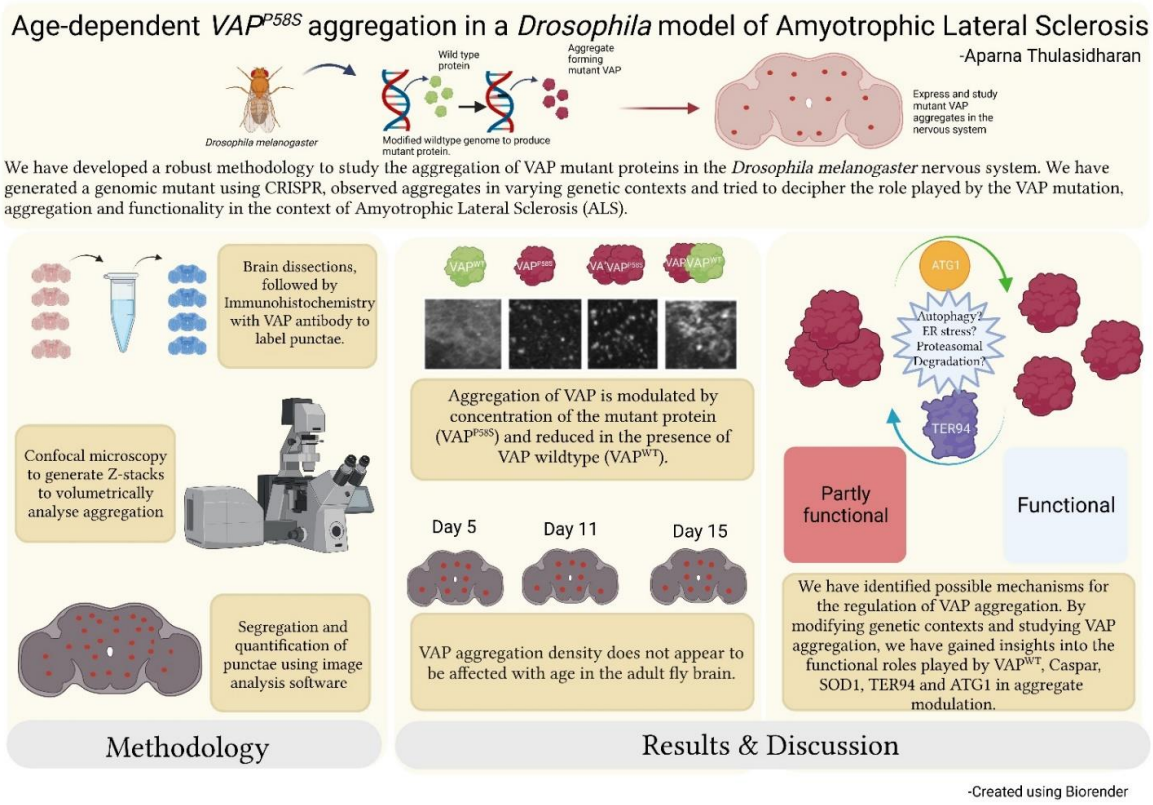


**Manuscripts and Publications:**

1) Caspar, an adapter for VAPB and TER94, modulates the progression of ALS8 by regulating IMD/ NFκB-mediated glial inflammation in a *Drosophila* model of human disease. *Human Molecular Genetics*, 2022, Vol. 31, 17, 2857–2875
   -Shweta Tendulkar, Sushmitha Hegde, Lovleen Garg, Aparna Thulasidharan, Bhagyashree Kaduskar, Anuradha Ratnaparkhi and Girish S Ratnaparkhi.
   (Detailed in Chapter 3)
2) Age-dependant VAPB aggregation dynamics in a *Drosophila* model of ALS (manuscript under preparation.)
   -Aparna Thulasidharan, Shweta Tendulkar, Lovleen Garg and Girish S Ratnaparkhi.
   (Detailed in Chapter 2)

3) *VAP*$^{P58S}$ plays a role in the modulation of circadian rhythm in a *Drosophila* model of *ALS8* (manuscript under preparation.)
-Vidhyadheesh Kelkar, Aparna Thulasidharan, Namrata Kulkarni, and Girish S Ratnaparkhi.

# Table of Contents

## List of figures

# Chapter 1

## Aggregation in Neurodegenerative disorders

### Introduction

Neurodegenerative disorders are a heterogeneous group of diseases that result in the progressive loss of neurological structures and functions. They often result in heavily compromised motor functions, coordination, sensory perception, strength, and cognitive function. They are known to be highly debilitating, leading to paralysis, loss of memory, mood changes, disruption of sleep patterns, and even death. Alzheimer's Disease (AD) and Parkinson's Disease (PD) are two of the most prevalent.

There is currently a great deal of interest and urgency in the studying of neurodegenerative disorders. We are currently living in a rapidly growing and aging society. Access to improved health care, better nutrition, and general scientific advancements have resulted in an increase in lifespan for the global population. This, in turn has resulted in the prevalence of older populations across the globe. Unfortunately, this also means an increase in the prevalence of neurological disorders. We, however, have a very limited understanding of the pathogenesis and mechanisms of these diseases. The available cure and therapy options are also limited. Thus, it becomes critical that we focus our efforts on trying to understand the mechanisms behind the pathogenesis of these diseases and try to develop methods for alleviating and curing them.

In order to understand how to treat diseases, knowledge on how and why they are caused is essential. To answer these questions, we must be able to identify processes or cellular mechanisms that are malfunctioning. These aberrations can provide us clues as to why there are problems in the system. When looking at neurodegenerative disorders collectively, we find certain common features in their pathogenesis. We regularly see a dysregulation of cellular pathways pertaining to the regulation of Reactive Oxidative Species (ROS), ER stress, protein aggregation, autophagy, inflammation, and RNA metabolism. Understanding how a pathway is affected will give us insight into developing treatment options.

### Reactive Oxidative Species (ROS) and Oxidative Stress (OS)

ROS is a common entity within the cellular environment. They are the highly reactive products of oxidative reactions taking place within the cell and are known to have signalling

roles, particularly in stem cells (Sinenko et al. 2021). ROS are also capable of causing damage to the cellular components by altering their structure or composition, especially in neurons, and hence cells have their own anti-oxidant mechanisms (Dröge 2002). When these fail or there is an increase in ROS, there is a resultant oxidative stress that can cause widespread damage to the cellular system. In the case of AD, affected brains have been found to show signs of ROS-mediated injury, with an increase in malondialdehyde and 4-hydroxynonenal in the patient brain and cerebrospinal fluid samples compared to control samples (Lovell et al. 1995). Transgenic animal models of AD also show protein and lipid peroxidation of the frontal cortex and hippocampus prior to the formation of plaques or tangles associated with AD pathology (Praticò 2008). In the case of PD, both protein oxidation and lipid peroxidation markers are seen to be increased in the substantia nigra (Beal 2002; Dalfó et al. 2005). In addition there have also been findings of deletions in the mitochondrial DNA of surviving dopaminergic neurons, which is believed to be a sign of oxidative damage (Bender et al. 2006). In Amyotrophic Lateral Sclerosis (ALS), a disorder affecting motor neurons, an increase in lipid peroxidation markers in cerebrospinal fluid have been identified in cases of sporadic ALS (Simpson et al. 2004).

Because of the prevalence of oxidative stress in neurodegenerative disorders, it has often been targeted for therapeutic intervention. Though initial studies with antioxidants indicated ameliorative effects, particularly in reduction of amyloid deposits in AD, larger randomised studies showed no significant benefit for either AD nor PD (Dumont, Lin, and Beal 2010). In the case of ALS, Edaravone is an FDA approved drug that acts as an antioxidant which is currently used in a few countries for treatment. The widespread usage of this drug was fairly recent with more studies needing to be done to get a clear idea of its effectiveness, but from currently available studies, it does not drastically improve the disease outcome (Ortiz et al. 2020).

The failure of antioxidants to act as effective therapeutic drug candidates has been widely debated. It is generally thought that this was a result of poor translation of results seen in animal models to human models, caused by inherent differences in the models and ineffectiveness of dosages used in animal models (Gandhi and Abramov 2012). Further, the exact aetiology of ROS in disease is not very clear because of which treatment of oxidative stress may relieve only one small facet of the entire pathogenesis, thus resulting in minor or no benefit. The correct time period during which OS is to be treated may also affect whether there is a beneficial effect. Oxidative Stress is now often treated as a secondary factor in the

progression of neurodegenerative disorders as many other systemic disruptions such as neuroinflammation, protein aggregation, mitochondrial defects are also seen in the affected tissues.

**ER stress**

Neurodegenerative disorders are characterized by aberrant proteostatic regulation. The involvement of processes involved in the amelioration of protein misfolding and accumulation is a widely studied phenomenon in these diseases. The cellular Unfolded Protein Response (UPR), is a normal process triggered by the presence of misfolded proteins (Hetz 2012). The UPR sets into motion a number of ameliorative responses including increased transcription of chaperones, reduction of protein synthesis and removal of misfolded proteins via clearance pathways such as the ERAD (Yoshida et al. 2003; Schröder and Kaufman 2005; Qu, Zou, and Lin 2021). If the UPR is unable to reduce the misfolded protein load, it is often responsible for the triggering of ER stress. The activation of ATF6, PERK and IRE1 is a key activation event for the UPR and consequently ER stress (Hetz and Saxena 2017). Once triggered, ER stress results in an overall slowing down of protein synthesis and if it is not resolved by either proper refolding or removal of misfolded protein, it can trigger the activation of pro-apoptotic pathways, leading to cell death.

ER stress has been hypothesized as a cause of cell death in NDs. Signs of increased levels of UPR have been identified in several tauopathies, including in AD, Pick's Disease, and FTLD (Nijholt et al. 2012). UPR activation has been observed early on in the case of PD, and was seen to be associated with increased phosphorylation of PERK and eIF2α in neuromelanin positive cells of the substantia nigra (J. J. M. Hoozemans et al. 2007; Jeroen J. M. Hoozemans et al. 2012). In ALS, all three pathways of the UPR were found to be upregulated in spinal cord samples of sporadic ALS patients (Sasaki 2010). Data from global gene expression profiles of patients with a C9orf72 repeat expansion revealed UPR alterations were a signature of the diseased cerebellum (Prudencio et al. 2015). Upregulation of ER stress linked transcription factor CHOP has been identified in the brains of AD patients along with downstream effectors like GADD34 and caspase-12, pointing to the possibility of apoptosis (Santos and Ferreira 2018).

Though there is evidence for the presence and activation of the UPR and ERAD pathways, whether ER stress plays a central role in neurodegeneration is still debated. ER stress is

currently thought to play an additive role to the damage caused by ROS, neuroinflammation and proteostatic imbalances.

**Autophagy**

Autophagy is a cellular process wherein unwanted and large macromolecules are removed from the system. It also plays a role in maintaining the turnover of damaged organelles and misfolded proteins in systems where cells aren't replaceable, such as post mitotic neurons. Autophagy can be triggered in response to starvation and it can also trigger apoptosis in certain cases.

Neurons are particularly sensitive to disruptions in autophagy. Younger neurons are much more efficient at clearing autophagic substrates, but older neurons often struggle with autophagic clearance (Boland et al. 2008; Nixon 2013). Autophagy has been implicated in NDs as the process is involved in the clearing of aggregated proteins, a feature of NDs. p62 and other components of the autophagy pathway are often seen as components of aggregates in neurodegenerative diseases(Mori et al. 2012; Bjørkøy et al. 2005) indicating autophagic involvement. Loss of autophagy has been demonstrated to lead to neurodegeneration in mice models (Hara et al. 2006; Komatsu et al. 2006). Lysosomal pathologies are associated with AD, this has been found to lead to disruptions in macroautophagy as well (Nixon et al. 2005). Mice models of PD where α-Synuclein is overexpressed show the accumulation autophagic vacuoles (Spencer et al. 2009; Yu et al. 2009). Overexpression of Beclin-1 was found to be protective in mouse models of Machado-Joseph disease, highlighting how autophagic regulation could restore disease pathology (Nascimento-Ferreira et al. 2011).

Autophagy has been explored as a promising target for therapeutics. Rapamycin and Rapamycin analogues have been popularly used as and studied as an agent to induce autophagy and has been shown to ameliorate disease phenotypes such as motor dysfunction, toxic aggregates and cognitive defects in model organisms (Djajadikerta et al. 2020; Menzies et al. 2010; Spilman et al. 2010). Rapamycin, however, affects autophagy via the suppression of the mTOR pathway, which results in a host of undesirable side effects. Alternatives which affect autophagy, without affecting mTOR have also been developed. These include inositol synthesis modulators like carbamazepine. Trehalose, has also been found to affect autophagy and its administration has been found to be neuroprotective in mouse models of taupathies and ALS (Rodríguez-Navarro et al. 2010; Menzies, Fleming, and Rubinsztein 2015). Upregulation of autophagy may not be a viable solution in all cases of neurodegeneration

such as in cases where there is lysosomal accumulation, such as in lysosomal storage disorders.

**Aggregation in neurodegenerative disorders**

Protein aggregation is a prominent feature seen in neurodegenerative disorders. They indicate a defect in proteostatic functions within the affected cells. Protein misfolding is a normal, biological phenomenon that is usually dealt with effectively by cells either through refolding or by removal of misfolded/aggregated proteins through processes like autophagy or degradation via ubiquitin proteasome systems. In certain diseases, however, protein quality control is adversely affected, which leads to protein misfolding and their accumulation (Dobson 2001). Misfolded proteins have been known to aggregate as well as cause cellular oxidative stress, trigger the unfolded protein responses (UPR) and cause ER stress. In fact, a large number of human diseases have been identified where protein aggregation is a prominent feature. Neurodegenerative diseases are one group of disorders where one sees protein aggregation prominently.

First observed by Alois Alzheimer in the brains of dementia patients, protein aggregation has since been thought of as playing a crucial role in disease onset and progression (Caughey and Lansbury 2003). Aggregated masses of proteins have been observed in nervous tissues of patients and animal models of Huntington's Disease(HD) (Scherzinger et al. 1997), Parkinson's Disease(PD) (Baba et al., 1998), Alzheimer's Disease (AD) and motor neuron diseases (Cleveland and Rothstein 2001). The link between protein aggregation and disease pathology is not well understood, with induction of aggregation alone being sufficient to trigger disease in certain cases (Wong et al., 2002). Mechanisms by which aggregates affect cellular and animal physiology are varied. Aggregates have been known to be toxic to the cell by affecting autophagy, triggering apoptosis and inhibiting proteasomal machinery (Hipp, Park, and Hartl 2014). Protein aggregation can also remove soluble functional protein from the available pool and reduce the functional dose of wild- type protein of the same. While generally thought of as harmful, in some cases aggregates have also shown to be benign or even beneficial as can be seen by inducing regulated aggregation is a cell protective mechanism in certain cases of stresses (McDonald et al. 2011).

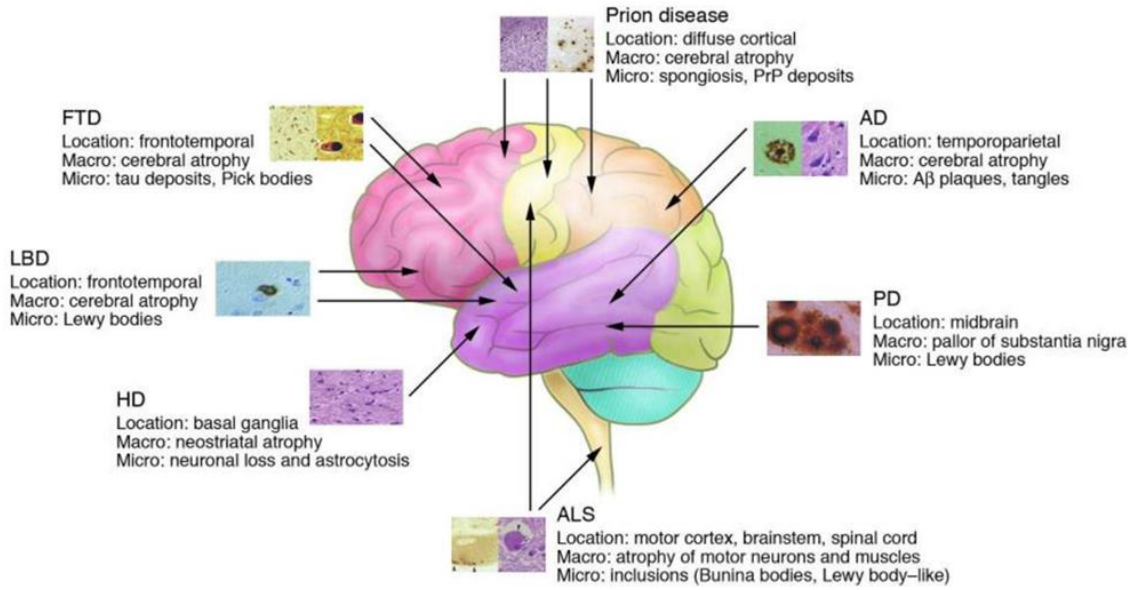


**Figure 1.1: Protein aggregation is a common feature of neurodegenerative disorders.** Protein aggregates are a common feature seen across several neurodegenerative disorders. An overview of the position of these aggregates in different common neurodegenerative disorders, along with the observed pathology, is shown in this representative figure. Image has been adapted from Bertram and Tanzi, *JCI*, 2005 (Bertram and Tanzi 2005)

Alzheimers's Disease (AD):

The presence of plaques and tangles is used to confirm the diagnosis of AD post-mortem. The affected brain shows presence of extracellular amyloid plaques and intraneuronal neurofibrillary tangles. There are two forms of Aβ, $A\beta_{40}$ is the more common variant while $A\beta_{42}$ is the form associated with the disease. The more compact and neuritic deposits consist of both forms and are also fibrillary. Diffuse plaques are not fibrillar and consist of mainly $A\beta_{42}$. They are considered precursors to the more compact neuritic plaques as they are seen in AD patients before the onset of cognitive symptoms as well as in young patients suffering from Down's syndrome (Lemere et al. 1996). The presence of neuritic plaques is associated with active microglia and astrocytes, along with dilated and dystrophic neurons in the vicinity. Neurofibrillary tangles (NFTs) are seen in several other disorders as well as in aged brains. They are made up of hyperphosphorylated tau, a microtubule protein (Grundke-Iqbal

et al. 1986). Their presence is more closely associated with disease progression than that of the amyloid deposits (Irvine et al. 2008). The role played by NFTs in the disease progression is widely debated. The number of NFTs in the neocortex positively correlates with cognitive decline in the brains of AD patients (Arriagada et al. 1992). It has also been seen that neurons with NFTs in transgenic mouse models expressing Tau have a relatively healthy nuclear morphology, with the dying neurons showing a lesser load of NFTs (Andorfer et al. 2005). There is experimental evidence to suggest that the tau pathology is downstream of Aβ accumulation and both pathologies influence each other (Umeda et al. 2014). Tau appears to play a clear role in the cognitive defects seen in some transgenic mouse models, with suppression of tau being capable of reversing the cognitive effects (Santacruz et al. 2005; Van der Jeugd et al. 2013; Tatebayashi et al. 2002; Andorfer et al. 2003).

Parkinson's Disease (PD):

Parkinson's Disease is the second most common ND after AD. The disease is slowly progressive and characterized by rigidity, postural instability and abnormal gait (Jankovic 2008). Mental faculties are also known to be affected in later stages of the disease. The Substantia Nigra pars compacta (SNc) is the region of the brain wherein the dopaminergic neurons are seen to degenerate as a result of PD. The disease is characterized by the presence of inclusions rich in α-Synuclein, which may have a variety of post translational modifications on it. They are also known to sequester other proteins in them. Abnormal protein accumulation is seen in both sporadic as well as familial PD (McNaught and Olanow 2006). In several forms of PD, structures called Lewy Bodies have been identified. They are large structures with a dense central core of ubiquitinated proteins and a diffuse outer layer made up of fibrillar α-Synuclein and neurofilaments. They are predominantly made up of α-Synuclein. They also contain components of the UPS and HSPs (Ii et al. 1997). Lewy pathology is often associated with neuron loss and has been observed in the substantia nigra , dorsal nucleus of the vagal nerve and the amygdala (Harding et al. 2002; Chartier and Duyckaerts 2018). It has been seen in models that the soluble monomeric forms of α-Synuclein are toxic to the cell (Emin et al. 2022; Winner et al. 2011) and the fibrillar form seen in Lewy bodies might be formed as a neuroprotective mechanism.

Lewy bodies have been thought to act like aggresomes and perform neuroprotective functions by sequestering and degrading toxic proteins formed in affected neurons, wherein other

modes of clearance are compromised. There have been attempts at developing therapeutic strategies aimed at reducing aggregates. *Drosophila* models of PD have been developed, that show the presence of aggregates containing α-Synuclein and ubiquitin. Expressing the chaperone HSP70 has been shown to reduce the death of dopaminergic neurons in the model (Auluck et al, 2002).Co-expression of HSP70 with mutant synuclein in a mouse model has also been shown to reduce aggregates (Klucken et al. 2004). Thus the use of chaperones targeting misfolded proteins looks like a promising target for clinical trials based on animal studies.

Huntington's Disease (HD):

HD is a disease caused by a mutation in the *HTT* gene, which results in an abnormal number of CAG nucleotide repeats.(Walker 2007) As a result of this, the protein produced has several glutamines (polyQ) that make it prone to aggregate.(Williams and Paulson 2008). Following the discovery of the causative gene, mouse models were generated to understand the pathogenesis (Schilling et al. 1999; Mangiarini et al. 1996; Sathasivam et al. 1999). With the help of these models, and antibodies targeting the irregular polyQ, densely staining intraneuronal inclusions called inclusion bodies (IB) were identified. They have been seen to occur in the nucleus though they have later been found to occur cytoplasmically as well. (DiFiglia et al. 1997) They have been seen to occur in many regions throughout the brain, including the striatum, cerebral cortex, cerebellum, and the spinal cord.

IBs were initially thought to be responsible for the pathology associated with HD, but a series of studies showed that the presence of IBs was not as reflective of the disease state . This was because the degeneration of certain regions of the brain, particularly the caudate-accumbens-putamen and globus pallidus did not seem to be affected by the number of IBs . IBs are seen more commonly in the cortex where neuronal losses are lesser than those in the striatum. In the striatum, IBs are more common in the interneurons and not the more vulnerable medium spiny projection neurons (Kuemmerle et al. 1999).Thus IBs don't appear to localise with neurons which are more vulnerable to die from the disease. Following these observations, questions arose regarding the role of these IBs, of why they were formed and if they were in some way beneficial. Further studies revealed that the presence of diffuse mutant HTT in the neuron was correlated with neuron death. The presence of IBs appeared to alter the diseased state of the neurons by reducing levels of diffuse HTT (Arrasate et al. 2004).The formation of IBs was then considered an adaptive change to protect neurons from death caused by diffuse forms of HTT.

Current therapeutic approaches targeting aggregation:

There have been several attempts at developing treatments for neurodegenerative disorders, where the principal target of action was the formation of aggregates and their removal. There have been studies showing how in the case of certain NDs, the major toxic player among aggregates are the soluble oligomeric forms, which are also one of the first to be formed.(Chung, Lee, and Lee 2018) Certain polyphenolic compounds have also been identified which have been shown to reduce aggregation. Myricetin is a polyphenolic flavonoid that has been found to have favorable effects on neurodegenerative disease like ALS and PD. The exact mechanisms behind its action is unknown, however, it has been shown to clear accumulated SOD1 mutant protein in a cell culture system(Joshi et al. 2019). Myricetin has also been shown to have neuroprotective effects ,could reduce inflammation and increase dopamine levels in a rodent model of PD (Maher 2019). Curcumin, another plant derived polyphenol has also been shown to inhibit the formation of amyloid beta oligomers in mouse models of AD and also promote the disaggregation of formed plaques(Yang et al. 2005) It has also been shown to reduce PolyQ aggregation in a mouse knock in model of Huntington's Disease (Hickey et al. 2012). While a lot of compounds have been identified and even shown to have beneficial impact of disease, they have had very limited success at the level of clinical trials.

Antibodies have also been looked at as a promising means of treatment. Antibodies targeting Aβ toxic species have been generated. These antibodies are designed to target, bind and neutralize the Aβ aggregates. They can also stimulate microglial clearance or stimulate Aβ clearance from the brain (D et al. 2017). Aducanumab (BIIB037) is a fully human, monoclonal antibody targeting a conformational epitope on the Aβ. It is currently in the phase III stage of clinical trials. Crenezumab is another antibody which recognizes multiple forms of Aβ. It also stimulates amyloid phagocytosis and inhibits release of inflammatory cytokines, which helps reduce vasogenic edema (Adolfsson et al. 2012). Solanezumab is another monoclonal antibody that works to aggregate the soluble Aβ,thereby shifting the equilibrium towards forming aggregates and hence removing the toxic soluble forms(Siemers et al. 2016).Antibodies have also been developed to target misfolded SOD1.These vaccines were found to generate robust and sustained immune response and increase the lifespan of treated animals (Zhao et al. 2019).For treatment of HD, the use of small ,bioactive fragments of antibodies called intrabodies have been employed (Messer and Butler 2020). They bind with high affinity to the N terminal of the HTT protein and have been shown to suppress the

formation of mutant HTT positive aggregates. They have been shown to ameliorate the disease phenotype in several animal models of HD as well (Minakawa and Nagai 2021).

## Aging

Aging is considered a primary risk factor for developing Alzheimer's Disease (AD) and Parkinson's Disease (PD) with the prevalence of developing the disease increasing with age (Hou et al. 2019). The number of cases of dementia is expected to rise from 57.4 million in 2000 to 152.8 million in 2050 (Nichols et al. 2022) The economic burden being placed on society by the rapid increase in incidences of neurodegenerative disease has also been estimated to increase significantly.

Aging is a natural biological process which involves a gradual breakdown and slowing of metabolic pathways, leading to senescence. Proteostasis has been shown to get disrupted with the age of an organism, leading to more amounts of insoluble proteins in the cell(Rai et al. 2021). Aging is also associated with defects in autophagy (Barbosa, Grosso, and Fader 2019), increased ROS and oxidative damage (Bokov, Chaudhuri, and Richardson 2004)and higher levels of inflammation. These are all associated with worse out-comes for neurodegeneration. Another hall mark for aging is genome instability(López-Otín et al. 2013) There are also studies that point to an increase in genomic aberrations such as increased somatic mutations, with the age (Tucker et al. 1999; Martin et al. 1996) Certain proteins such as α- synuclein , phosphorylated tau and aβ aggregates are known to be found in the brains of elderly people though whether they affect cognition is unclear. There is a natural breakdown of pathways associated with normal, healthy aging, however these effects tend to worsen already compromised systems in NDs.

## ALS: A debilitating, motor neuro degenerative disorder

Amyotrophic lateral sclerosis (ALS) The disease is marked by the progressive decline of motor function in patients, terminating in respiratory failure and death. There is selective death of motor neurons and loss of muscle innervation which results in the loss of motor ability in patients (Kiernan et al. 2011). Most diagnosed patients do not survive beyond 30 months post-symptom onset. There are currently two FDA-approved drugs, neither of which can cure the disease. Riluzole which is most widely used for the treatment, works by blocking glutamatergic transmission in the CNS and protecting against anoxic damage (Doble 1996) , while Edaravone works by removing oxidative free radicals and reducing oxidative stress (Yoshino and Kimura 2006). Both the drugs slow the progression of the degeneration, with

Riluzole extending patient life by only a few months. Thus, there are huge efforts behind finding a practical therapy for curing ALS. The exact causes and events which lead up to the disease are still unclear with errors in RNA metabolism, cellular trafficking, protein misfolding , autophagy and increased levels of Reactive Oxidative Species(ROS) being implicated (Taylor, Brown, and Cleveland 2016) for the initiation and progression of the disease.

A large number of cases reported are found to not have any known familial history or cause and are referred to as sporadic ALS (sALS), but about 5-10% cases reported in the USA have been found to have a familial pattern of occurrence and are termed as familial ALS (fALS) (Mehta et al. 2018). Approximately 30-35 genes have been implicated so far, for fALS in being involved with the disease pathology (Abel et al., 2012).

***Table 1: List of Familial ALS loci, their genetic location and function .Adapted from (Mejzini et al. 2019)***

| *Gene Name* | *Location* | | *Function of protein* |
|---|---|---|---|
| *C9ORF72* | 9p21.3 | C9ORF72 | Transcription and pre-mRNA splicing regulation; membrane traffic via Rab GTPase family |
| *SOD1* | 21q22 | SOD1 | Major cytosolic antioxidant |
| *TARDBP* | 1p36.2 | TDP-43 | Transcription and pre-mRNA splicing regulation; micRNA biogenesis; RNA transport and stabilization; translational regulation of *ApoE-II* and *CFTR* |
| *FUS* | 16p11.2 | FUS (or TLS) | Transcription and pre-mRNA splicing regulation; micRNA processing; mRNA transport and stabilization; maintenance of genomic integrity; regulating protein synthesis at synapse |
| *OPTN* | 10p13 | Optineurin | Golgi maintenance; exocytosis; vesicular trafficking; regulator of NF-kB signaling pathway; autophagy process |

| | | | |
|---|---|---|---|
| *PFN1* | 17p13 | Profilin 1 | Regulates ATP-mediated actin polymerization |
| *VCP* | 9p13 | VCP or p97 | Protein degradation via UPS, autophagy, and the ER; membrane fusion |
| *ANG* | 14q11.2 | Angiogenin | RNA processing and tRNA modification; vascularization; RNAase activity and assembly of stress granules; neurite outgrowth and pathfinding |
| *TUBA4A* | 2q35 | Tubulin α4A | Major component of microtubules; neuronal cell skeleton |
| *UBQLN2* | Xp11 | Ubiquilin 2 | Protein degradation via UPS |
| *TAF15* | 17q11 | TAF15 | Transcription initiation; RNA polymerase II gene component |
| *EWSR1* | 22q12.2 | EWSR1 | Transcriptional repressor |
| *hnRNPA1* | 12q13 | hnRNPA1 | Packing and transport of mRNA; micRNA biogenesis |
| *hnRNPA2B1* | 7p15 | hnRNPA2/B1 | Packing and transport of mRNA; micRNA biogenesis |
| *SETX* | 9q34.13 | Senataxin | DNA/RNA helicase activity; DNA/RNA metabolism |
| *CREST* | 20q13.3 | SS18L1 | $Ca^{2+}$-dependent transcriptional activator |
| *MATR3* | 5q31.2 | Matrin 3 | RNA processing; stabilizing mRNAs; gene silencing; chromatin organization |
| *ATXN2* | 12q24 | Ataxin 2 | RNA processing; regulation of receptor tyrosine kinase endocytosis |
| *ELP3* | 8p21.1 | ELP3 | RNA processing; transcript elongation; histone acetylation; modification of tRNA wobble nucleosides |

| | | | |
|---|---|---|---|
| *SQSTM1* | 5q35 | p62 or SQSTM1 | Autophagy and UPS degradation; regulator of NF-kB signaling pathway; immune response |
| *CHMP2B* | 3p11 | CHMP2B | MVBs formation; protein trafficking between plasma membrane, trans-Golgi network, and lysosome |
| *ALS2* | 2q33.1 | Alsin | Activation of the small GTPase Rac1 macropinocytosis-associated endosome fusion and trafficking; neurite outgrowth |
| *VAPB* | 20q13 | VAPB | Regulation of ER–Golgi transport and secretion |
| *SIGMAR1* | 9p13.3 | SIGMAR1 | Lipid transport through ER; BDNF and EGF signaling |
| *DCTN1* | 2p13 | Dynactin | ER–Golgi transport; centripetal movement of lysosomes and endosomes; spindle formation, chromosome movement; nuclear positioning; axonogenesis |
| *FIG4* | 6q21 | $PI_{3,5}P_2$ | Phosphoinositide phosphatase activity; endosomal vesicle trafficking to the trans-Golgi network; regulation of autophagy |
| *SPG11* | 15q21.1 | Spatascin | Neuronal cell skeleton; axonal transport; involved in synaptic vesicles |
| *NEFH* | 22q12.2 | NEFH | Maintaining axon diameter |
| *PRPH* | 12q13 | Peripherin | Regulating neurite elongation during development and axonal regeneration after injury |
| *NTE* | 19p13 | Neuropathy target esterase | Regulating the neuronal membrane composition |

| | | | |
|---|---|---|---|
| *PON1-3* | 7q21 | Paraoxonase 1-3 | Enzymatic breakdown of nerve toxins |
| *DAO* | 12q22 | DAO | Regulating levels of D-serine, NMDAR function |
| *CHRNA3*, *CHRNA4*, *CHRNB4* | 15q24, 20q13, 15q24 | nAChR | Cholinergic neurotransmission |
| *ERBB4* | 2q34 | Receptor tyrosine-protein kinase ErbB-4 | Neuronal cell mitogenesis and differentiation |
| *CHCHD10* | 22q11 | Mitochondrial protein | Mitochondrial genome stability; cristae integrity and mitochondrial fusion |
| *C19orf12* | 9q12 | Mitochondrial protein | Unknown |
| *ALS3* | 18q21 | Disulfide redox protein | Unknown |
| *ALS7* | 20p13 | Unknown | Unknown |
| *ALS6-21* | 6p25, 21q22 | Unknown | Unknown |
| *ALS-FTD* | 16p12 | Unknown | Unknown |
| *UNC13A* | 19p13 | Unc-13 homolog A | Regulating neurite outgrowth and synaptic neurotransmission |
| *EPHA4* | 2q36.1 | Ephrin receptor A4 | Receptor tyrosine kinase activity Modulation of cell morphology and integrin-dependent cell adhesion; regulation of synaptic plasticity and CNS development |
| *CHGB* | 20p12.3 | CHGB | Involved in the ER–Golgi system |
| *KIFAP3* | 1q24.2 | Kinesin-associated protein 3 | Tethering chromosomes to spindle pole; chromosome movement; axonal transport of choline acetyl-transferase |

| | | | |
|---|---|---|---|
| *SMN* | 5q13 | Germin 1 | Regulating biogenesis of snRNPs |

**ALS Loci and Protein aggregation**

The presence of cytoplasmic aggregates in degenerating motor neurons and surrounding oligodendrocytes is a characteristic feature in ALS pathology. Protein inclusions or aggregates, with SOD1 and TDP43 containing inclusions are found in most cases (Arai et al., 2006). Aggregates are found in the spinal cord, hippocampus, cerebellum and the frontal and temporal cortices (Al-Chalabi et al. 2012) There are two major types of ubiquitinated aggregates seen in ALS: lewy body like hyaline inclusions and skein like aggregates. A third type, called Bunina bodies are small, eosinophilic and negative for ubiquitination (Okamoto, Mizuno, and Fujita 2008) Several loci implicated in fALS like *OPTN*,*FUS* and *C9orf72* have been known to harbour mutations which produce protein inclusions (Blokhuis et al., 2013). The presence of aggregates in most sporadic cases of ALS also show the presence of aggregates, mostly immunopositive for SOD1 and TDP-43 (Mackenzie et al. 2007; Medinas et al. 2018) The presence of aggregates in all these cases point towards a common disruption of proteostasis and clearance mechanisms. The presence of certain molecules in the aggregates could also be a sign of the involvement of their associated pathway in the disease. For example, *UBQLN2*, *SQSTM1*, *OPTN* are all loci identified with ALS, with the protein being present and identified in aggregates (Blokhuis et al. 2013). They are associated with UPS and autophagy, and their presence signals issues with the pathways.

Several loci are also known to interact with other loci and this could affect the functioning of other loci. The oligogenic nature of ALS has been hypothesised, with the chance of multiple mutations being responsible for an outcome. In such cases, protein aggregates can be a means through which one loci might affect another. For example, in the case of *SOD1*, *SOD1 G85R* mutant mice were seen to develop inclusions which were immune-positive for SOD1 and Ubiquitin (Bruijn et al. 1997). Mutant SOD1 has also been shown to aggregate along with other proteins like the components of the Dynein complex (Zhang et al. 2007), Bcl-2 (Pasinelli et al. 2004) and several proteins involved in the Heat Shock responses (Crippa et al. 2010). TDP-43, another ALS locus, is an RNA-binding protein which was found to be mislocalized in cases of ALS. It was found in ubiquitinated cytoplasmic inclusions in affected brain and spinal cord cells, displaced from its normal intra-nuclear position (Arai et al. 2006). TDP-43 inclusions are also implicated in the neurodegenerative disease, Fronto-temporal Dementia (FTD) lacking Tau inclusions and are also a secondary pathological feature for a

fraction of people with AD and PD (Taylor, Brown, and Cleveland 2016). The normal protein was seen to be mislocalized in all cases of sALS and all cases of non-SOD1 fALS. TDP-43 has been shown to interact with a large number of factors important in RNA quality control, Protein translation, Splicing, Protein folding and so on. (Blokhuis et al., 2013). TDP-43 has been found to interact with a number of DNA binding and repair proteins, Heat Shock factors, translational regulators and components of the NFκB pathway (Zhu, Cynader, and Jia 2015). Further, it was shown that mislocalized cytoplasmic TDP-43 co-localized with inclusions, called stress granules (SRs) (Freibaum et al. 2010). Mutant TDP-43 has also been shown to interact with other proteins implicated in ALS-like FUS (Fused In Sarcoma) (Ling et al., 2010). VAPB is another locus associated with ALS and is known to have a large number of interactors like microtubules, ER and proteins like SNAREs, FFAT domain containing proteins and viral proteins within the cell (Lev et al. 2008). The mutant form of the VAPB protein was found to aggregate and inhibit the Unfolded Protein Response (UPR), which was at that time thought to explain the pathogenesis (Kanekura et al., 2006). The VAP(P56S) mutant was found to alter these interactions (Huttlin et al. 2015).

**Goals and aim of our study**

Aggregation of proteins in neurodegenerative disorders is a common pathological hallmark, however, there remains a lot of unanswered questions regarding aggregation in each disease context. There are different types of aggregates ,with each type affecting the cell in different ways. The response to an aggregate within the cell is also varied. We wished to understand the role played by the neuronal VAP aggregates in ALS. The VAPB locus was identified as an ALS causative locus in a Brazilian family (Nishimura et al. 2004). The mutant protein has been shown to aggregate and give rise to cellular inclusions (Kanekura et al. 2006).Since the initial discovery of the locus, several studies have established model systems for studying the role of the mutation in disease pathogenesis. VAP aggregation has been observed in model organisms in systems where the mutant protein is overexpressed. These studies focus mainly on a single time point to understand aspects of the aggregation. Aging is a very important factor in the development of neurodegeneration and how it affects aggregation of VAP protein is a question that was not tackled previously. We wished to study the role played by the cellular aggregation of VAP protein in disease progression in a Drosophila model of the disease.

**Objective of the study**

To study and characterize age-dependant aggregation dynamics of $VAPB^{P58S}$ in a *Drosophila* model of Amyotrophic Lateral Sclerosis 8.

**Specific aims:**

1) Establishing and characterizing $VAP^{P58S}$ aggregation in *Drosophila* ALS8 disease models (Tsuda model *vs* CRISPR genome-edited model)

2) Quantitative measurement of the density of $VAP^{P58S}$ aggregation in relation to age, disease progression and pathology

3) Identify possible modulators of VAP aggregation in the disease

**References**

Adolfsson, O., M. Pihlgren, N. Toni, Y. Varisco, A. L. Buccarello, K. Antoniello, S. Lohmann, et al. 2012. "An Effector-Reduced Anti- -Amyloid (A ) Antibody with Unique A Binding Properties Promotes Neuroprotection and Glial Engulfment of A." *Journal of Neuroscience* 32 (28): 9677–89. https://doi.org/10.1523/JNEUROSCI.4742-11.2012.

Al-Chalabi, Ammar, Ashley Jones, Claire Troakes, Andrew King, Safa Al-Sarraj, and Leonard H. van den Berg. 2012. "The Genetics and Neuropathology of Amyotrophic Lateral Sclerosis." *Acta Neuropathologica* 124 (3): 339–52. https://doi.org/10.1007/s00401-012-1022-4.

Andorfer, Cathy, Christopher M. Acker, Yvonne Kress, Patrick R. Hof, Karen Duff, and Peter Davies. 2005. "Cell-Cycle Reentry and Cell Death in Transgenic Mice Expressing Nonmutant Human Tau Isoforms." *The Journal of Neuroscience: The Official Journal of the Society for Neuroscience* 25 (22): 5446–54. https://doi.org/10.1523/JNEUROSCI.4637-04.2005.

Andorfer, Cathy, Yvonne Kress, Marisol Espinoza, Rohan de Silva, Kerry L. Tucker, Yves-Alain Barde, Karen Duff, and Peter Davies. 2003. "Hyperphosphorylation and Aggregation of Tau in Mice Expressing Normal Human Tau Isoforms." *Journal of Neurochemistry* 86 (3): 582–90. https://doi.org/10.1046/j.1471-4159.2003.01879.x.

Arai, Tetsuaki, Masato Hasegawa, Haruhiko Akiyama, Kenji Ikeda, Takashi Nonaka, Hiroshi Mori, David Mann, et al. 2006. "TDP-43 Is a Component of Ubiquitin-Positive Tau-Negative Inclusions in Frontotemporal Lobar Degeneration and Amyotrophic Lateral Sclerosis." *Biochemical and Biophysical Research Communications* 351 (3): 602–11. https://doi.org/10.1016/j.bbrc.2006.10.093.

Arrasate, Montserrat, Siddhartha Mitra, Erik S. Schweitzer, Mark R. Segal, and Steven Finkbeiner. 2004. "Inclusion Body Formation Reduces Levels of Mutant Huntingtin and the Risk of Neuronal Death." *Nature* 431 (7010): 805–10. https://doi.org/10.1038/nature02998.

Arriagada, Paulina V., John H. Growdon, E. Tessa Hedley-Whyte, and Bradley T. Hyman. 1992. "Neurofibrillary Tangles but Not Senile Plaques Parallel Duration and Severity of Alzheimer's Disease." *Neurology* 42 (3): 631–631. https://doi.org/10.1212/WNL.42.3.631.

Barbosa, María Carolina, Rubén Adrián Grosso, and Claudio Marcelo Fader. 2019. "Hallmarks of Aging: An Autophagic Perspective." *Frontiers in Endocrinology* 9. https://www.frontiersin.org/articles/10.3389/fendo.2018.00790.

Beal, M. Flint. 2002. "Oxidatively Modified Proteins in Aging and Disease1, 2 1Guest Editor: Earl Stadtman 2This Article Is Part of a Series of Reviews on 'Oxidatively Modified Proteins in Aging and Disease.' The Full List of Papers May Be Found on the Homepage of the Journal." *Free Radical Biology and Medicine* 32 (9): 797–803. https://doi.org/10.1016/S0891-5849(02)00780-3.

Bender, Andreas, Kim J. Krishnan, Christopher M. Morris, Geoffrey A. Taylor, Amy K. Reeve, Robert H. Perry, Evelyn Jaros, et al. 2006. "High Levels of Mitochondrial DNA Deletions in Substantia Nigra Neurons in Aging and Parkinson Disease." *Nature Genetics* 38 (5): 515–17. https://doi.org/10.1038/ng1769.

Bertram, Lars, and Rudolph E. Tanzi. 2005. "The Genetic Epidemiology of Neurodegenerative Disease." *Journal of Clinical Investigation* 115 (6): 1449–57. https://doi.org/10.1172/JCI24761.

Bjørkøy, Geir, Trond Lamark, Andreas Brech, Heidi Outzen, Maria Perander, Aud Øvervatn, Harald Stenmark, and Terje Johansen. 2005. "P62/SQSTM1 Forms Protein Aggregates Degraded by Autophagy and Has a Protective Effect on Huntingtin-Induced Cell Death." *Journal of Cell Biology* 171 (4): 603–14. https://doi.org/10.1083/jcb.200507002.

Blokhuis, Anna M., Ewout J. N. Groen, Max Koppers, Leonard H. van den Berg, and R. Jeroen Pasterkamp. 2013. "Protein Aggregation in Amyotrophic Lateral Sclerosis." *Acta Neuropathologica* 125 (6): 777–94. https://doi.org/10.1007/s00401-013-1125-6.

Bokov, Alex, Asish Chaudhuri, and Arlan Richardson. 2004. "The Role of Oxidative Damage and Stress in Aging." *Mechanisms of Ageing and Development*, Hormone receptors, genes, ageing and Arun Roy: A tribute to Professor Arun K. Roy, 125 (10): 811–26. https://doi.org/10.1016/j.mad.2004.07.009.

Boland, Barry, Asok Kumar, Sooyeon Lee, Frances M. Platt, Jerzy Wegiel, W. Haung Yu, and Ralph A. Nixon. 2008. "Autophagy Induction and Autophagosome Clearance in Neurons: Relationship to Autophagic Pathology in Alzheimer's Disease." *Journal of Neuroscience* 28 (27): 6926–37. https://doi.org/10.1523/JNEUROSCI.0800-08.2008.

Bruijn, L.I., M.W. Becher, M.K. Lee, K.L. Anderson, N.A. Jenkins, N.G. Copeland, S.S. Sisodia, et al. 1997. “ALS-Linked SOD1 Mutant G85R Mediates Damage to Astrocytes and Promotes Rapidly Progressive Disease with SOD1-Containing Inclusions.” *Neuron* 18 (2): 327–38. https://doi.org/10.1016/S0896-6273(00)80272-X.

Caughey, Byron, and Peter T. Lansbury. 2003. “PROTOFIBRILS, PORES, FIBRILS, AND NEURODEGENERATION: Separating the Responsible Protein Aggregates from The Innocent Bystanders.” *Annual Review of Neuroscience* 26 (1): 267–98. https://doi.org/10.1146/annurev.neuro.26.010302.081142.

Chartier, Suzanne, and Charles Duyckaerts. 2018. “Is Lewy Pathology in the Human Nervous System Chiefly an Indicator of Neuronal Protection or of Toxicity?” *Cell and Tissue Research* 373 (1): 149–60. https://doi.org/10.1007/s00441-018-2854-6.

Chung, Chang Geon, Hyosang Lee, and Sung Bae Lee. 2018. “Mechanisms of Protein Toxicity in Neurodegenerative Diseases.” *Cellular and Molecular Life Sciences* 75 (17): 3159–80. https://doi.org/10.1007/s00018-018-2854-4.

Cleveland, Don W., and Jeffrey D. Rothstein. 2001. “From Charcot to Lou Gehrig: Deciphering Selective Motor Neuron Death in Als.” *Nature Reviews Neuroscience* 2 (11): 806–19. https://doi.org/10.1038/35097565.

Crippa, Valeria, Daniela Sau, Paola Rusmini, Alessandra Boncoraglio, Elisa Onesto, Elena Bolzoni, Mariarita Galbiati, et al. 2010. “The Small Heat Shock Protein B8 (HspB8) Promotes Autophagic Removal of Misfolded Proteins Involved in Amyotrophic Lateral Sclerosis (ALS).” *Human Molecular Genetics* 19 (17): 3440–56. https://doi.org/10.1093/hmg/ddq257.

D, Pietrobono, Giacomelli C, Trincavelli Ml, Daniele S, and Martini C. 2017. “Inhibitors of Protein Aggregates as Novel Drugs in Neurodegenerative Diseases.” *Global Drugs and Therapeutics* 2 (3). https://doi.org/10.15761/GDT.1000119.

Dalfó, Esther, Manuel Portero-Otín, Victoria Ayala, Anna Martínez, Reinald Pamplona, and Isidre Ferrer. 2005. “Evidence of Oxidative Stress in the Neocortex in Incidental Lewy Body Disease.” *Journal of Neuropathology & Experimental Neurology* 64 (9): 816–30. https://doi.org/10.1097/01.jnen.0000179050.54522.5a.

DiFiglia, M., E. Sapp, K. O. Chase, S. W. Davies, G. P. Bates, J. P. Vonsattel, and N. Aronin. 1997. “Aggregation of Huntingtin in Neuronal Intranuclear Inclusions and Dystrophic Neurites in Brain.” *Science (New York, N.Y.)* 277 (5334): 1990–93. https://doi.org/10.1126/science.277.5334.1990.

Djajadikerta, Alvin, Swati Keshri, Mariana Pavel, Ryan Prestil, Laura Ryan, and David C. Rubinsztein. 2020. “Autophagy Induction as a Therapeutic Strategy for Neurodegenerative Diseases.” *Journal of Molecular Biology* 432 (8): 2799–2821. https://doi.org/10.1016/j.jmb.2019.12.035.

Doble, A. 1996. “The Pharmacology and Mechanism of Action of Riluzole.” *Neurology* 47 (6 Suppl 4): S233-241. https://doi.org/10.1212/wnl.47.6_suppl_4.233s.

Dobson, Christopher M. 2001. “The Structural Basis of Protein Folding and Its Links with Human Disease.” Edited by C. M. Dobson, R. J. Ellis, and A. R. Fersht. *Philosophical Transactions of the Royal Society of London. Series B: Biological Sciences* 356 (1406): 133–45. https://doi.org/10.1098/rstb.2000.0758.

Dröge, Wulf. 2002. “Free Radicals in the Physiological Control of Cell Function.” *Physiological Reviews* 82 (1): 47–95. https://doi.org/10.1152/physrev.00018.2001.

Dumont, Magali, Michael T. Lin, and M. Flint Beal. 2010. “Mitochondria and Antioxidant Targeted Therapeutic Strategies for Alzheimer’s Disease.” Edited by Xiongwei Zhu, M. Flint Beal, Xinglong Wang, George Perry, and Mark A. Smith. *Journal of Alzheimer’s Disease* 20 (s2): S633–43. https://doi.org/10.3233/JAD-2010-100507.

Emin, Derya, Yu P. Zhang, Evgeniia Lobanova, Alyssa Miller, Xuecong Li, Zengjie Xia, Helen Dakin, et al. 2022. “Small Soluble α-Synuclein Aggregates Are the Toxic Species in Parkinson’s Disease.” *Nature Communications* 13 (1): 5512. https://doi.org/10.1038/s41467-022-33252-6.

Freibaum, Brian D., Raghu Chitta, Anthony A. High, and J. Paul Taylor. 2010. “Global Analysis of TDP-43 Interacting Proteins Reveals Strong Association with RNA Splicing and Translation Machinery.” *Journal of Proteome Research* 9 (2): 1104–20. https://doi.org/10.1021/pr901076y.

Gandhi, Sonia, and Andrey Y. Abramov. 2012. “Mechanism of Oxidative Stress in Neurodegeneration.” *Oxidative Medicine and Cellular Longevity* 2012 (May): e428010. https://doi.org/10.1155/2012/428010.

Grundke-Iqbal, I., K. Iqbal, Y. C. Tung, M. Quinlan, H. M. Wisniewski, and L. I. Binder. 1986. “Abnormal Phosphorylation of the Microtubule-Associated Protein Tau (Tau) in Alzheimer Cytoskeletal Pathology.” *Proceedings of the National Academy of Sciences of the United States of America* 83 (13): 4913–17. https://doi.org/10.1073/pnas.83.13.4913.

Hara, Taichi, Kenji Nakamura, Makoto Matsui, Akitsugu Yamamoto, Yohko Nakahara, Rika Suzuki-Migishima, Minesuke Yokoyama, et al. 2006. “Suppression of Basal Autophagy in Neural Cells Causes Neurodegenerative Disease in Mice.” *Nature* 441 (7095): 885–89. https://doi.org/10.1038/nature04724.

Harding, Antony J., Emily Stimson, Jasmine M. Henderson, and Glenda M. Halliday. 2002. “Clinical Correlates of Selective Pathology in the Amygdala of Patients with Parkinson’s Disease.” *Brain* 125 (11): 2431–45. https://doi.org/10.1093/brain/awf251.

Hetz, Claudio. 2012. “The Unfolded Protein Response: Controlling Cell Fate Decisions under ER Stress and Beyond.” *Nature Reviews Molecular Cell Biology* 13 (2): 89–102. https://doi.org/10.1038/nrm3270.

Hetz, Claudio, and Smita Saxena. 2017. “ER Stress and the Unfolded Protein Response in Neurodegeneration.” *Nature Reviews Neurology* 13 (8): 477–91. https://doi.org/10.1038/nrneurol.2017.99.

Hickey, Miriam A., Chunni Zhu, Vera Medvedeva, Renata P. Lerner, Stefano Patassini, Nicholas R. Franich, Panchanan Maiti, et al. 2012. “Improvement of Neuropathology and Transcriptional Deficits in CAG 140 Knock-in Mice Supports a Beneficial Effect of Dietary Curcumin in Huntington’s Disease.” *Molecular Neurodegeneration* 7 (1): 12. https://doi.org/10.1186/1750-1326-7-12.

Hipp, Mark S., Sae-Hun Park, and F. Ulrich Hartl. 2014. “Proteostasis Impairment in Protein-Misfolding and -Aggregation Diseases.” *Trends in Cell Biology* 24 (9): 506–14. https://doi.org/10.1016/j.tcb.2014.05.003.

Hoozemans, J. J. M., E. S. van Haastert, P. Eikelenboom, R. a. I. de Vos, J. M. Rozemuller, and W. Scheper. 2007. “Activation of the Unfolded Protein Response in Parkinson’s

Disease." *Biochemical and Biophysical Research Communications* 354 (3): 707–11. https://doi.org/10.1016/j.bbrc.2007.01.043.

Hoozemans, Jeroen J. M., Elise S. van Haastert, Diana A. T. Nijholt, Annemieke J. M. Rozemuller, and Wiep Scheper. 2012. "Activation of the Unfolded Protein Response Is an Early Event in Alzheimer's and Parkinson's Disease." *Neuro-Degenerative Diseases* 10 (1–4): 212–15. https://doi.org/10.1159/000334536.

Hou, Yujun, Xiuli Dan, Mansi Babbar, Yong Wei, Steen G. Hasselbalch, Deborah L. Croteau, and Vilhelm A. Bohr. 2019. "Ageing as a Risk Factor for Neurodegenerative Disease." *Nature Reviews Neurology* 15 (10): 565–81. https://doi.org/10.1038/s41582-019-0244-7.

Huttlin, Edward L., Lily Ting, Raphael J. Bruckner, Fana Gebreab, Melanie P. Gygi, John Szpyt, Stanley Tam, et al. 2015. "The BioPlex Network: A Systematic Exploration of the Human Interactome." *Cell* 162 (2): 425–40. https://doi.org/10.1016/j.cell.2015.06.043.

Ii, K., H. Ito, K. Tanaka, and A. Hirano. 1997. "Immunocytochemical Co-Localization of the Proteasome in Ubiquitinated Structures in Neurodegenerative Diseases and the Elderly." *Journal of Neuropathology and Experimental Neurology* 56 (2): 125–31. https://doi.org/10.1097/00005072-199702000-00002.

Irvine, G. Brent, Omar M. El-Agnaf, Ganesh M. Shankar, and Dominic M. Walsh. 2008. "Protein Aggregation in the Brain: The Molecular Basis for Alzheimer's and Parkinson's Diseases." *Molecular Medicine* 14 (7): 451–64. https://doi.org/10.2119/2007-00100.Irvine.

Jankovic, J. 2008. "Parkinson's Disease: Clinical Features and Diagnosis." *Journal of Neurology, Neurosurgery & Psychiatry* 79 (4): 368–76. https://doi.org/10.1136/jnnp.2007.131045.

Joshi, Vibhuti, Ribhav Mishra, Arun Upadhyay, Ayeman Amanullah, Krishna Mohan Poluri, Sarika Singh, Amit Kumar, and Amit Mishra. 2019. "Polyphenolic Flavonoid (Myricetin) Upregulated Proteasomal Degradation Mechanisms: Eliminates Neurodegenerative Proteins Aggregation." *Journal of Cellular Physiology* 234 (11): 20900–914. https://doi.org/10.1002/jcp.28695.

Kanekura, Kohsuke, Ikuo Nishimoto, Sadakazu Aiso, and Masaaki Matsuoka. 2006. "Characterization of Amyotrophic Lateral Sclerosis-Linked P56S Mutation of Vesicle-

Associated Membrane Protein-Associated Protein B (VAPB/ALS8).” *J. Biol. Chem.* 281 (40): 30223–33.

Kiernan, Matthew C, Steve Vucic, Benjamin C Cheah, Martin R Turner, Andrew Eisen, Orla Hardiman, James R Burrell, and Margaret C Zoing. 2011. “Amyotrophic Lateral Sclerosis.” *The Lancet* 377 (9769): 942–55. https://doi.org/10.1016/S0140-6736(10)61156-7.

Klucken, Jochen, Youngah Shin, Eliezer Masliah, Bradley T. Hyman, and Pamela J. McLean. 2004. “Hsp70 Reduces α-Synuclein Aggregation and Toxicity *.” *Journal of Biological Chemistry* 279 (24): 25497–502. https://doi.org/10.1074/jbc.M400255200.

Komatsu, Masaaki, Satoshi Waguri, Tomoki Chiba, Shigeo Murata, Jun-ichi Iwata, Isei Tanida, Takashi Ueno, et al. 2006. “Loss of Autophagy in the Central Nervous System Causes Neurodegeneration in Mice.” *Nature* 441 (7095): 880–84. https://doi.org/10.1038/nature04723.

Kuemmerle, S., C. A. Gutekunst, A. M. Klein, X. J. Li, S. H. Li, M. F. Beal, S. M. Hersch, and R. J. Ferrante. 1999. “Huntington Aggregates May Not Predict Neuronal Death in Huntington’s Disease.” *Annals of Neurology* 46 (6): 842–49.

Lemere, C. A., J. K. Blusztajn, H. Yamaguchi, T. Wisniewski, T. C. Saido, and D. J. Selkoe. 1996. “Sequence of Deposition of Heterogeneous Amyloid β-Peptides and APO E in Down Syndrome: Implications for Initial Events in Amyloid Plaque Formation.” *Neurobiology of Disease* 3 (1): 16–32. https://doi.org/10.1006/nbdi.1996.0003.

Lev, Sima, Daniel Ben Halevy, Diego Peretti, and Nili Dahan. 2008. “The VAP Protein Family: From Cellular Functions to Motor Neuron Disease.” *Trends Cell Biol.* 18 (6): 282–90.

López-Otín, Carlos, Maria A. Blasco, Linda Partridge, Manuel Serrano, and Guido Kroemer. 2013. “The Hallmarks of Aging.” *Cell* 153 (6): 1194–1217. https://doi.org/10.1016/j.cell.2013.05.039.

Lovell, M. A., W. D. Ehmann, S. M. Butler, and W. R. Markesbery. 1995. “Elevated Thiobarbituric Acid-Reactive Substances and Antioxidant Enzyme Activity in the Brain in Alzheimer’s Disease.” *Neurology* 45 (8): 1594–1601. https://doi.org/10.1212/WNL.45.8.1594.

Mackenzie, Ian R. A., Eileen H. Bigio, Paul G. Ince, Felix Geser, Manuela Neumann, Nigel J. Cairns, Linda K. Kwong, et al. 2007. “Pathological TDP-43 Distinguishes Sporadic Amyotrophic Lateral Sclerosis from Amyotrophic Lateral Sclerosis with SOD1 Mutations.” *Annals of Neurology* 61 (5): 427–34. https://doi.org/10.1002/ana.21147.

Maher, Pamela. 2019. “The Potential of Flavonoids for the Treatment of Neurodegenerative Diseases.” *International Journal of Molecular Sciences* 20 (12): 3056. https://doi.org/10.3390/ijms20123056.

Martin, George M., Charles E. Ogburn, Lorel M. Colgin, Allen M. Gown, Steven D. Edland, and Raymond J. Monnat. 1996. “Somatic Mutations Are Frequent and Increase with Age in Human Kidney Epithelial Cells.” *Human Molecular Genetics* 5 (2): 215–21. https://doi.org/10.1093/hmg/5.2.215.

McDonald, Karli K., Anaïs Aulas, Laurie Destroismaisons, Sarah Pickles, Evghenia Beleac, William Camu, Guy A. Rouleau, and Christine Vande Velde. 2011. “TAR DNA-Binding Protein 43 (TDP-43) Regulates Stress Granule Dynamics via Differential Regulation of G3BP and TIA-1.” *Human Molecular Genetics* 20 (7): 1400–1410. https://doi.org/10.1093/hmg/ddr021.

McNaught, Kevin St. P., and C. Warren Olanow. 2006. “Protein Aggregation in the Pathogenesis of Familial and Sporadic Parkinson’s Disease.” *Neurobiology of Aging*, This issue includes a special issue section:Protein misfolding in Alzheimer’s and other age-related neurodegenerative diseases, 27 (4): 530–45. https://doi.org/10.1016/j.neurobiolaging.2005.08.012.

Medinas, Danilo B., Pablo Rozas, Francisca Martínez Traub, Ute Woehlbier, Robert H. Brown, Daryl A. Bosco, and Claudio Hetz. 2018. “Endoplasmic Reticulum Stress Leads to Accumulation of Wild-Type SOD1 Aggregates Associated with Sporadic Amyotrophic Lateral Sclerosis.” *Proceedings of the National Academy of Sciences* 115 (32): 8209–14. https://doi.org/10.1073/pnas.1801109115.

Mehta, Paul, Wendy Kaye, Jaime Raymond, Ruoming Wu, Theodore Larson, Reshma Punjani, Daniel Heller, et al. 2018. “Prevalence of Amyotrophic Lateral Sclerosis — United States, 2014.” *Morbidity and Mortality Weekly Report* 67 (7): 216–18. https://doi.org/10.15585/mmwr.mm6707a3.

Mejzini, Rita, Loren L. Flynn, Ianthe L. Pitout, Sue Fletcher, Steve D. Wilton, and P. Anthony Akkari. 2019. “ALS Genetics, Mechanisms, and Therapeutics: Where Are We Now?” *Frontiers in Neuroscience* 13: 1310. https://doi.org/10.3389/fnins.2019.01310.

Menzies, Fiona M., Angeleen Fleming, and David C. Rubinsztein. 2015. “Compromised Autophagy and Neurodegenerative Diseases.” *Nature Reviews Neuroscience* 16 (6): 345–57. https://doi.org/10.1038/nrn3961.

Menzies, Fiona M., Jeannette Huebener, Maurizio Renna, Michael Bonin, Olaf Riess, and David C. Rubinsztein. 2010. “Autophagy Induction Reduces Mutant Ataxin-3 Levels and Toxicity in a Mouse Model of Spinocerebellar Ataxia Type 3.” *Brain* 133 (1): 93–104. https://doi.org/10.1093/brain/awp292.

Messer, Anne, and David C. Butler. 2020. “Optimizing Intracellular Antibodies (Intrabodies/Nanobodies) to Treat Neurodegenerative Disorders.” *Neurobiology of Disease* 134 (February): 104619. https://doi.org/10.1016/j.nbd.2019.104619.

Minakawa, Eiko N., and Yoshitaka Nagai. 2021. “Protein Aggregation Inhibitors as Disease-Modifying Therapies for Polyglutamine Diseases.” *Frontiers in Neuroscience* 15. https://www.frontiersin.org/articles/10.3389/fnins.2021.621996.

Mori, Fumiaki, Kunikazu Tanji, Yasuko Toyoshima, Mari Yoshida, Akiyoshi Kakita, Hitoshi Takahashi, and Koichi Wakabayashi. 2012. “Optineurin Immunoreactivity in Neuronal Nuclear Inclusions of Polyglutamine Diseases (Huntington’s, DRPLA, SCA2, SCA3) and Intranuclear Inclusion Body Disease.” *Acta Neuropathologica* 123 (5): 747–49. https://doi.org/10.1007/s00401-012-0956-x.

Nascimento-Ferreira, Isabel, Tiago Santos-Ferreira, Lígia Sousa-Ferreira, Gwennaëlle Auregan, Isabel Onofre, Sandro Alves, Noëlle Dufour, et al. 2011. “Overexpression of the Autophagic Beclin-1 Protein Clears Mutant Ataxin-3 and Alleviates Machado–Joseph Disease.” *Brain* 134 (5): 1400–1415. https://doi.org/10.1093/brain/awr047.

Nichols, Emma, Jaimie D Steinmetz, Stein Emil Vollset, Kai Fukutaki, Julian Chalek, Foad Abd-Allah, Amir Abdoli, et al. 2022. “Estimation of the Global Prevalence of Dementia in 2019 and Forecasted Prevalence in 2050: An Analysis for the Global Burden of Disease Study 2019.” *The Lancet Public Health* 7 (2): e105–25. https://doi.org/10.1016/S2468-2667(21)00249-8.

Nijholt, Diana A. T., Elise S. van Haastert, Annemieke J. M. Rozemuller, Wiep Scheper, and Jeroen J. M. Hoozemans. 2012. “The Unfolded Protein Response Is Associated with Early Tau Pathology in the Hippocampus of Tauopathies.” *The Journal of Pathology* 226 (5): 693–702. https://doi.org/10.1002/path.3969.

Nishimura, Agnes L, Miguel Mitne-Neto, Helga C A Silva, Antônio Richieri-Costa, Susan Middleton, Duilio Cascio, Fernando Kok, et al. 2004. “A Mutation in the Vesicle-Trafficking Protein VAPB Causes Late-Onset Spinal Muscular Atrophy and Amyotrophic Lateral Sclerosis.” *Am. J. Hum. Genet.* 75 (5): 822–31.

Nixon, Ralph A. 2013. “The Role of Autophagy in Neurodegenerative Disease.” *Nature Medicine* 19 (8): 983–97. https://doi.org/10.1038/nm.3232.

Nixon, Ralph A., Jerzy Wegiel, Asok Kumar, Wai Haung Yu, Corrinne Peterhoff, Anne Cataldo, and Ana Maria Cuervo. 2005. “Extensive Involvement of Autophagy in Alzheimer Disease: An Immuno-Electron Microscopy Study.” *Journal of Neuropathology and Experimental Neurology* 64 (2): 113–22. https://doi.org/10.1093/jnen/64.2.113.

Okamoto, Koichi, Yuji Mizuno, and Yukio Fujita. 2008. “Bunina Bodies in Amyotrophic Lateral Sclerosis.” *Neuropathology* 28 (2): 109–15. https://doi.org/10.1111/j.1440-1789.2007.00873.x.

Ortiz, Juan Fernando, Sawleha Arshi Khan, Amr Salem, Zayar Lin, Zafar Iqbal, and Nusrat Jahan. 2020. “Post-Marketing Experience of Edaravone in Amyotrophic Lateral Sclerosis: A Clinical Perspective and Comparison With the Clinical Trials of the Drug.” *Cureus* 12 (10). https://doi.org/10.7759/cureus.10818.

Pasinelli, Piera, Mary Elizabeth Belford, Niall Lennon, Brian J. Bacskai, Bradley T. Hyman, Davide Trotti, and Robert H. Brown. 2004. “Amyotrophic Lateral Sclerosis-Associated SOD1 Mutant Proteins Bind and Aggregate with Bcl-2 in Spinal Cord Mitochondria.” *Neuron* 43 (1): 19–30. https://doi.org/10.1016/j.neuron.2004.06.021.

Praticò, Domenico. 2008. “Evidence of Oxidative Stress in Alzheimer’s Disease Brain and Antioxidant Therapy: Lights and Shadows.” *Annals of the New York Academy of Sciences* 1147 (1): 70–78. https://doi.org/10.1196/annals.1427.010.

Prudencio, Mercedes, Veronique V. Belzil, Ranjan Batra, Christian A. Ross, Tania F. Gendron, Luc J. Pregent, Melissa E. Murray, et al. 2015. “Distinct Brain Transcriptome

Profiles in C9orf72-Associated and Sporadic ALS." *Nature Neuroscience* 18 (8): 1175–82. https://doi.org/10.1038/nn.4065.

Qu, Junyan, Tingting Zou, and Zhenghong Lin. 2021. "The Roles of the Ubiquitin-Proteasome System in the Endoplasmic Reticulum Stress Pathway." *International Journal of Molecular Sciences* 22 (4): 1526. https://doi.org/10.3390/ijms22041526.

Rai, Mamta, Michelle Curley, Zane Coleman, Anjana Nityanandam, Jianqin Jiao, Flavia A. Graca, Liam C. Hunt, and Fabio Demontis. 2021. "Analysis of Proteostasis during Aging with Western Blot of Detergent-Soluble and Insoluble Protein Fractions." *STAR Protocols* 2 (3): 100628. https://doi.org/10.1016/j.xpro.2021.100628.

Rodríguez-Navarro, Jose A., Laura Rodríguez, María J. Casarejos, Rosa M. Solano, Ana Gómez, Juan Perucho, Ana María Cuervo, Justo García de Yébenes, and María A. Mena. 2010. "Trehalose Ameliorates Dopaminergic and Tau Pathology in Parkin Deleted/Tau Overexpressing Mice through Autophagy Activation." *Neurobiology of Disease* 39 (3): 423–38. https://doi.org/10.1016/j.nbd.2010.05.014.

Santacruz, K., J. Lewis, T. Spires, J. Paulson, L. Kotilinek, M. Ingelsson, A. Guimaraes, et al. 2005. "Tau Suppression in a Neurodegenerative Mouse Model Improves Memory Function." *Science (New York, N.Y.)* 309 (5733): 476–81. https://doi.org/10.1126/science.1113694.

Santos, Luis E., and Sergio T. Ferreira. 2018. "Crosstalk between Endoplasmic Reticulum Stress and Brain Inflammation in Alzheimer's Disease." *Neuropharmacology* 136 (Pt B): 350–60. https://doi.org/10.1016/j.neuropharm.2017.11.016.

Sasaki, Shoichi. 2010. "Endoplasmic Reticulum Stress in Motor Neurons of the Spinal Cord in Sporadic Amyotrophic Lateral Sclerosis." *Journal of Neuropathology and Experimental Neurology* 69 (4): 346–55. https://doi.org/10.1097/NEN.0b013e3181d44992.

Scherzinger, Eberhard, Rudi Lurz, Mark Turmaine, Laura Mangiarini, Birgit Hollenbach, Renate Hasenbank, Gillian P. Bates, Stephen W. Davies, Hans Lehrach, and Erich E. Wanker. 1997. "Huntingtin-Encoded Polyglutamine Expansions Form Amyloid-like Protein Aggregates In Vitro and In Vivo." *Cell* 90 (3): 549–58. https://doi.org/10.1016/S0092-8674(00)80514-0.

Schröder, Martin, and Randal J. Kaufman. 2005. “The Mammalian Unfolded Protein Response.” *Annual Review of Biochemistry* 74 (1): 739–89. https://doi.org/10.1146/annurev.biochem.73.011303.074134.

Siemers, Eric R., Karen L. Sundell, Christopher Carlson, Michael Case, Gopalan Sethuraman, Hong Liu-Seifert, Sherie A. Dowsett, Michael J. Pontecorvo, Robert A. Dean, and Ronald Demattos. 2016. “Phase 3 Solanezumab Trials: Secondary Outcomes in Mild Alzheimer’s Disease Patients.” *Alzheimer’s & Dementia* 12 (2): 110–20. https://doi.org/10.1016/j.jalz.2015.06.1893.

Simpson, E. P., Y. K. Henry, J. S. Henkel, R. G. Smith, and S. H. Appel. 2004. “Increased Lipid Peroxidation in Sera of ALS Patients: A Potential Biomarker of Disease Burden.” *Neurology* 62 (10): 1758–65. https://doi.org/10.1212/WNL.62.10.1758.

Sinenko, Sergey A., Tatiana Yu. Starkova, Andrey A. Kuzmin, and Alexey N. Tomilin. 2021. “Physiological Signaling Functions of Reactive Oxygen Species in Stem Cells: From Flies to Man.” *Frontiers in Cell and Developmental Biology* 9. https://www.frontiersin.org/articles/10.3389/fcell.2021.714370.

Spencer, Brian, Rewati Potkar, Margarita Trejo, Edward Rockenstein, Christina Patrick, Ryan Gindi, Anthony Adame, Tony Wyss-Coray, and Eliezer Masliah. 2009. “Beclin 1 Gene Transfer Activates Autophagy and Ameliorates the Neurodegenerative Pathology in α-Synuclein Models of Parkinson’s and Lewy Body Diseases.” *The Journal of Neuroscience* 29 (43): 13578–88. https://doi.org/10.1523/JNEUROSCI.4390-09.2009.

Spilman, Patricia, Natalia Podlutskaya, Matthew J. Hart, Jayanta Debnath, Olivia Gorostiza, Dale Bredesen, Arlan Richardson, Randy Strong, and Veronica Galvan. 2010. “Inhibition of MTOR by Rapamycin Abolishes Cognitive Deficits and Reduces Amyloid-β Levels in a Mouse Model of Alzheimer’s Disease.” *PLOS ONE* 5 (4): e9979. https://doi.org/10.1371/journal.pone.0009979.

Tatebayashi, Yoshitaka, Tomohiro Miyasaka, De-Hua Chui, Takumi Akagi, Ken-ichi Mishima, Katsunori Iwasaki, Michihiro Fujiwara, et al. 2002. “Tau Filament Formation and Associative Memory Deficit in Aged Mice Expressing Mutant (R406W) Human Tau.” *Proceedings of the National Academy of Sciences of the United States of America* 99 (21): 13896–901. https://doi.org/10.1073/pnas.202205599.

Taylor, J. Paul, Robert H. Brown, and Don W. Cleveland. 2016. “Decoding ALS: From Genes to Mechanism.” *Nature* 539 (7628): 197–206. https://doi.org/10.1038/nature20413.

Tucker, James D, Michelle D Spruill, Marilyn J Ramsey, Alison D Director, and Joginder Nath. 1999. “Frequency of Spontaneous Chromosome Aberrations in Mice: Effects of Age.” *Mutation Research/Fundamental and Molecular Mechanisms of Mutagenesis* 425 (1): 135–41. https://doi.org/10.1016/S0027-5107(99)00036-6.

Umeda, Tomohiro, Satomi Maekawa, Tetsuya Kimura, Akihiko Takashima, Takami Tomiyama, and Hiroshi Mori. 2014. “Neurofibrillary Tangle Formation by Introducing Wild-Type Human Tau into APP Transgenic Mice.” *Acta Neuropathologica* 127 (5): 685–98. https://doi.org/10.1007/s00401-014-1259-1.

Van der Jeugd, Ann, Ben Vermaercke, Maxime Derisbourg, Adrian C. Lo, Malika Hamdane, David Blum, Luc Buée, and Rudi D’Hooge. 2013. “Progressive Age-Related Cognitive Decline in Tau Mice.” *Journal of Alzheimer’s Disease* 37 (4): 777–88. https://doi.org/10.3233/JAD-130110.

Walker, Francis O. 2007. “Huntington’s Disease.” *Lancet (London, England)* 369 (9557): 218–28. https://doi.org/10.1016/S0140-6736(07)60111-1.

Williams, Aislinn J., and Henry L. Paulson. 2008. “Polyglutamine Neurodegeneration: Protein Misfolding Revisited.” *Trends in Neurosciences* 31 (10): 521–28. https://doi.org/10.1016/j.tins.2008.07.004.

Winner, Beate, Roberto Jappelli, Samir K. Maji, Paula A. Desplats, Leah Boyer, Stefan Aigner, Claudia Hetzer, et al. 2011. “In Vivo Demonstration That α-Synuclein Oligomers Are Toxic.” *Proceedings of the National Academy of Sciences of the United States of America* 108 (10): 4194–99. https://doi.org/10.1073/pnas.1100976108.

Yang, Fusheng, Giselle P. Lim, Aynun N. Begum, Oliver J. Ubeda, Mychica R. Simmons, Surendra S. Ambegaokar, Pingping P. Chen, et al. 2005. “Curcumin Inhibits Formation of Amyloid β Oligomers and Fibrils, Binds Plaques, and Reduces Amyloid in Vivo*.” *Journal of Biological Chemistry* 280 (7): 5892–5901. https://doi.org/10.1074/jbc.M404751200.

Yoshida, Hiderou, Toshie Matsui, Nobuko Hosokawa, Randal J. Kaufman, Kazuhiro Nagata, and Kazutoshi Mori. 2003. “A Time-Dependent Phase Shift in the Mammalian Unfolded

Protein Response." *Developmental Cell* 4 (2): 265–71. https://doi.org/10.1016/s1534-5807(03)00022-4.

Yoshino, Hiide, and Akio Kimura. 2006. "Investigation of the Therapeutic Effects of Edaravone, a Free Radical Scavenger, on Amyotrophic Lateral Sclerosis (Phase II Study)." *Amyotrophic Lateral Sclerosis* 7 (4): 247–51. https://doi.org/10.1080/17482960600881870.

Yu, Wai Haung, Beatriz Dorado, Helen Yvette Figueroa, Lili Wang, Emmanuel Planel, Mark R. Cookson, Lorraine N. Clark, and Karen E. Duff. 2009. "Metabolic Activity Determines Efficacy of Macroautophagic Clearance of Pathological Oligomeric α-Synuclein." *The American Journal of Pathology* 175 (2): 736–47. https://doi.org/10.2353/ajpath.2009.080928.

Zhang, Fujian, Anna-Lena Ström, Kei Fukada, Sangmook Lee, Lawrence J. Hayward, and Haining Zhu. 2007. "Interaction between Familial Amyotrophic Lateral Sclerosis (ALS)-Linked SOD1 Mutants and the Dynein Complex *." *Journal of Biological Chemistry* 282 (22): 16691–99. https://doi.org/10.1074/jbc.M609743200.

Zhao, Beibei, Kristen Marciniuk, Ebrima Gibbs, Masoud Yousefi, Scott Napper, and Neil R. Cashman. 2019. "Therapeutic Vaccines for Amyotrophic Lateral Sclerosis Directed against Disease Specific Epitopes of Superoxide Dismutase 1." *Vaccine* 37 (35): 4920–27. https://doi.org/10.1016/j.vaccine.2019.07.044.

Zhu, Jingyan, Max S. Cynader, and William Jia. 2015. "TDP-43 Inhibits NF-KB Activity by Blocking P65 Nuclear Translocation." *PLoS ONE* 10 (11): e0142296. https://doi.org/10.1371/journal.pone.0142296.

# Chapter 2

# Characterization of VAP aggregation in the *Drosophila* nervous system

**Abstract:**

Amyotrophic Lateral Sclerosis (ALS) is a fatal neurodegenerative disorder with no known cure and limited treatment options. We have a very limited understanding of the disease aetiology. While a large number of cases are sporadic, around 5 to 10% of the cases have a familial origin, with close to 40 genes being identified as causative loci. VAPB, the eighth locus to be identified, is an interesting candidate for study as it is involved in the regulation of several functions including vesicular trafficking, maintaining UPR, lipid biosynthesis, maintenance of ER structure and signaling via its MSP domain. A Proline to Serine substitution in its 56$^{th}$ residue has been identified as a causative mutation in the development of ALS. The mutant protein has been shown to misfold and aggregate, often sequestering functional protein, thus disrupting functional homeostasis (Kanekura et al. 2006; Teuling et al. 2007). While several models have been suggested for explaining how VAP aggregation affects the cellular system in a diseased state, there is still a lack of clarity behind the processes involved in generation and clearance of VAP aggregates in native systems. In order to study and understand VAP aggregation in a native context, we employed the use of a *Drosophila* model, which could express *VAP$^{P58S}$* at genomic levels. For this we used two approaches, the first involved using a fly model developed in Hiroshi Tsuda's lab, involving a null rescued with a genomically expressing *VAP$^{P58S}$*. This line showed phenotypes reported in ALS, progressive motor degeneration and reduced lifespan (Moustaqim-Barrette et al. 2014). We modified this line and characterized motor degeneration, lifespan and aggregation in our adapted model. The second approach involved generating a genomic mutant using a CRISPR-Cas9 strategy and validating the results obtained from the null rescue model. (Refer chapter 5.)

In this chapter, I will discuss how we characterized the null rescue model we generated in the lab in terms of VAP aggregation. We looked at larval and adult nervous tissue and used immunohistochemistry and confocal imaging to visualize aggregation. We also studied how VAP aggregation changes with age. To get a clearer understanding of VAP function and how the mutation affects it, we studied aggregation in flies rescued with a double copy of VAP,

where one allele expressed the wild-type protein and the other allele expressed the mutant protein. We also carried out an age-dependent characterization of BiP staining in the null rescue lines to gain an understanding of both wild-type and mutant protein functioning.

**VAMP Associated Protein B (VAPB)**

Vesicle Associated Membrane Protein (VAMP) Associated Protein B (VAPB) is an integral membrane protein, belonging to the VAP family of proteins. The VAPs are ER resident, single-pass proteins, with three major domains: the major sperm protein domain (MSP), a coiled-coil domain (CCD) and a Transmembrane domain (TMD) (Fig 2.1 A). The MSP domain lies in the cytosol and has been shown to get secreted and interact with ligand receptors (Tsuda et al. 2008) (Fig. 2.1 B). The two major members of the VAP protein family are VAPA and VAPB. In addition to these forms, a splice variant of VAPB called VAPC has also been identified. Currently, Motile Sperm Domain containing proteins (MOSPD1, MOSPD2, MOSPD3) have also been added to this family due to the presence of an MSP domain and similarities in binding partners (Di Mattia et al. 2018; Cabukusta et al. 2020) . VAPA and VAPB are expressed ubiquitously in humans and show high sequence similarity (60% amino-acid sequence similarity) (Nishimura et al. 1999). The VAPs are involved in vesicle trafficking, endocytosis and the establishment of neuromuscular architecture. VAPB is known to interact with several other cellular components like microtubules, ER and also several proteins (Lev et al., 2008) .VAPs are also known to facilitate the formation and maintenance of membrane contact sites (MCS) between ER and other organelles (Murphy and Levine 2016; Cabukusta et al. 2020).

In the early 2000s, the VAPB locus was identified as an ALS causative locus, making it the eighth locus to be associated with the disease. The causative mutation was first identified in a Brazilian family and was found to be autosomal dominant. A missense mutation in the *VAPB* gene which results in the substitution of the 56th conserved Proline to Serine was identified in these patients, and was shown to cause protein misfolding and aggregation (Nishimura et al., 2004). The manner in which the mutation affected normal cellular functioning, causing disease pathogenesis has since been widely studied. The *VAP (P56S)* mutation was shown to act in a dominant negative manner by sequestering wild-type VAP into tubular aggregates (Teuling et al., 2007). Loss of *VAPB* was associated with neuromuscular defects in zebrafish and mild, late onset motor defects in mice (Kabashi et al. 2013).

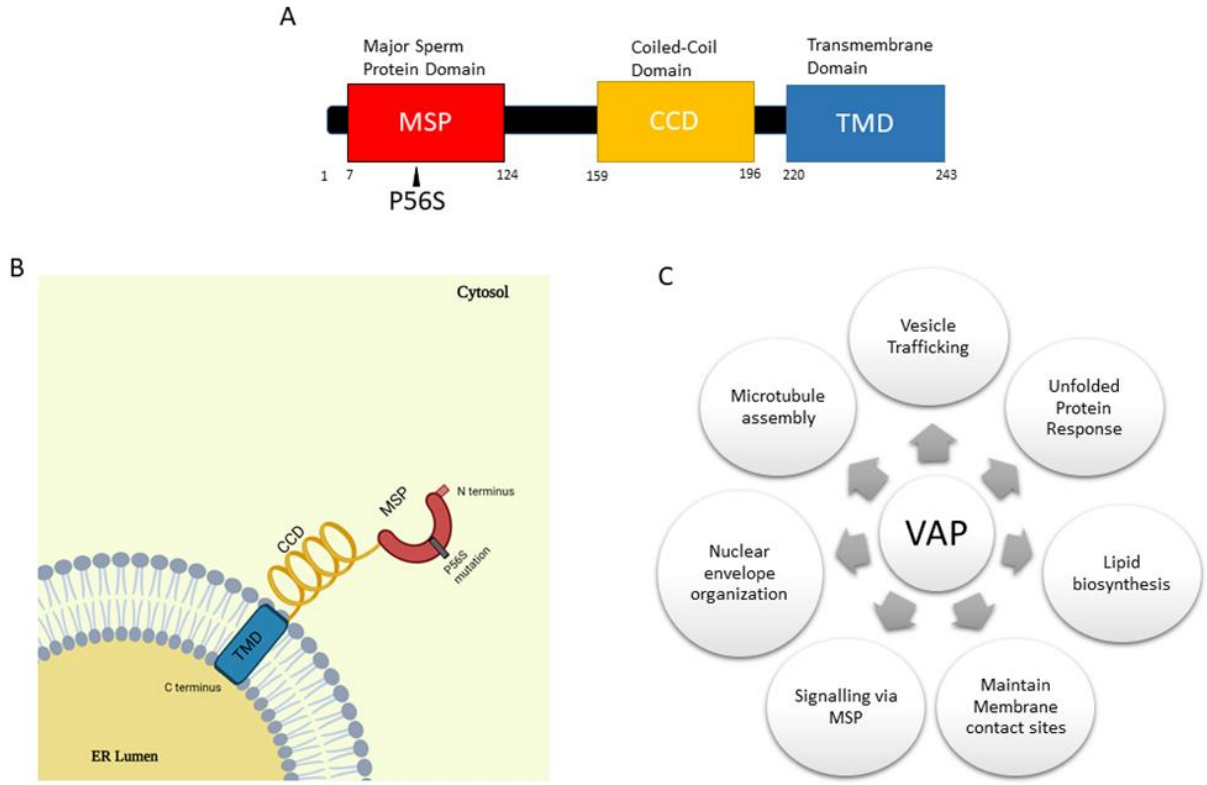


***Figure 2.1: VAPB is an ALS locus involved in a myriad of cellular functions.***

VAPB is a familial ALS locus that was identified first in a Brazilian family. It is a type II integral membrane protein with three major domains, a Major Sperm Protein (MSP) domain, a Coiled Coil Domain (CCD) and a Transmembrane Domain (TMD). The ALS causative mutation P56S occurs in the MSP (A). VAPB is an ER resident. The MSP domain faces the cytosol, with the TMD inserted into the membrane (B). The VAP family is known to perform a wide variety of cellular functions, listed in (C).

VAPB is highly conserved evolutionarily, because of which several animal models could be developed to study the mutation. *VAPB* function has been studied in yeast, *C.elegans*, *Drosophila* and mice (Lev et al., 2008). *Drosophila melanogaster* has emerged as a powerful tool for this enterprise. They have a single VAP protein-VAP33-1, and the mutation homologous to P56S in this system is at the 58$^{th}$ residue. VAP null *Drosophila* larvae show enlarged boutons at the neuromuscular junction and the expression of $VAP^{P58S}$ in the neurons results in a similar phenotype (Pennetta et al., 2002). $VAP^{P58S}$ was also found to aggregate in this system, supporting the hypothesis that $VAP^{P58S}$ acts in a dominant negative manner by sequestering functional VAP into aggregates, thus depleting functional VAP (Ratnaparkhi et al., 2008). Aggregation models of VAP, however, do not appear to show motor defects. Possible explanations put forward for these were the presence of endogenous

VAP in the system being functional, which needed to be evaluated for understanding the allelic function.

**The Tsuda model of *VAPB* ALS**

*VAP*$^{P58S}$ activity has been studied in *Drosophila* using a few different systems to drive expression. The most used and documented involve the expression of VAP protein using the UAS-Gal4 system. The protein of interest in this system is driven by the generation of Gal4 by a promoter, which triggers a UAS sequence upstream of the gene of interest (Duffy 2002). This allows us to have both spatial and temporal control over the expression of the protein of interest (in our case, VAP). This system was critical in establishing the role of VAP in flies, the effects of VAP$^{P58S}$ and identification of VAP interactors (Pennetta et al. 2002; Ratnaparkhi et al. 2008; Deivasigamani et al. 2014). VAP$^{P58S}$ aggregation was also demonstrated in flies using *VAP*$^{P58S}$ overexpression in the muscle (Ratnaparkhi et al. 2008) and in the nervous system (Chaplot et al. 2019). Working with the Gal4 system did pose a few issues, primarily in terms of the level of protein expressed and the presence of endogenous wild-type protein. In the GAL4 system, the level of protein expression might not always match the level of normal genomic expression and it could also not always account for fluctuations in expression which occurred naturally in development. To circumvent this problem, the use of a genomic promoter to drive expression is a good option. When coupled with a protein null background, the genomic promoter driven expression of protein can effectively simulate physiological characteristics of its behavior and interactions.

The Hiroshi Tsuda lab developed one such system in their lab to study the role of the *VAP*$^{P58S}$ mutation in ALS disease aetiology. For this system, they used a VAP null allele, *Δ31*, as the null background. Using VAP constructs under the expression of a genomic promoter, they managed to rescue the lethality seen in VAP null mutants. The VAP constructs could either be of the native or wild-type (WT) sequence or the ALS mutant *VAP*$^{P58S}$ and both of these rescued pupal lethality. They however had different ageing phenotypes following eclosion. The wild-type flies had a normal lifespan and developed no motor defects with ageing, while the *VAP*$^{P58S}$ flies had a severely shortened lifespan with progressive development of motor defects. This phenotype mimicked the disease progression in ALS and was a good system to study disease pathogenesis, in context to phenotypes observed in the disease. The genetic rescue in this model was carried out by insertion of genomic VAP constructs via phiC31 integrase mediated transgenesis into the VK31 and VK33 sites on the third chromosome, separate from the original locus (Moustaqim-Barrette et al. 2014). This opened up the

possibility of studying VAP$^{P58S}$ activity without endogenous VAP$^{WT}$ by selecting male flies for the required experiment (Fig 2.2). In addition to single copy rescues, another important observation was how the addition of a copy of *VAP$^{WT}$* to the *VAP$^{P58S}$* background could rescue both the lifespan and motor defects.

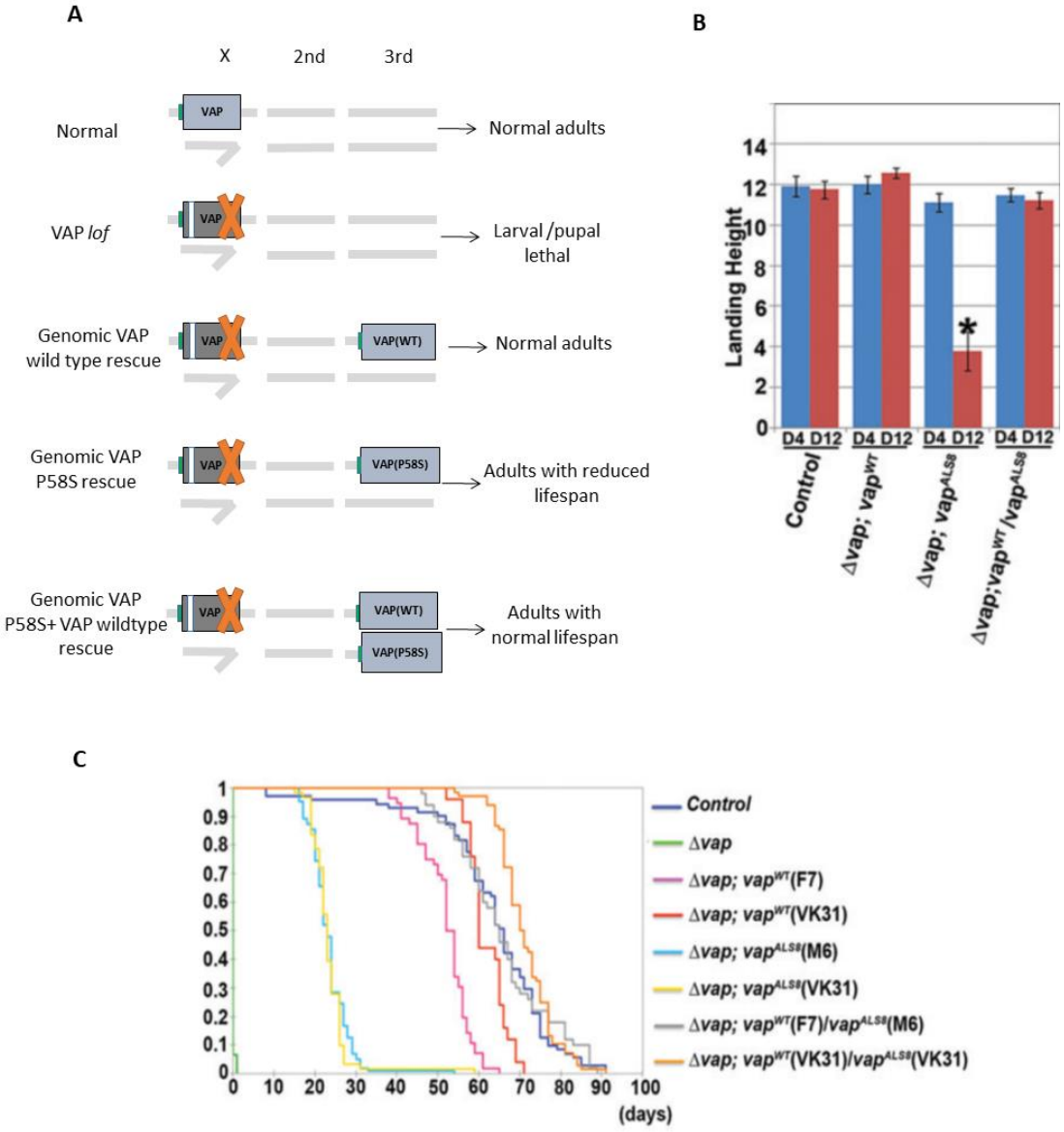


***Figure 2.2: The Drosophila model developed for studying ALS8 by the Hiroshi Tsuda lab demonstrates both motor defects and shortened lifespan (Moustaqim-Barrette et al, 2014).***

A) The following schematic shows the genetic background used for studying the *VAP$^{P58S}$* mutation in ALS phenotype. For this, a VAP null background was used in tandem with a VAP construct under a genomic promoter. This construct was incorporated into the VK31 site on the third chromosome, away from the original VAP locus, thus providing an option to not have endogenous VAP protein in the

background. With this system, it is possible to create fly lines which solely express the mutant VAP protein. An additional genetic copy of $VAP^{WT}$ in this background completely rescues the motor and lifespan defects associated with the $VAP^{P58S}$ rescue. B) Data comparing the flight ability of flies at different ages using the landing height as a parameter for comparison. The abilities of ALS8 flies were shown to deteriorate with age. This deterioration was rescued by adding a copy of $VAP^{WT}$. C) Lifespan data from the lines demonstrated that the VAP null flies rescued with the $VAP^{P58S}$ mutation lived far fewer days than VAP null flies rescued with $VAP^{WT}$. This reduction in lifespan could also be rescued by adding an allele of $VAP^{WT}$ in the system.

In order to study VAP aggregation we decided to use the fly lines generated using the Tsuda lab strategy. We used genomic promoter driven $VAP^{P58S}$ and $VAP^{WT}$ generated from Tsuda lab. We tried to combine these with the null originally used by them, but faced issues with obtaining and maintaining the same. We decided to use an alternative, a strongly hypomorphic line, *Δ166*, generated by the Bellen lab. This line also shows pupal lethality similar to that seen in the other null lines (Pennetta et al. 2002). This line was balanced and crossed with fly lines containing the genomic promoter driven VAP constructs and the resulting rescue lines were balanced and stabilized. The fly lines with the genomic VAP constructs were a gift from the Tsuda lab and they have been made as described previously, with the constructs inserted into the VK31 and VK33 sites on the third chromosome (Moustaqim-Barrette et al. 2014). They were validated using lifespan and motor assays and they demonstrate the same phenotypes as the ones originally observed (Fig 2.3). Data has been contributed by Shweta Tendulkar. Henceforth, we will refer to this set of lines as the null rescue set of lines.

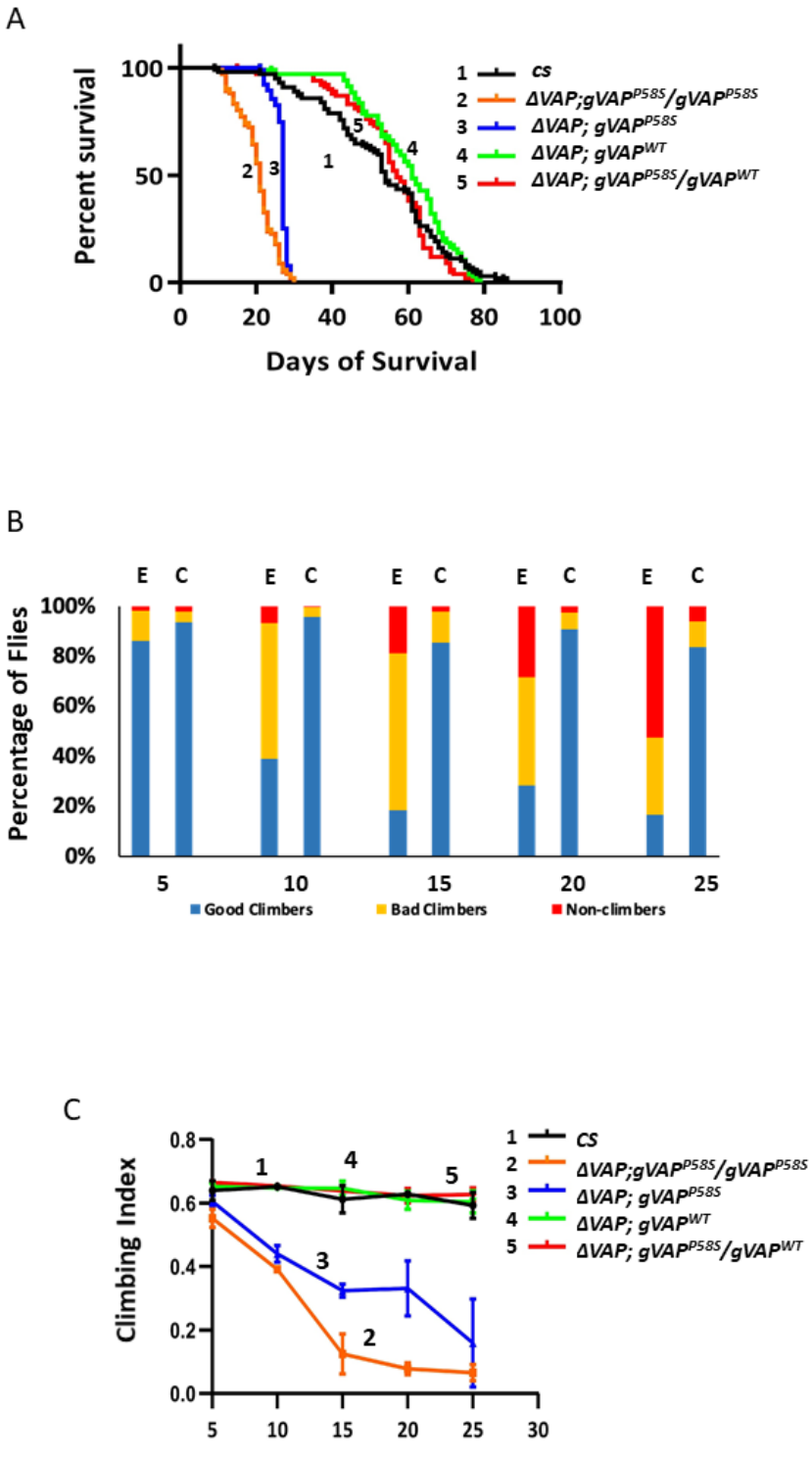


***Figure 2.3: ΔVAP;; gVAP$^{P58S}$ /+ (Null rescue) flies show lifespan defects and progressive motor degeneration***

A) Survival plots for CS (wild type, master control, black curve, number 1), ΔVAP; gVAP$^{P58S}$/gVAP$^{P58S}$ (orange curve, number 2), ΔVAP; ;gVAP$^{P58S}$ (blue curve, number 3), ΔVAP;

$gVAP^{WT}$ (light green curve, number 4) and ΔVAP; $gVAP^{WT}/gVAP^{P58S}$ (red curve, number 5). Introduction of a $gVAP^{wt}$ copy in the ΔVAP or ΔVAP; $gVAP^{P58S}$ background rescues the lifespan defect. Curve comparison was done using log-rank (Mantel-Cox test). Combined p-value for the whole set is <0.001(n=80-100).

B) Percentage of good climbers goes down with the age of ΔVAP; $gVAP^{P58S}$ /+ flies (marked as E), whereas it remains constant for the wild type control (marked as C). The blue refers to percentage of good climbers, the yellow refers to percentage of bad climbers while the red section refers to percentage of non-climbers.

C) Climbing index of ΔVAP; $gVAP^{P58S}$ /+ flies (blue) is significantly reduced as compared to wild type control flies (black) when observed from day 10 to day 30 of the life of the flies. We observe a rescue in this decline upon adding a $VAP^{WT}$ allele to the $VAP^{P58S}$ genetic background (red). n=15-20 flies, N=1. Statistical analysis was done using unpaired Student's t-test. Combined p-value for the whole set is <0.01

(Data from Thulasidharan et al, Manuscript in preparation)

While working with this system it is important to remember a few points. Because of the position of the VAP locus being on the first chromosome (X chromosome), only male flies can be used for experiments if we don't want endogenous $VAP^{WT}$ in our background. Thus, for most of our experiments, we have used male flies.

**Methodology**

We have primarily used immunohistochemistry in combination with confocal microscopy to identify and characterize VAP localization in different genetic backgrounds (Fig 2.4). Briefly, *Drosophila* nervous system tissue, at either larval or adult stages, would be dissected, fixed and stained for the presence of VAP using an in-house generated VAP antibody. This antibody has been used and validated in different studies (Yadav et al. 2017; Chaplot et al. 2019). Following this, samples would be imaged using confocal microscopy, wherein they were acquired as a Z-stack. Manual thresholding was used to segment the punctae from background. From our experience, different genetic backgrounds gave varying amounts of background intensity, which arose mainly from the difference in VAP solubility, number of VAP aggregates and presence of $VAP^{WT}$. We thus, used a manual thresholding protocol for overcoming this issue. Following segmentation, three Regions of Interest (ROIs) were defined in the stack and punctae in each were measured and counted. This measure was normalized to the volume of the ROI and is called Aggregation Density or Aggregate Density. For a detailed methodology, refer materials and methods.

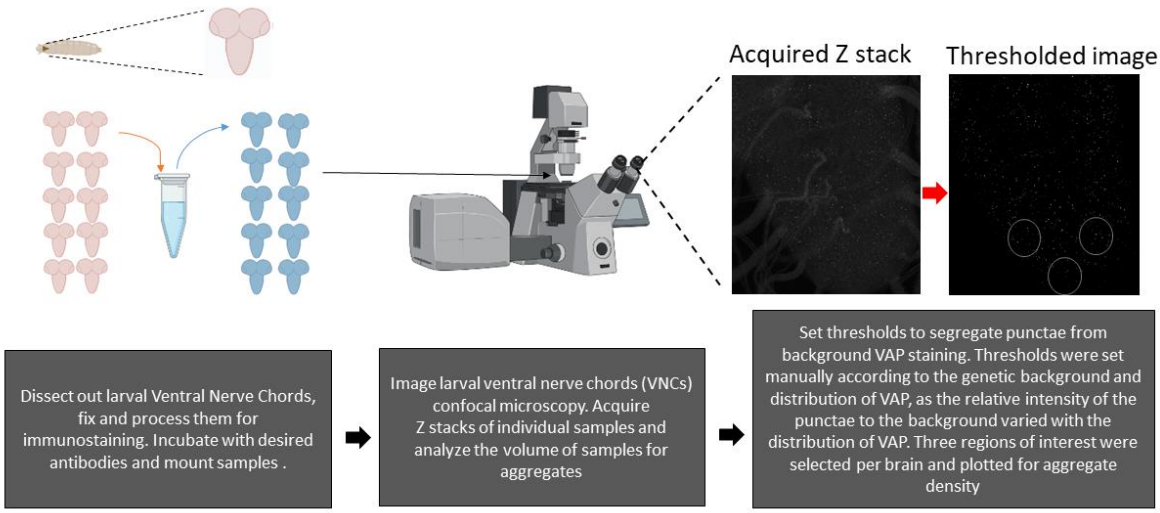


***Figure 2.4: Methodology developed for studying aggregation in Drosophila larval Ventral Nerve Cords.***

Drosophila Larval Ventral Cords (VNCs) are used to study VAP aggregation in our model. The process has been visualised as a schematic, a more detailed methodology for the same is discussed in the material and methods section.

## Results

1) Punctate localization of VAP is seen in the genomic *VAP*$^{P58S}$ line, the aggregate size, aggregation density and intensity increase with the dosage of the mutant protein.

The larval VNCs of wild type (CS), *VAP*$^{WT}$ genomic rescue and *VAP*$^{P58S}$ were processed and imaged as described in the materials and methods. We observed that the *VAP*$^{P58S}$ larvae show punctate localization of VAP as opposed to the cytoplasmic staining shown by VAP wild type rescues and wild type larvae (Fig.2.5 A,B and C). These punctae are found throughout the ventral nerve cord. Previous studies to understand VAP$^{P58S}$ aggregation were carried out using *VAP*$^{P58S}$ overexpression (Ratnaparkhi et al. 2008; Chaplot et al. 2019) and the presence of ubiquitinated VAP aggregates were observed in the tissues where overexpression was driven. With the Tsuda system, we needed to understand how we could measure and compare the aggregation we saw and in order to do that we decided to compare aggregation in genetic backgrounds with varying dosages of the *VAP*$^{P58S}$. For this we used the null rescue lines generated in our lab, where one had a single *VAP*$^{P58S}$ allele, the other had two alleles of the *VAP*$^{P58S}$(Fig. 2.5 D, E). We also used the *VAP*$^{P58S}$ neuronal overexpression system previously

used in the field to study the VAP mutation (Chaplot et al. 2019) ( Fig 2.5 F). We compared different parameters used to describe the properties of the aggregates, and observed that there is an increase in the size, intensity and density of aggregates upon increase of $VAP^{P58S}$ dosage (Fig.2.5 G- I). Of the parameters observed, we saw a more pronounced change with the aggregate intensity and density (Fig.2.5 H and I). We observed that these parameters increased with an increase in genetic dosage of $VAP^{P58S}$ implying that more of the mutant protein in the system would lead to more aggregates, with higher intensity in the given volume. This was in agreement with a previous study from our lab where increased expression of $VAP^{P58S}$ was shown to give a higher aggregation density (Chaplot et al. 2019). We have thus decided to use the aggregation density in this system as well to quantify aggregation.

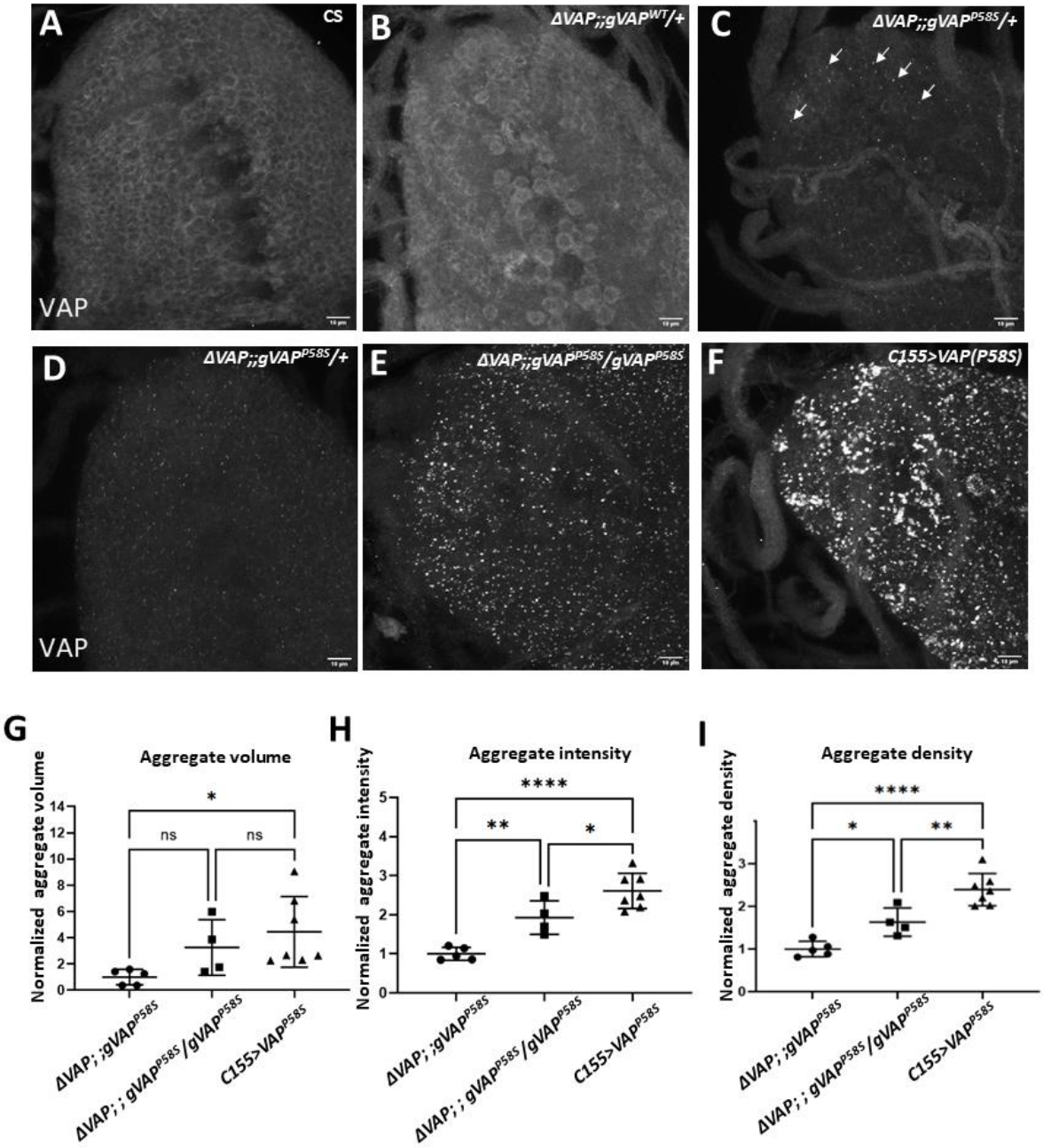


***Figure 2.5: VAP antibody staining of $VAP^{P58S}$ larval Ventral Nerve Cords demonstrates VAP aggregation, which shows a dose dependent variation in size , intensity and number.***

Figures (A-F) show representative Maximum Intensity Projections (MIPs) of the larval VNCs of different genotypes stained with VAP antibody. Wild-type CS and *ΔVAP* rescued with $VAP^{WT}$ (A and B) show non punctate diffuse staining of VAP protein. *ΔVAP* rescued with a single copy of $VAP^{P58S}$ shows the presence of puncta, marked by the white arrows (C). (D-F) are representative images demonstrating an increase in size, intensity and aggregation density with increase in VAP dosage. The change in aggregate volume (G), aggregate intensity (H) and aggregate density (I) are depicted graphically. Each point represents an average value calculated from 3 ROIs (for G, ns=non-

significant,*P= 0.0387. For H, *P= 0.0333, **P=0.079,****P<0.0001. For I, *P=0.0287 ,**P= 0.0057 ,****P<0.0001. One-way ANOVA with Tukey's multiple comparisons. Error bars represent SD). Scale bars denote 10µm.

2) Addition of $VAP^{WT}$ rescues aggregation in the larval ventral cord

One of the striking phenotypes observed while working with the Tsuda model was the complete rescue of both motor and lifespan defects observed in heterozygous flies, having a copy of both $VAP^{P58S}$ and $VAP^{WT}$. We wished to see how VAP localized in this genetic background and for that we looked at the VNCs of $\Delta VAP; ; gVAP^{P58S}/gVAP^{WT}$ ( Fig.2.6 C). Surprisingly, we observe a significant lack of aggregates in the heterozygous larval VNCs. The VAP localization in the VNCs closely resembles that of the wild-type alone (Fig.2.6 A). The aggregate intensity, size and aggregation density are seen to be lowered in the heterozygous background (Fig.2.6 D-F). In our experiments so far, we have always observed VAP punctae in genetic backgrounds having $VAP^{P58S}$, with increasing amounts of $VAP^{P58S}$ resulting in more aggregates, while in this scenario we see a near absence of VAP aggregates. From the data it appears that addition of $VAP^{WT}$ to the $VAP^{P58S}$ background rescues VAP aggregation in the larval VNC. $VAP^{WT}$ appears to be involved in the regulation of aggregation of $VAP^{P58S}$.

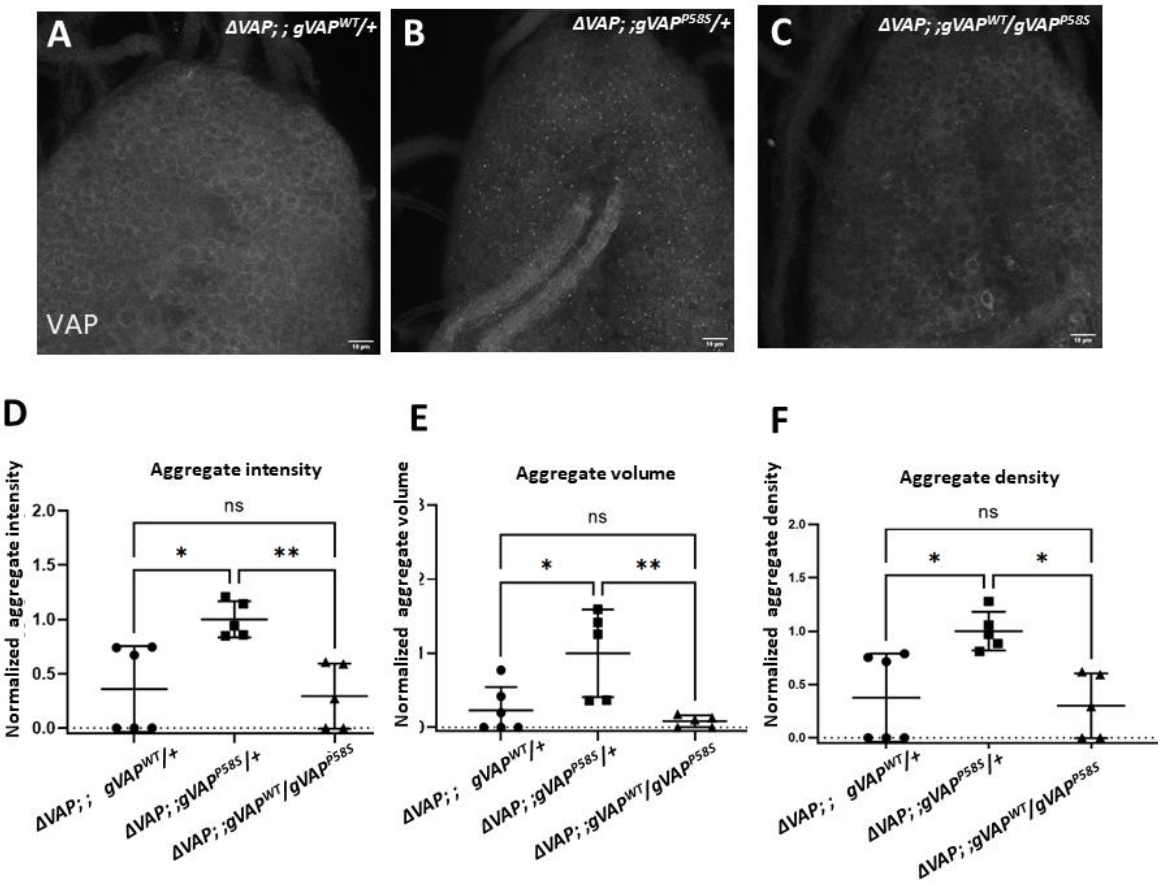


***Figure 2.6: Addition of $VAP^{WT}$ rescues aggregation in the larval ventral cord.***

Figures (A-C) show representative Maximum Intensity Projections (MIPs) of the larval VNCs of $\Delta VAP; ; gVAP^{WT}/+$, $\Delta VAP; ;gVAP^{P58S}/+$ and $\Delta VAP; ;gVAP^{P58S}/gVAP^{WT}$ stained with VAP antibody. The aggregate intensity (D), volume (E) and aggregation density (F) are reduced in the heterozygous null rescue. Each point represents an average of 3 ROIs from one animal. (For D, ns=non-significant, *P= 0.012, **P= 0.0084. For E, ns= non-significant, *P=0.0144, **P=0.006. For F, ns=non-significant, *P= 0.01. One-way ANOVA with Tukey's multiple comparisons was used for all three graphs. Error bars denote SD.) Scale bars denote 10µm.

3) Aggregation does not appear to change with age and aggregation density increases with genetic dosage of $VAP^{P58S}$

From our experiments in the larval VNCs, we developed a system to quantify aggregation in the tissue using aggregation density as a measurement. We now wondered if it were possible to look at aggregation in the adults, as this was the stage at which one saw motor and lifespan defects. For carrying out our experiments in the adult fly, we chose to look at the *Drosophila* adult brain. We adapted the protocol used for staining, imaging and quantification of

aggregation density from the larval experiments (described in methods). We first looked at the brains of *ΔVAP;; gVAP$^{P58S}$/+* and *ΔVAP;; gVAP$^{WT}$/+* and saw the presence of VAP punctae (Fig.2.7 A-F). As the motor defects are seen to be progressive with age, after confirming the presence of VAP punctae in the adult brain, we wanted to see if there was a relationship between age and VAP aggregation. We also wished to see if the genetic dosage of *VAP$^{P58S}$* would affect aggregation. We compared the brains of 5 day old, 11 day old and 15 day old flies of both genotypes (Fig.2.7 D-I). We did not observe a significant change in aggregation density with age in either of the genotypes (Fig.2.7 J). We did see an increase in aggregation density when comparing the single copy to the double copy.

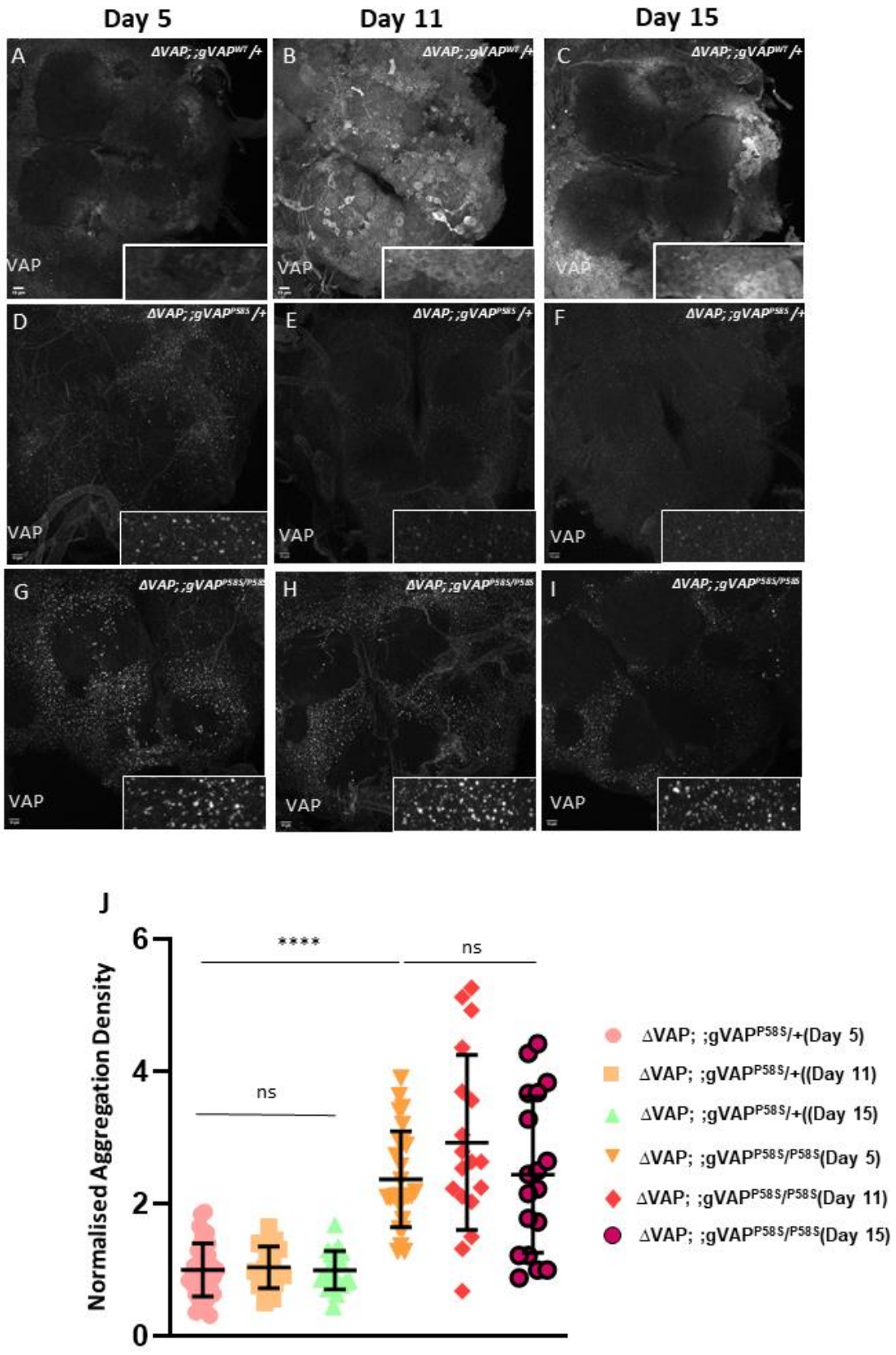


***Figure 2.7 : VAP aggregation density does not change with age and increases with increase in dosage.***

(A-C) Representative images of adult brain anti VAP staining for Δ*VAP; ;gVAP*$^{WT}$/+(A-C), Δ*VAP; ;gVAP*$^{P58S}$/+(D-F),and Δ*VAP; ;gVAP*$^{P58S}$/$^{P58S}$ (G-I) across 5, 11 and 15 day old flies . Δ*VAP; ;gVAP*$^{WT}$/+ show diffuse, non-punctate localization of VAP at all observed ages (A-C). Δ*VAP; ;gVAP*$^{P58S}$/+ shows the presence of aggregates at all three ages (D-F), they, however, do not change in density across age point ( J , ns=non-significant, ****P<0.0001. Kruskal-Wallis test, followed by Dunn's multiple comparisons (n=3, N=8-12).Error bars depict SD). Scale bar denote 10µm.

4) Addition of a copy of *VAP*$^{WT}$ reduces VAP$^{P58S}$ aggregation in an age dependant manner.

Addition of a copy of *VAP*$^{WT}$ to the *VAP*$^{P58S}$ background was shown to rescue motor defects and lifespan defects in the null rescue line and VAP aggregation in the larval VNC. We now wanted to see how aggregation was affected in this genetic context, where there was one copy of *VAP*$^{WT}$ and one copy of *VAP*$^{P58S}$. We looked at the brains of 5 day old, 11 day old and 15 day old flies. As seen previously, the *ΔVAP;; gVAP*$^{P58S}$/+ flies show aggregates at all three age points, without a significant difference in aggregation density with age (Fig 2.8 A-C, G). With the *ΔVAP;; gVAP*$^{P58S}$/*gVAP*$^{WT}$ flies, we observed VAP aggregates at 5 days (Fig 2.8 D). The aggregation density in these flies were comparable to that seen in 5 day old *ΔVAP;; gVAP*$^{P58S}$/+. However, as the fly ages, the aggregate density drops significantly, resulting in a clearance of the VAP aggregation (Fig 2.8 E, F, G). This was a novel observation as the VAP$^{P58S}$ protein was previously shown to be dominant negative in its pathogenic mechanism. The VAP aggregates were believed to be sequestering functional VAP resulting in ,compromised VAP activity. Our data show that addition of *VAP*$^{WT}$ rescues VAP aggregation seen as a result of *VAP*$^{P58S}$. The clearance is a progressive phenotype, with VAP aggregation density reducing with the age of the fly.

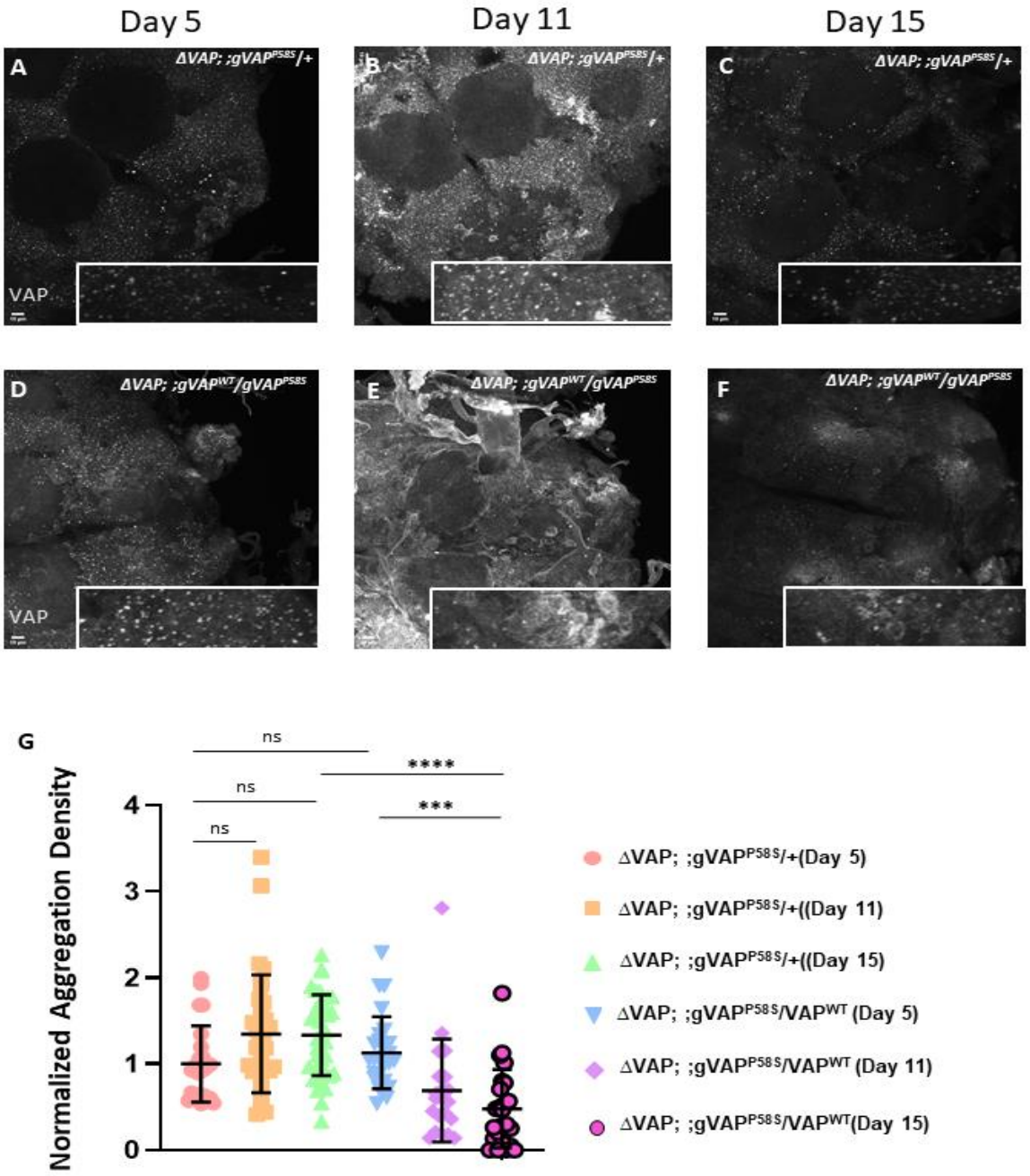


***Figure 2.8: VAP aggregation in the adult fly brain is cleared with age upon addition of a wild-type VAP allele.***

(A-F) Representative images of adult brain anti VAP staining for Δ*VAP; ;gVAP*$^{P58S}$/+ and Δ*VAP; ;gVAP*$^{P58S}$*/gVAP*$^{WT}$ across 5, 11 and 15 day old flies . When compared to *VAP*$^{P58S}$ brain (A,B,C), adults with a copy of *VAP*$^{WT}$ in the background (D,E,F) show progressive decrease in aggregation. Quantification of aggregation in terms of normalized aggregate density, depicting a decrease in aggregation upon addition of *VAP*$^{WT}$ in the *VAP*$^{P58S}$ background. Each point represents a single ROI in a brain (G , *P=0.0187,***P=0.0002, ****P<0.0001, ns=Non significant, Kruskal-Wallis with Dunn's multiple comparison (n=3 ,N=8-12). Error bars depict SD). Scale bar depicts 10µm.

5) A copy of $VAP^{WT}$ to the $VAP^{P58S}$ background reduces BiP aggregation.

*VAPB* has previously been shown to be a regulator of the UPR and ER stress responses (Suzuki et al. 2009; Gkogkas et al. 2008). VAP null flies are known to show ER stress (Moustaqim-Barrette et al. 2014). Over expression of the mutant $VAP^{P58S}$ has also been shown to trigger ER stress and lead to BiP aggregation (Tsuda et al. 2008) . BiP or Grp78 is an important player in the series of events leading to ER stress. The binding of BiP to ATF6, PERK and IRE1 keeps them in an off state. The presence of misfolded proteins causes BiP to unbind from them and rebind to the misfolded proteins. BiP can attempt to refold the proteins by functioning as a chaperone (Lee 2005) and once the misfolded proteins are removed, the BiP dissociates and relocalizes with ATF6, IRE1 and PERK (Bertolotti et al. 2000). As these studies were carried out in either a *VAP* null, or with endogenous VAP in the background, we wondered how BiP localization was being affected in our null rescue model. We stained the brains of old flies at day 15 to check for differences in BiP localization between wild-type, $\Delta VAP; ;gVAP^{P58S}/+$ and $\Delta VAP; ;gVAP^{P58S}/gVAP^{WT}$ (Fig 2.9). We observe a very diffuse pattern of BiP staining in the case of 15 day old wild-type flies (Fig 2.9 A). In contrast, the $\Delta VAP; ;gVAP^{P58S}/+$ shows punctate BiP staining (Fig.2.9 B). We thus observe a difference in BiP localisation from the wild type, indicative of compromised BiP activity and UPR. We compared this with the samples from $\Delta VAP; ;gVAP^{P58S}/gVAP^{WT}$ and observed a decrease in BiP punctae (Fig 2.9 C-D). Our observations indicate that the presence of $VAP^{WT}$ is affecting BiP aggregation at 15 days.

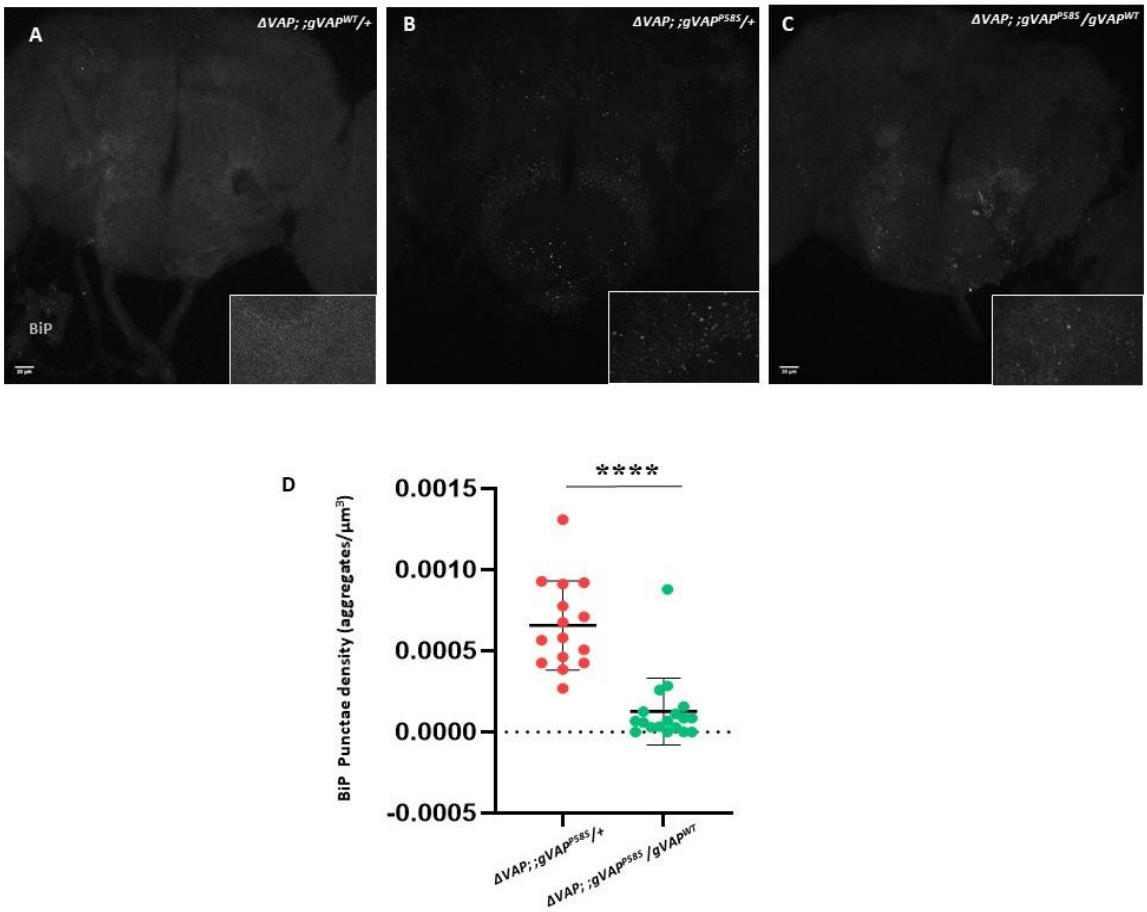


***Figure 2.9: A copy of VAP$^{WT}$ to the VAP$^{P58S}$ background reduces BiP aggregation.***
Representative images of adult brain anti BiP staining for Δ*VAP; ;gVAP*$^{WT}$/+ (A), Δ*VAP; ;gVAP*$^{P58S}$/+ (B) and Δ*VAP; ;gVAP*$^{P58S}$/*gVAP*$^{WT}$ (C) at 15 days . Δ*VAP; ;gVAP*$^{P58S}$/+ (B) shows the presence of punctae not seen in wild type (A). Lesser punctae are observed in (C). Quantification for the BiP puncta density of Δ*VAP; ;gVAP*$^{P58S}$/+ *and* Δ*VAP; ;gVAP*$^{P58S}$/*gVAP*$^{WT}$. Each point represents a single ROI in a brain (****P<0.0001, Mann-Whitney test). Error bars depict SD. Scale bars represent 20 µm.

6) BiP aggregation reduces with age in the disease model, the presence of VAP$^{WT}$ enhances this reduction.

The observation of BiP aggregation in the Δ*VAP; ;gVAP*$^{P58S}$/+ line led us to the question of whether BiP aggregation in the system was a progressive phenotype that worsened with age. In order to answer this we compared the BiP punctae density of 5 day old Δ*VAP;;gVAP*$^{P58S}$/+ fly brains with 15 day old Δ*VAP; ;gVAP*$^{P58S}$/+ fly brains (Fig 2.10 A-B). We notice a decrease in the puncta density at 15 days when compared to the 5 day old brains. The BiP aggregation phenotype does not appear to be progressive, rather it seems to ameliorate with

age (Fig. 2.10 C). Following this observation, we were curious to see how the addition of $VAP^{WT}$ affected this phenotype. We repeated the same experiment but with $\Delta VAP;;gVAP^{P58S}/gVAP^{WT}$ flies. We observe the same decline in BiP aggregation with age, but we see the aggregation drop to a far lower value of puncta density than that seen in the $\Delta VAP;;gVAP^{P58S}/+$ ( Fig 2.10 E). This demonstrates that the clearance of BiP punctae with age is compromised in the absence of $VAP^{WT}$ protein.

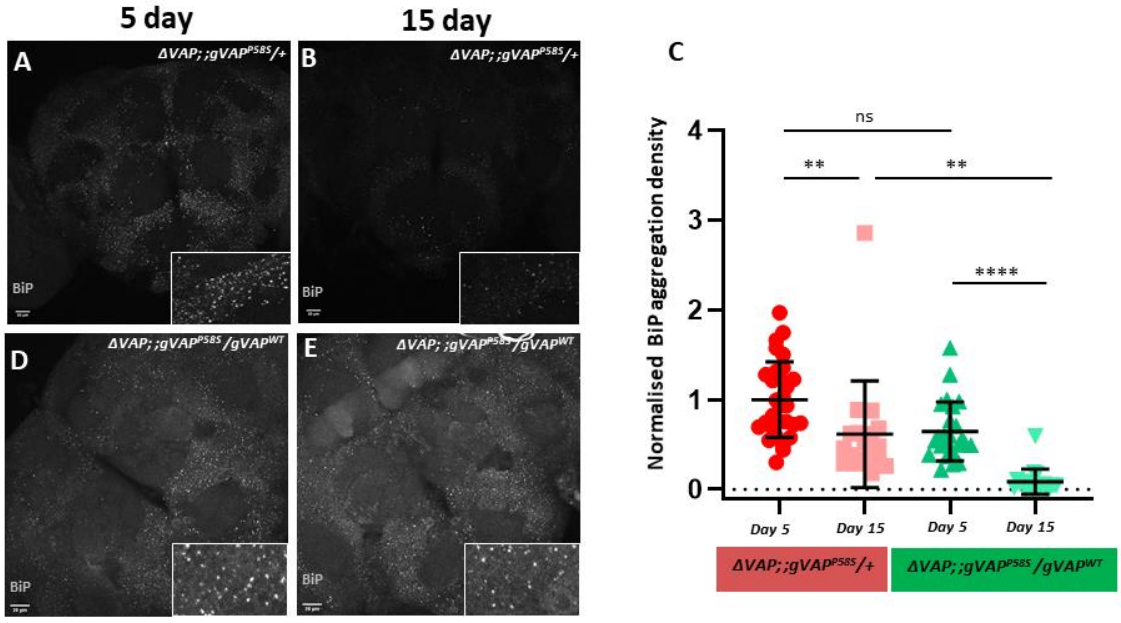


***Figure 2.10: BiP aggregation reduces with age in the disease model, the presence of $VAP^{WT}$ enhances this reduction.***

BiP punctae observed in $\Delta VAP;;gVAP^{P58S}/+$(A and B) and $\Delta VAP;;gVAP^{P58S}/gVAP^{WT}$ (D and E) show a difference in BiP aggregation density when compared between 5 and 15 day time-points. (C) Aggregation density is lower at the 15 day time points for both genotypes (A and D, **P=0.0074, for D and E, ****P<0.0001) when comparing between the genotypes at 5 day, ns=non-significant. When comparing between genotypes at day 15, **P=0.0034. The test used was Kruskal-Wallis followed by Dunn's multiple comparisons. Error bars depict SD. Scale bar represents 20 μm.

## Discussion

In order to study VAP aggregation and processes affected by it, we have developed a system for studying VAP protein aggregation using a workflow involving tissue dissection, immunostaining, fluorescence confocal microscopy and analysis of generated image stacks. We chose to study these in an animal model which phenocopied the hallmarks of human ALS, in order to understand how variation in VAP aggregation may influence the progressive defects observed in the human disease. The Drosophila models for VAP ALS have been demonstrated in various studies to show several hallmarks of the disease including increased ubiquitinated protein accumulation, increased ER stress, motor defects, reduced lifespan and showed lipid defects (Tsuda et al. 2008; Ratnaparkhi et al. 2008; Moustaqim-Barrette et al. 2014; Tendulkar et al. 2022). Ageing is a known risk factor for the development of several neurodegenerative disorders, with an increase in age being linked to an increase in risk for development of Alzheimer's, Parkinson's, ALS and so on. Ageing has been shown to result in a lot of undesirable variations in cellular functions, including decrease in proteostatic clearance, disruptions in autophagy, increases in ROS and cellular inflammation. Thus studying neurodegeneration in the context of changes caused by ageing becomes important for determining aetiology. With the null rescue system used in our study, we have a *Drosophila* model, showing progressive motor defects and reduced lifespan, similar to the human ALS symptoms. Using this system, we could not only look at VAP aggregates in a single time-point, but compare with the aggregation seen at different time-points (ages) or genetic backgrounds (Fig 2.7).

While ageing has been shown to increase the concentration of insoluble proteins in cells (Reis-Rodrigues et al. 2012; Rai et al. 2021) and reduce proteasomal activity (Tsakiri et al. 2013), how it affects misfolding of proteins is not clearly known. In our study, we made a few critical observations regarding VAP aggregation with age. We observe that the aggregation density does not vary significantly with the age of the fly. We know from our studies on this line that the flies show a progression in motor defects with age, but such a correlation is not observed with VAP aggregation. This could imply that the VAP aggregates are not solely responsible for the progression of defects. These observations point us towards a hypothesis that the aggregates are not directly toxic. The disease progression may be occurring due to VAP loss of function. Aggregation may be limiting the functioning of VAP, and aggregates by themselves may not be toxic.

Aggregation of the VAP mutant protein has been hypothesized as being dominant negative in the field (Ratnaparkhi et al. 2008; M Mitne-Neto et al. 2007; Teuling et al. 2007; Suzuki et al. 2009), the deleterious effects observed being a result of $VAP^{WT}$ sequestration. We noticed in our null rescue models that the addition of $VAP^{WT}$ appears to clear VAP aggregates along with rescue life span, motor defects and BiP punctae. While aggregates are observed in the 5 day old flies, we see them clearing up by the fifteenth day in this genetic background. Thus the presence of aggregates does not appear to be sequestering and blocking $VAP^{WT}$ function when they are both expressed in equal genetic dosages. Combined with the fact that flies heterozygous for both alleles show a normal lifespan and motor function, the mode of pathogenicity for $VAP^{P58S}$ appears to be due to a partial loss of function, rendering it incapable of performing cellular functions. This leads us to propose a hypomorphic model for $VAP^{P58S}$ associated ALS progression. It has been shown in the field previously that haplo-insufficiency of *VAPB* may be responsible for some of the observed dysfunctions. The spinal cord lysates of patients show reduced VAPB levels (Tsuda et al. 2008). Certain models shown in mice and zebra fish, where expression of the mutant protein alone is not responsible for the onset of motor defects, rather it is the loss of VAP function itself that leads to defects (Kabashi et al. 2013). iPSc derived motor neurons taken from ALS patients with the VAP (P56S) mutation also show a decreased concentration of VAPB (Miguel Mitne-Neto et al. 2011).

The cycling of BiP is critical for both effecting, maintaining and terminating UPR. Inadequate availability of BiP can lead to ER stress (Vitale et al. 2019). Prolonged UPR can lead to ER stress which, if not managed and brought under control, can trigger pro-apoptotic pathways (Szegezdi et al. 2006). We see an upregulation in BiP in terms of BiP punctae when we compare 15 day old, $\Delta VAP;;gVAP^{P58S}/+$ flies to wild type or $\Delta VAP;;gVAP^{P58S}/gVAP^{WT}$ flies (Fig 2.9). This implies an upregulated UPR response in the $\Delta VAP;;gVAP^{P58S}/+$ flies. We also characterized this aggregation in younger flies and compared it with the older flies. Our results demonstrate a decline in the BiP punctae with age in both, $\Delta VAP;;gVAP^{P58S}/+$ and $\Delta VAP;;gVAP^{P58S}/gVAP^{WT}$. This would imply that an active removal mechanism for the BiP punctae exists and is functional. The extent to which the punctae are removed however is greatly affected by the presence of $VAP^{WT}$ and its presence ensures a near complete removal of BiP punctae. Our experiment demonstrates that regulation of BiP aggregation also appears to be a function of VAP that is compromised in the $\Delta VAP;;gVAP^{P58S}/+$ flies.

VAPB models of ALS do show ER stress. *VAPB* knock in mice expressing the P56S mutation show progressive motor defects, with starker defects observed with more genetic dosage of the mutant protein. These mice also display an upregulation of ER markers in their motor neurons before the onset of motor defects (Larroquette et al. 2015). Drosophila *VAP* null mutants also display upregulation in ER stress markers (Moustaqim-Barrette et al. 2014). Our current understanding is that the wild-type VAPB interacts with components in the UPR pathway including IRE1 and ATF6 and initialize the UPR (Gkogkas et al. 2008; Suzuki et al. 2009). The VAP (P56S) mutant appears to not be able to splice XBP-1, resulting in a lack of UPR initiation (Suzuki et al. 2009). Our model indicates that BiP punctae develop early on in the $VAP^{P58S}$ backgrounds. In the scenario where we do not have $VAP^{WT}$, the punctae are not effectively removed with age, which might be causing persistent ER stress. With $VAP^{WT}$ in the system, the punctae are cleared much more effectively. These observations point us towards thinking of $VAP^{P58S}$ being only partially functional in maintaining UPR, which would be in agreement with a loss of function mode of pathogenicity for the $VAP^{P58S}$ allele.

**Future Directions**

With the null rescue model, we have developed a fly line showing phenotypes similar to those observed in human ALS. We have also developed a quantitative method for studying VAP and BiP aggregation in this line for both larval and adult fly nervous systems. Our study shows us that wild type VAP protein is a modulator of VAP aggregation. The exact mechanism through which this modulation occurs is not clear. One of our future goals would be to identify the pathways through which VAP aggregation is regulated, particularly in the adults. We further hope to adapt and use the methods developed to study VAP aggregation to study the aggregation of other candidate loci such as *SOD1* and *TDP-43.*

**Contributions:**

Shweta Tendulkar carried out the lifespan and motor assay based characterization of the null rescue lines. Lovleen Garg assisted with image analysis for the larval aggregate assays.

**Materials and methods**

## *Drosophila* maintenance and husbandry

All flies were grown on standard corn meal agar at 25 degrees Celsius. All crosses were set up at 25 degrees Celsius unless specified otherwise.

## *Drosophila* stocks and reagents

The flies expressing genomic $VAP^{WT}$ and genomic $VAP^{P58S}$ were a gift from Hiroshi Tsuda. These lines were balanced with a null line, *Δ166*, as described previously (Tendulkar et al. 2022).The UAS –VAP(P58S) line was generated in the Jackson lab (Ratnaparkhi et al. 2008). Canton S (0001) lines were procured from Bloomington Drosophila stock center (BDSC).

## Larval Ventral Nerve cord preparation

Wandering third-instar larvae were selected and dissected in 1X PBS. They were fixed in 4% PFA with 0.3% PBST for 20 minutes. Post fixation, the samples were washed thrice in 1X PBS and then transferred to blocking solution (2% BSA in 0.3% PBST) for 1 hour, followed by incubation in primary antibody for 12 hours. This was followed by 3 washes with blocking each lasting 20 minutes and then an overnight incubation with the secondary antibody. Post-secondary, the samples are washed thrice with blocking, each lasting 20 minutes. DAPI is added to the second wash to visualize cell nuclei. Samples are given one final wash in PBS before mounting in antifade mounting media.

## Adult brain dissections

Flies of the desired genotype are collected and aged to the requirement. Adult brains are dissected out into cold 1X PBS, followed by a 24-hour fixation in 1.2% PFA at 4 degrees Celsius. This is followed by permeabilization in 5% PBST (2 washes for 20 minutes each) followed by 2 washes in PAT buffer (30 minutes each). Samples were then blocked in 5% BSA in 0.5% PBST for two hours. This was followed by incubation in primary antibodies for 36 hours at 4 degrees Celsius. Post-primary incubation, 4 PAT buffer washes each lasting 30 minutes are administered. Samples are then incubated in secondary antibodies for 36 hours. This is followed by another 4 PAT buffer washes. DAPI (1:1000) is added in the second wash to visualize nuclei. This is followed by a wash in 1X PBS and subsequently stored in PBS with Vectashield mounting media in a 1:1 ratio at 4 degrees Celsius overnight.
For mounting, samples are placed with the antennal lobes facing the coverslip. Samples are bridge-mounted. We have used SlowFade mounting medium (Vectashield, S36937).

Antibodies used: Rabbit Anti-BiP (1:200)(Cell signalling) , Rat Anti-ELAV (DSHB; 1:100) and Rabbit Anti-VAP (1:500) (Yadav et al. 2017; Chaplot et al. 2019).

## Microscopy

Mounted samples were imaged using Zeiss LSM710 or Leica SP8 confocal microscopes with 63x objectives. Images were acquired at 16-bit depth as Z stacks. For larval ventral chords, the tip of the ventral cord was imaged at 1X zoom. For the adult brains, the main body of the brain was imaged at 0.75X zoom. Acquisition parameters were kept constant across experimental sets.

## Image analysis

We have used both ImageJ and Huygens Professional software for image segmentation and analysis. The analysis protocol is similar to that used in (Chaplot et al. 2019) with modifications for analysing adult brain images. Briefly, a threshold is set to segment high intensity punctae from the background signal from the tissue. The threshold is manually adjusted for each genotype in order to segment punctae from the tissue background. Object filters were used to remove objects larger than 200 voxels and smaller than 8 voxels. The punctae were quantified per micrometre of the larval ventral nerve chord or the adult brain and has been defined as aggregation density. Three 3D ROIs were selected from each brain from the tip of the VNC (larval) or the sub oesophageal zone (SEZ) (adult) and measured. The aggregation density for each ROI was normalized to the mean value for the control group in each experiment. We have used 6 to 12 brains per genotype per experiment. ROI volume has been calculated as the range of the z stack of the image. The 3D objects calculator and Visikol plugin has been used in the case of ImageJ to count aggregates and calculate volume.

## Lifespan assays

Survival assays were carried out for characterisation of the $VAP^{P58S}$ and for testing genetic interactions. 80-100 male flies of the appropriate genotype were collected and maintained in media containing vials. All flies were maintained at 25 ºC. Each vial had 15 or fewer, age-matched individuals. Vials were flipped every fourth day to avoid accidental death caused by sticking to dry media. The daily death toll of each genotype was recorded. The assay was followed up till the death of every fly in both the experimental and control vials. Data was plotted and analyzed using the log-rank test in prism7 survival assay which computes a value of significance by comparing the survival curves of the assayed genotypes. We have also taken

into account the median lifespan of each genotype as an additional criterion for comparison (Piper and Partridge 2016; Moustaqim-Barrette et al. 2014; Estes et al. 2011).

## Motor Function

Motor performance of the different genotypes were analyzed using the startle induced negative geotaxis climbing assay (Madabattula et al. 2015; Azuma et al. 2014), with minor modifications. Three separate sets (biological replicates) of 30 age-matched adult males each were raised at 25 ºC. At the beginning of an experiment, a set of 30 flies was emptied in a 250 ml glass cylinder and tapped sufficiently to startle the flies in the cylinder. As a result of the startle response, flies would fall to the bottom, or zero mark of the cylinder. Following this, flies start climbing to the top of the cylinder. The flies were ranked into three groups, based on their position at the end of 60 seconds, post startling. Flies which could not climb at all were ranked 0 (Non-Climbers), flies which climbed till 80 mL mark were ranked 1 (Bad Climbers) and flies which climbed further up from 80 mL to the top were ranked 2 (Good Climbers). The assay was repeated thrice for each set of 30 flies. The climbing assays was repeated for every genotype at an interval of 5 days until flies in at least one of the genotypes completely stopped climbing or were dead.

This motor assay does not account for the death occurring as the assay proceeds. Each time a set was transferred from the vial to the cylinder for the assay, acclimatization was done for approximately 5 minutes. Also, the flies were exposed to CO2 only after a day's trial was complete, ensuring no effect of CO2 on the assay. Flies were transferred to a new vial every four days to avoid accidental death due to dry media. The conditions at which the assays were performed were constant for every set. Data was analyzed by calculating the climbing index for each technical repeat, which was then averaged. This average was averaged with other biological replicates to obtain a final value of the climbing index with error values. This data was plotted using Prism7 grouped representations and statistically analyzed using two -way ANOVA followed by multiple comparison testing by Tukey test.

The Climbing index is a proxy indicator for the fitness of a particular fly/genotype on a particular day. It helps in recognizing any progression of the motor defect in a set of flies. The formula for climbing index is

Climbing Index (CI)=Sum of all three values (Each Score X Number of flies with that score)/3 X Total number of flies examined.(Azuma et al. 2014)

**References**

Azuma, Yumiko, Takahiko Tokuda, Mai Shimamura, Akane Kyotani, Hiroshi Sasayama, Tomokatsu Yoshida, Ikuko Mizuta, et al. 2014. "Identification of Ter94, Drosophila VCP, as a Strong Modulator of Motor Neuron Degeneration Induced by Knockdown of Caz, Drosophila FUS." *Human Molecular Genetics* 23 (13): 3467–80. https://doi.org/10.1093/hmg/ddu055.

Bertolotti, Anne, Yuhong Zhang, Linda M. Hendershot, Heather P. Harding, and David Ron. 2000. "Dynamic Interaction of BiP and ER Stress Transducers in the Unfolded-Protein Response." *Nature Cell Biology* 2 (6): 326–32. https://doi.org/10.1038/35014014.

Cabukusta, Birol, Ilana Berlin, Daphne M. van Elsland, Iris Forkink, Menno Spits, Anja W. M. de Jong, Jimmy J. L. L. Akkermans, et al. 2020. "Human VAPome Analysis Reveals MOSPD1 and MOSPD3 as Membrane Contact Site Proteins Interacting with FFAT-Related FFNT Motifs." *Cell Reports* 33 (10): 108475. https://doi.org/10.1016/j.celrep.2020.108475.

Chaplot, Kriti, Lokesh Pimpale, Balaji Ramalingam, Senthilkumar Deivasigamani, Siddhesh S Kamat, and Girish S Ratnaparkhi. 2019. "SOD1 Activity Threshold and TOR Signalling Modulate VAP (P58S) Aggregation via Reactive Oxygen Species-Induced Proteasomal Degradation in a Drosophila Model of Amyotrophic Lateral Sclerosis." *Dis. Model. Mech.* 12 (2): dmm033803.

Deivasigamani, Senthilkumar, Hemant Kumar Verma, Ryu Ueda, Anuradha Ratnaparkhi, and Girish S Ratnaparkhi. 2014. "A Genetic Screen Identifies Tor as an Interactor of VAPB in a Drosophila Model of Amyotrophic Lateral Sclerosis." *Biol. Open* 3 (11): 1127–38.

Di Mattia, Thomas, Léa P Wilhelm, Souade Ikhlef, Corinne Wendling, Danièle Spehner, Yves Nominé, Francesca Giordano, et al. 2018. "Identification of MOSPD2, a Novel Scaffold for Endoplasmic Reticulum Membrane Contact Sites." *EMBO Reports* 19 (7): e45453. https://doi.org/10.15252/embr.201745453.

Duffy, Joseph B. 2002. "GAL4 System in Drosophila: A Fly Geneticist's Swiss Army Knife." *Genesis (New York, N.Y.: 2000)* 34 (1–2): 1–15. https://doi.org/10.1002/gene.10150.

Estes, Patricia S., Ashley Boehringer, Rebecca Zwick, Jonathan E. Tang, Brianna Grigsby, and Daniela C. Zarnescu. 2011. "Wild-Type and A315T Mutant TDP-43 Exert Differential

Neurotoxicity in a Drosophila Model of ALS." *Human Molecular Genetics* 20 (12): 2308–21. https://doi.org/10.1093/hmg/ddr124.

Gkogkas, Christos, Susan Middleton, Anna M Kremer, Caroline Wardrope, Matthew Hannah, Thomas H Gillingwater, and Paul Skehel. 2008. "VAPB Interacts with and Modulates the Activity of ATF6." *Hum. Mol. Genet.* 17 (11): 1517–26.

Kabashi, Edor, Hajer El Oussini, Valérie Bercier, François Gros-Louis, Paul N. Valdmanis, Jonathan McDearmid, Inge A. Mejier, et al. 2013. "Investigating the Contribution of VAPB/ALS8 Loss of Function in Amyotrophic Lateral Sclerosis." *Human Molecular Genetics* 22 (12): 2350–60. https://doi.org/10.1093/hmg/ddt080.

Kanekura, Kohsuke, Ikuo Nishimoto, Sadakazu Aiso, and Masaaki Matsuoka. 2006. "Characterization of Amyotrophic Lateral Sclerosis-Linked P56S Mutation of Vesicle-Associated Membrane Protein-Associated Protein B (VAPB/ALS8)." *J. Biol. Chem.* 281 (40): 30223–33.

Larroquette, Frédérique, Lesley Seto, Perrine L. Gaub, Brishna Kamal, Deeann Wallis, Roxanne Larivière, Joanne Vallée, Richard Robitaille, and Hiroshi Tsuda. 2015. "Vapb/Amyotrophic Lateral Sclerosis 8 Knock-in Mice Display Slowly Progressive Motor Behavior Defects Accompanying ER Stress and Autophagic Response." *Human Molecular Genetics* 24 (22): 6515. https://doi.org/10.1093/hmg/ddv360.

Lee, Amy S. 2005. "The ER Chaperone and Signaling Regulator GRP78/BiP as a Monitor of Endoplasmic Reticulum Stress." *Methods* 35 (4): 373–81. https://doi.org/10.1016/j.ymeth.2004.10.010.

Madabattula, Surya T., Joel C. Strautman, Andrew M. Bysice, Julia A. O'Sullivan, Alaura Androschuk, Cory Rosenfelt, Kacy Doucet, Guy Rouleau, and Francois Bolduc. 2015. "Quantitative Analysis of Climbing Defects in a Drosophila Model of Neurodegenerative Disorders." *Journal of Visualized Experiments: JoVE*, no. 100 (June): e52741. https://doi.org/10.3791/52741.

Mitne-Neto, M, C R R Ramos, D C Pimenta, J S Luz, A L Nishimura, F A Gonzales, C C Oliveira, and M Zatz. 2007. "A Mutation in Human VAP-B–MSP Domain, Present in ALS Patients, Affects the Interaction with Other Cellular Proteins." *Protein Expr. Purif.* 55 (1): 139–46.

Mitne-Neto, Miguel, Marcela Machado-Costa, Maria C.N. Marchetto, Mario H. Bengtson, Claudio A. Joazeiro, Hiroshi Tsuda, Hugo J. Bellen, et al. 2011. “Downregulation of VAPB Expression in Motor Neurons Derived from Induced Pluripotent Stem Cells of ALS8 Patients.” *Human Molecular Genetics* 20 (18): 3642–52. https://doi.org/10.1093/hmg/ddr284.

Moustaqim-Barrette, Amina, Yong Q Lin, Sreeparna Pradhan, Gregory G Neely, Hugo J Bellen, and Hiroshi Tsuda. 2014. “The Amyotrophic Lateral Sclerosis 8 Protein, VAP, Is Required for ER Protein Quality Control.” *Hum. Mol. Genet.* 23 (8): 1975–89.

Murphy, Sarah E, and Tim P Levine. 2016. “VAP, a Versatile Access Point for the Endoplasmic Reticulum: Review and Analysis of FFAT-like Motifs in the VAPome.” *Biochim. Biophys. Acta* 1861 (8 Pt B): 952–61.

Nishimura, Yuhei, Masaaki Hayashi, Hiroyasu Inada, and Toshio Tanaka. 1999. “Molecular Cloning and Characterization of Mammalian Homologues of Vesicle-Associated Membrane Protein-Associated (VAMP-Associated) Proteins.” *Biochemical and Biophysical Research Communications* 254 (1): 21–26. https://doi.org/10.1006/bbrc.1998.9876.

Pennetta, Giuseppa, Peter Robin Hiesinger, Ruth Fabian-Fine, Ian A Meinertzhagen, and Hugo J Bellen. 2002. “Drosophila VAP-33A Directs Bouton Formation at Neuromuscular Junctions in a Dosage-Dependent Manner.” *Neuron* 35 (2): 291–306.

Piper, Matthew D. W., and Linda Partridge. 2016. “Protocols to Study Aging in Drosophila.” *Methods in Molecular Biology (Clifton, N.J.)* 1478: 291–302. https://doi.org/10.1007/978-1-4939-6371-3_18.

Rai, Mamta, Michelle Curley, Zane Coleman, Anjana Nityanandam, Jianqin Jiao, Flavia A. Graca, Liam C. Hunt, and Fabio Demontis. 2021. “Analysis of Proteostasis during Aging with Western Blot of Detergent-Soluble and Insoluble Protein Fractions.” *STAR Protocols* 2 (3): 100628. https://doi.org/10.1016/j.xpro.2021.100628.

Ratnaparkhi, Anuradha, George M Lawless, Felix E Schweizer, Peyman Golshani, and George R Jackson. 2008. “A Drosophila Model of ALS: Human ALS-Associated Mutation in VAP33A Suggests a Dominant Negative Mechanism.” *PLoS One* 3 (6): e2334.

Reis-Rodrigues, Pedro, Gregg Czerwieniec, Theodore W. Peters, Uday S. Evani, Silvestre Alavez, Emily A. Gaman, Maithili Vantipalli, et al. 2012. “Proteomic Analysis of Age-

Dependent Changes in Protein Solubility Identifies Genes That Modulate Lifespan." *Aging Cell* 11 (1): 120–27. https://doi.org/10.1111/j.1474-9726.2011.00765.x.

Suzuki, Hiroaki, Kohsuke Kanekura, Timothy P Levine, Kenji Kohno, Vesa M Olkkonen, Sadakazu Aiso, and Masaaki Matsuoka. 2009. "ALS-Linked P56S-VAPB, an Aggregated Loss-of-Function Mutant of VAPB, Predisposes Motor Neurons to ER Stress-Related Death by Inducing Aggregation of Co-Expressed Wild-Type VAPB." *J. Neurochem.* 108 (4): 973–85.

Szegezdi, Eva, Susan E Logue, Adrienne M Gorman, and Afshin Samali. 2006. "Mediators of Endoplasmic Reticulum Stress-induced Apoptosis." *EMBO Reports* 7 (9): 880–85. https://doi.org/10.1038/sj.embor.7400779.

Tendulkar, S, S Hegde, L Garg, and others. 2022. "Caspar, an Adapter for VAPB and TER94, Modulates the Progression of ALS8 by Regulating IMD/NFκB Mediated Glial Inflammation in a Drosophila Model of Human …." *Hum. Mol. Genet.*

Teuling, Eva, Suaad Ahmed, Elize Haasdijk, Jeroen Demmers, Michel O Steinmetz, Anna Akhmanova, Dick Jaarsma, and Casper C Hoogenraad. 2007. "Motor Neuron Disease-Associated Mutant Vesicle-Associated Membrane Protein-Associated Protein (VAP) B Recruits Wild-Type VAPs into Endoplasmic Reticulum-Derived Tubular Aggregates." *Journal of Neuroscience* 27 (36): 9801–15.

Tsakiri, Eleni N., Gerasimos P. Sykiotis, Issidora S. Papassideri, Vassilis G. Gorgoulis, Dirk Bohmann, and Ioannis P. Trougakos. 2013. "Differential Regulation of Proteasome Functionality in Reproductive vs. Somatic Tissues of Drosophila during Aging or Oxidative Stress." *The FASEB Journal* 27 (6): 2407–20. https://doi.org/10.1096/fj.12-221408.

Tsuda, Hiroshi, Sung Min Han, Youfeng Yang, Chao Tong, Yong Qi Lin, Kriti Mohan, Claire Haueter, et al. 2008. "The Amyotrophic Lateral Sclerosis 8 Protein VAPB Is Cleaved, Secreted, and Acts as a Ligand for Eph Receptors." *Cell* 133 (6): 963–77.

Vitale, Milena, Anush Bakunts, Andrea Orsi, Federica Lari, Laura Tadè, Alberto Danieli, Claudia Rato, et al. 2019. "Inadequate BiP Availability Defines Endoplasmic Reticulum Stress." Edited by Peter Walter and Randy Schekman. *ELife* 8 (March): e41168. https://doi.org/10.7554/eLife.41168.

Yadav, Shweta, Rajan Thakur, Plamen Georgiev, Senthilkumar Deivasigamani, Harini K, Girish Ratnaparkhi, and Padinjat Raghu. 2017. “RDGBα Localization and Function at a Membrane Contact Site Is Regulated by FFAT/VAP Interactions.” *Journal of Cell Science*, January, jcs.207985. https://doi.org/10.1242/jcs.207985.

# Chapter 3

# Modulation of VAP aggregation by *Caspar* and *Ter94*

**Ter94 and Caspar**

VCP (Valosin Containing Protein) is a type II AAA ATPase, involved in the segregation of misfolded aggregates and feeding them into the proteasome (Neuwald et al. 1999). VCP plays a critical role in recognizing and removing ubiquitinated proteins from membranes, aggregates and chromatin. It can modulate their states of ubiquitination or deubiquitination and enhance their degradation by autophagic pathways or UPS. VCP is expressed ubiquitously (Koller and Brownstein 1987) and can bind with a variety of cofactors enabling it to modulate many different pathways, including ERAD, Autophagy, NF-κB activation, Chromatin–associated degradation and membrane fusion (Hill et al. 2021; Latterich, Fröhlich, and Schekman 1995; Fessart et al. 2013). Mutations in VCP are associated with a number of disorders, including cancers (Costantini et al. 2021), Inclusion Body Myopathy with early-onset Paget disease and Frontotemporal Dementia (IBMPFD) (Watts et al. 2004) and ALS. About 1% of fALS cases are due to mutations in the *VCP* gene (Johnson et al. 2010). The *Drosophila* homologue of *VCP*, *ter94*, was found to modulate polyQ induced neurodegeneration in a fly model (Higashiyama et al. 2002). *Ter94* has also been found to mediate the degeneration associated with *caz* and *TBPH*. (Azuma et al. 2014; Kushimura et al.,2018) The overexpression of $ter94^{R152H}$ and $ter94^{A229E}$, the *Drosophila* orthologues of the human mutations, causes toxicity and degeneration, which is mediated by TDP-43 and its mislocalization (Ritson et al. 2010).

*Caspar* is the *Drosophila* homologue of human *FAF1* (Fas Associated Factor 1) which is a known modulator of the apoptotic pathways. *FAF1* has also been identified as a suppressor of the NF-κB pathway through preventing the translocation of the nuclear factor p65 (Park et al. 2004) and also the suppression of the IκB Kinase (IKK) activation (Park et al. 2007). FAF1 is also known to interact with polyubiquitinated proteins through its N terminal UBA domain and the p97/VCP through its UBX domain (Fig 3.1 A) and was thought to act as a scaffold

for the ubiquitin proteasomal system (Song et al. 2005; Ewens et al. 2014). *FAF1* has also been demonstrated to promote the ERAD via a complex involving FAF1,VCP, Npl4, Ufd1 and polyubiquitinated proteins (Lee et al. 2013). FAF1 is also known to interact with VAP through its FFAT motif (Baron et al. 2014)

FAF1 and Caspar share a high sequence similarity with each other (Fig 3.4A). Caspar was found to act as a negative regulator of immunity in *Drosophila* via the IMD pathway by suppressing the nuclear translocation of Relish (Kim et al. 2006).

**The VAP-Caspar-VCP axis**

We have previously demonstrated that Ter94 is an interactor of the Caspar and Caspar interacts with VAP through its FFAT domain (Fig 3.1). Given the association of VCP with the ERAD, autophagic and proteostatic pathways for clearance and regulation of misfolded proteins, the Caspar-VAP- Ter94 axis became a target for us to check for the modulation of VAP aggregation. Further, we have observed that there is a rescue of lifespan associated with the glial overexpression of Caspar and TER94 mutants (Tendulkar et al. 2022). These observations prompted us to study VAP aggregation backgrounds where we modulated *Caspar* and *VCP* levels.

.

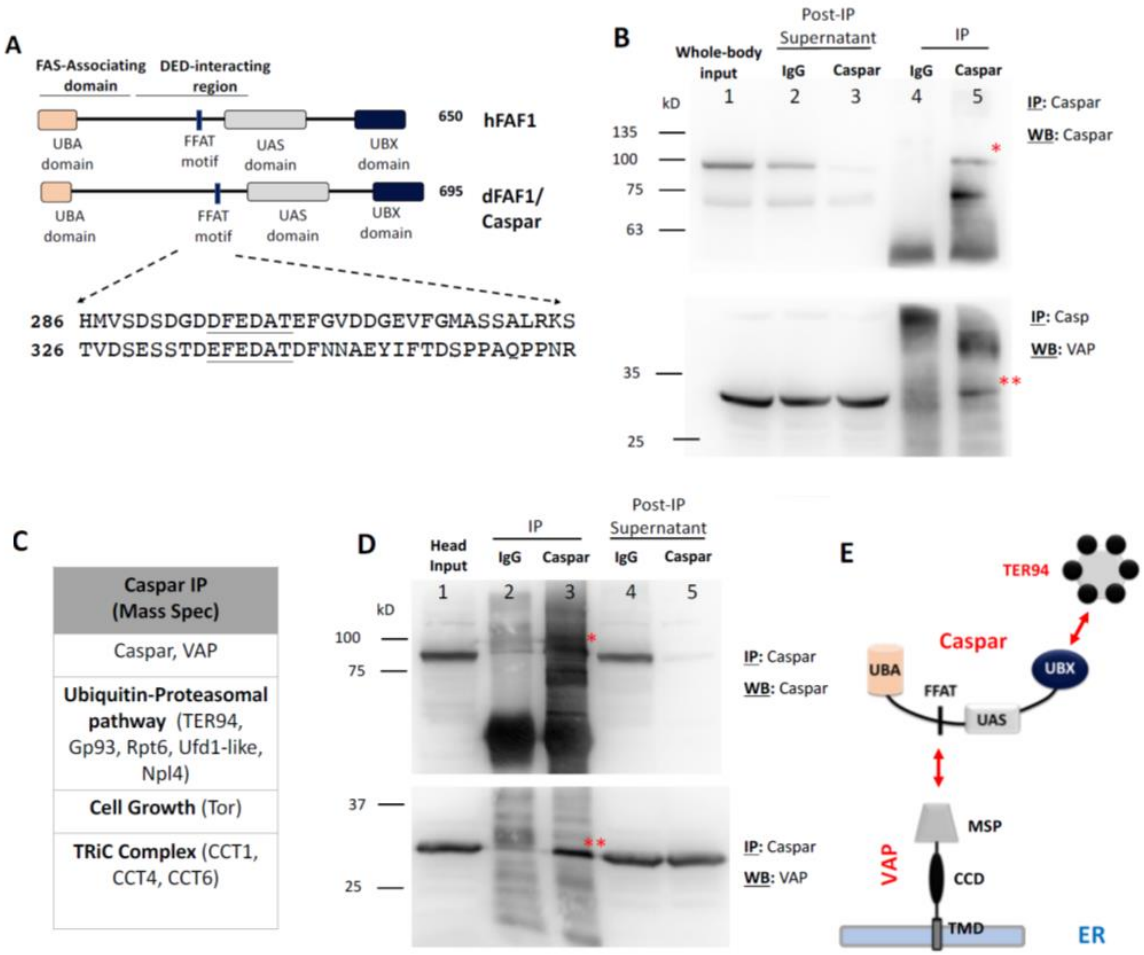


***Figure 3.1: Caspar, a Drosophila homologue of human FAF1, interacts with VAP and Ter94.***

A. Drosophila Caspar is an ortholog of human FAF1. The conserved N-terminal Ub-interacting and C-terminal Ter94 interacting domains suggest roles for Caspar as an adapter in the proteasomal degradation. A conserved FFAT motif (amino acids underlined), which is a well characterized VAP interactor is present in both polypeptides. This suggests that FFAT motif in Caspar may be the interface for an interaction with VAP.

B. Caspar antibody, previously generated and validated in the lab has been used to study interactions. When used for immunoprecipitation (IP) of whole animal lysates, the Rabbit Caspar antibody could affinity purify Caspar (*, 90 kD, lane 5, top panel) and also VAP (**, 25 kD, lane 5, bottom Panel). A concomitant decrease in Caspar in the supernatant (lane 3, top panel) is also seen, post IP. The ~70 kD reactive band is a feature of Caspar westerns.

C. Ter94, Gp93, Rpt6, Tor, CCT1 and CCT4 are detected by Mass Spectrometry in the Caspar antibody immune precipitates, using whole-body and embryonic lysates. Many of these are functionally associated with the ubiquitin-proteasomal system (UPS).

D. Caspar immune-precipitates using fly head lysates confirm that Caspar (*) is expressed in the head and can be enriched by the Caspar antibody (lane 3, top panel). Also, VAP (**) is a Caspar

interactor (lane3, bottom panel). A concomitant decrease in Caspar in the supernatant (lane 5, top panel) is seen, post IP.

E. A model for the interaction of VAP, an ER resident membrane protein, with cytoplasmic Caspar. Mass spectrometry interaction data suggests that ter94 and other proteins of the UPS are part of Caspar protein:protein interaction network in the cell.

***Figure from Tendulkar, Thulasidharan et al, 2022.***

**Results:**

1) Modulation of *Caspar* levels in the glia does not change VAP aggregation density. *Caspar* is the *Drosophila* homologue of *FAF1* and shares a high sequence similarity with FAF1. FAF1 acts as an adaptor for p97 via its UBX domain and polyubiquitinated proteins via its UBA domain (Lee et al. 2013). Previous studies from the lab had demonstrated that glial overexpression of *Caspar* strongly modulated lifespan and motor function in the null rescue model (Tendulkar et al. 2022). We hypothesized that *Caspar* plays a role in VAP aggregation, as FAF1 functions as an adapter for p97 or VCP through the UBX domain. In order to determine if glial Caspar levels affected VAP aggregation in the brain, we decided to look at adult fly brains of three age points, day 5, day 15 and day 30. We looked at the VAP aggregation density in three genotypes, $\Delta VAP;\ Repo>+;\ gVAP^{P58S}/+$ , $\Delta VAP;\ Repo>casp^{WT};\ gVAP^{P58S}/+$ and $\Delta VAP;\ Repo>casp^{RNAi};\ gVAP^{P58S}/+$ (Fig 3.2 A-I ). We do not see a significant change in aggregation density between any set (Fig 3.2 J-L, non-significant, one-way ANOVA followed by Tukey's multiple comparisons). Our result seems to indicate that glial overexpression of *Caspar* does not play a role in modulating VAP aggregation in the brain. This result indicated that lifespan and motor function rescue, seen in the glial overexpression may be the result of alternative pathways, such as ER stress or inflammation, being affected.

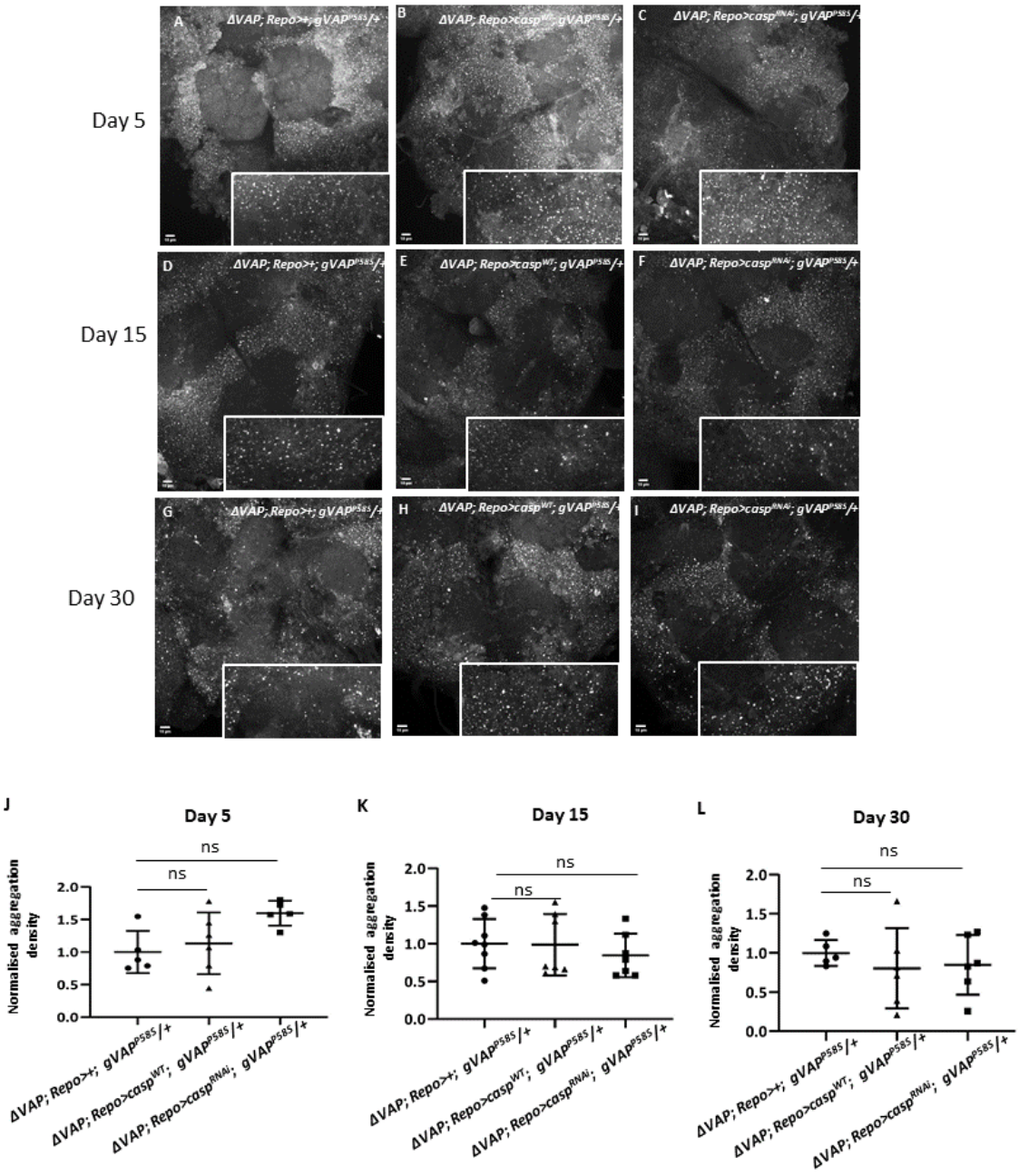


***Figure 3.2: VAP aggregation density in the brain of adult animals does not vary with Caspar levels.***

Representative images of VAP protein inclusions in adult brains for days 5, 15 and 30. The inclusions are marked with an anti-VAP antibody. The inclusions are seen more clearly in the inserted panel for each image (2X digital zoom).

**A,D,G**. Δ*VAP; Repo>+; gVAP*$^{P58S}$/+.

**B,E,H**. Δ*VAP; Repo>casp*$^{WT}$*; gVAP*$^{P58S}$/+

**C,F,I**. Δ*VAP; Repo>casp*$^{RNAi}$*; gVAP*$^{P58S}$/+

**J-O**. Graphical representation of normalised 'aggregate density' (J-L) and normalised 'aggregate volume' (M-O) of VAP inclusions. The genotypes compared are Δ*VAP;*

*Repo>+; gVAP*$^{P58S}$ /+ (control), Δ*VAP; Repo>casp*$^{WT}$*; gVAP*$^{P58S}$, and Δ*VAP; Repo>casp*$^{RNAi}$*; gVAP*$^{P58S}$. n= 5-10 brain samples. One-way ANOVA followed by Tukey's multiple comparison (*P<0.05, ***P<0.001, ****P<0.0001; ns, not significant). Error bars indicate SD. Scale bar denotes 10 μm.

2) Modulation of *Caspar* levels in the glia does not rescue BiP aggregation.

ER stress has been previously identified in the null rescue system by our lab as well as in VAP nulls in other studies (Moustaqim-Barrette et al. 2014). We also observed an amelioration in BiP aggregation in the rescue associated with the *VAP*$^{WT}$ in the *VAP*$^{P58S}$ background. *FAF1* is involved in the ERAD, through the VCP-Npl4-Ufd1 complex (Lee et al. 2013). We wondered if the rescue in lifespan and motor defects indicate a rescue in BiP aggregation in the glial *Caspar* overexpression lines. We tested this out by staining the brains of 15 day old flies of the CS , Δ*VAP; Repo>+; gVAP*$^{P58S}$/+and Δ*VAP; Repo>casp*$^{WT}$*; gVAP*$^{P58S}$/+ with BiP antibody to observe BiP aggregation density (Fig. 3.3 A-C). We observe a negligible number of aggregates in the *CS* flies (Fig 3.3 A). We observe a high density of BiP aggregation in the Δ*VAP; Repo>+; gVAP*$^{P58S}$/+ sample, similar to that observed in the Δ*VAP; gVAP*$^{P58S}$/+ line previously. We do not see a significant difference in aggregation density between this and the Δ*VAP; Repo>casp*$^{WT}$*; gVAP*$^{P58S}$/+ (Fig3.3 D, ns, Mann-Whitney). From this, we conclude that higher levels of glial *Caspar* does not affect BiP aggregation density.

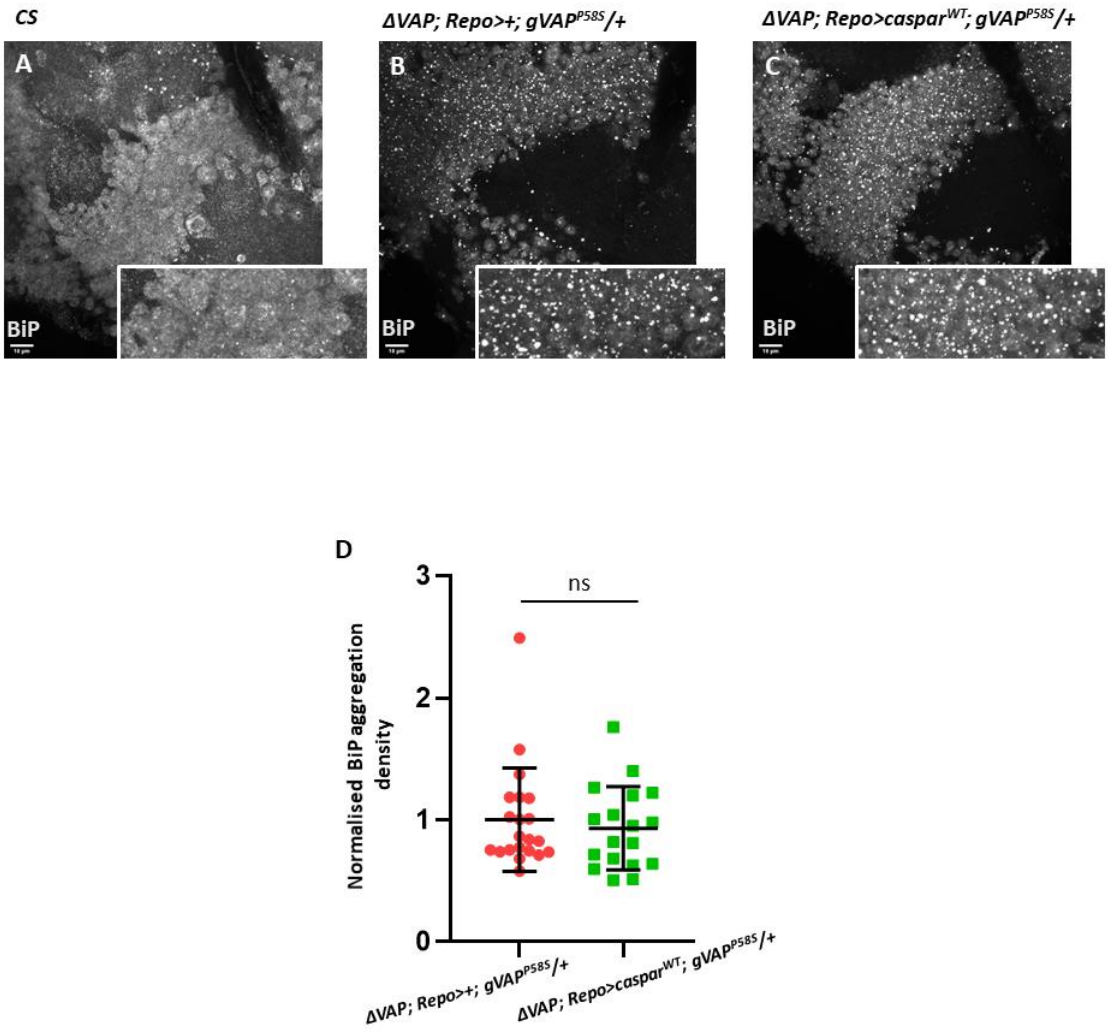


***Figure 3.3: Modulation of Caspar levels in the glia does not rescue BiP aggregation.***
Representative MIP images of the brains of 15 day old *CS* (A), *ΔVAP;Repo>+;gVAP*$^{P58S}$/+ (B) and *ΔVAP ;Repo>caspar*$^{WT}$*;gVAP*$^{P58S}$/+ (C) fly brains stained with BiP antibody. CS(A) shows negligible BiP punctae. The normalized BiP aggregation density for both the *ΔVAP;Repo>+;gVAP*$^{P58S}$/+ and *ΔVAP; Repo>caspar*$^{WT}$*;gVAP*$^{P58S}$/+ is similar to each other (D) (ns, non-significant. Mann-Whitney Test. Error bars represent SD). Scale bar denotes 10µm.

3) Modulation of *Caspar* levels in the neurons does not affect VAP aggregation density.

The glial population comprises around 5 -10% of the total cell population in the brain. Due to their number being small, it may be possible that we are unable to observe a global reduction in VAP aggregation. In order to confirm that *Caspar* levels does not affect VAP aggregation, we overexpressed *Caspar* in the neurons using the ELAV driver. Similar to the previous experiments, we compared the brains of 15 day old flies of the genotypes

*ΔVAP;Elav>casp$^{WT}$;gVAP$^{P58S}$/+*, *ΔVAP;Elav>+;gVAP$^{P58S}$/+* and *ΔVAP;Elav>casp$^{RNAi}$;gVAP$^{P58S}$/+* (Fig 3.4 A-C). We do not see a difference in the VAP aggregation densities between these three genotypes (Fig 3.4 D, non-significant, Kruskal-Wallis followed by Dunn's multiple comparisons). From this, we conclude that the Caspar levels in the brain does not appear to affect VAP aggregation density.

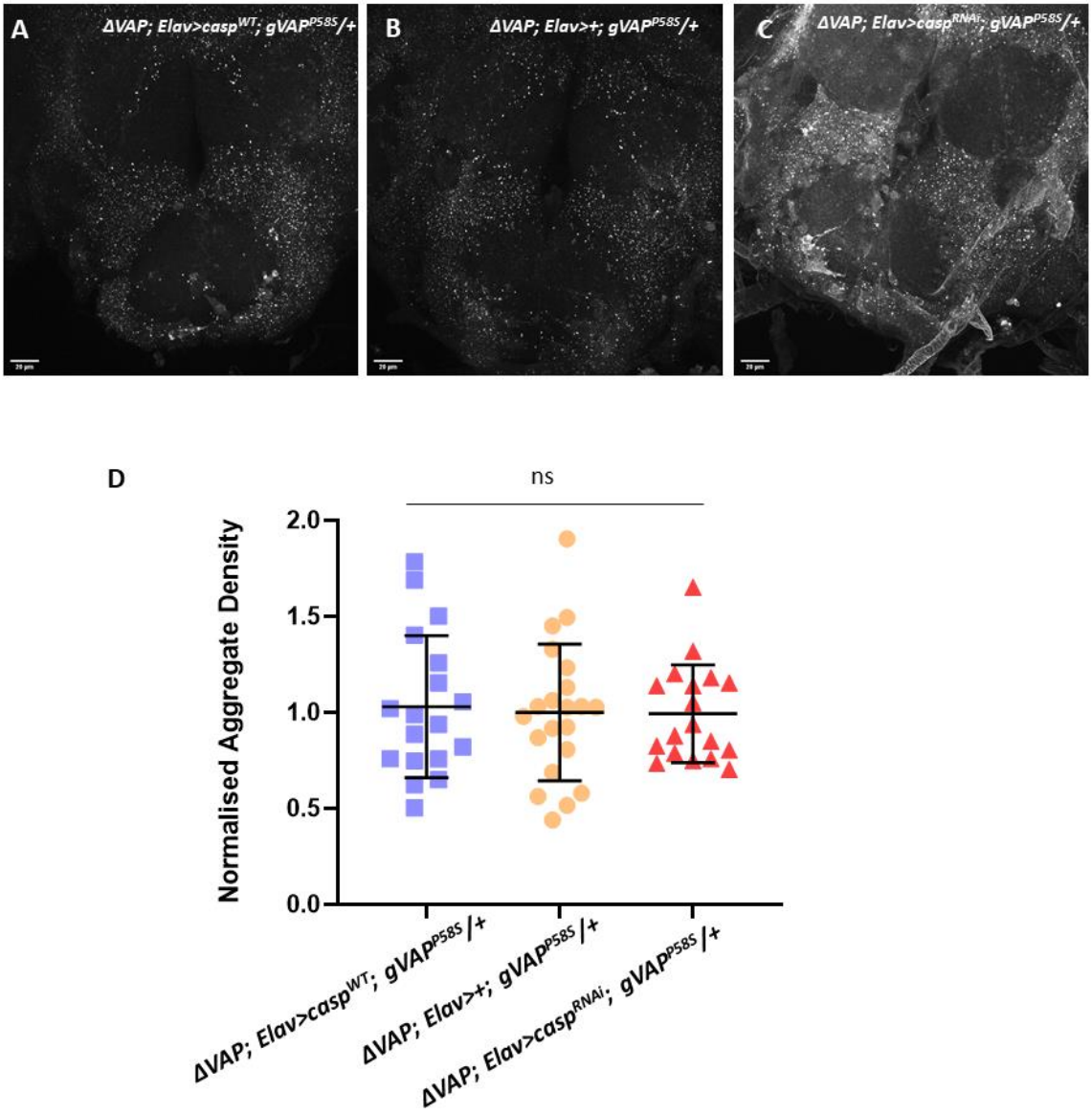


***Figure 3.4: Modulation of Caspar levels in the neurons does not affect VAP aggregation density.***

Representative MIP images of the brains of 15 day old ΔVAP; Elav>casp$^{WT}$;gVAP$^{P58S}$/+ (A) , ΔVAP;Elav>+;gVAP$^{P58S}$/+ (B) and ΔVAP; Elav>casp$^{RNAi}$;gVAP$^{P58S}$/+ (C) fly brains stained with VAP antibody. The aggregation density is similar for all three genotypes (D) (Kruskal-wallis followed by Dunn's multiple comparisons. Error bars represent SD). Scale bar denotes 20µm.

.

4) Knocking down *dVCP* in the neurons reduces VAP aggregation.

VCP is a known component of the ERAD pathway and is involved in the removal of misfolded proteins (Lee et al. 2013). *Ter94* is also a genetic interactor of VAP as understood from studies done previously in the lab. Ter94 was demonstrated to be present in complex with Caspar and VAP (Fig 3.1 C). All of these observations led us into investigating if *Ter94* was a modifier of $VAP^{P58S}$ aggregation. Our first experiment sought to understand if removal of Ter94 would affect the aggregation density of $VAP^{P58S}$ in a null rescue model. For this, we chose to compare the VAP aggregation in a background where *Ter94* was knocked down in the neurons using the ELAV driver (*ΔVAP; Elav>Ter94$^{RNAi}$; gVAP$^{P58S}$/+* , Fig 3.5 B) with aggregation seen in the null *VAP$^{P58S}$* background (*ΔVAP; Elav>+; gVAP$^{P58S}$/+* , Fig 3.5 A). We observed a sharp decrease in aggregation density in the *Ter94* neuronal knockdown (Fig 3.5 C). This result indicates that Ter94 is indeed a player in the regulation of VAP aggregation.

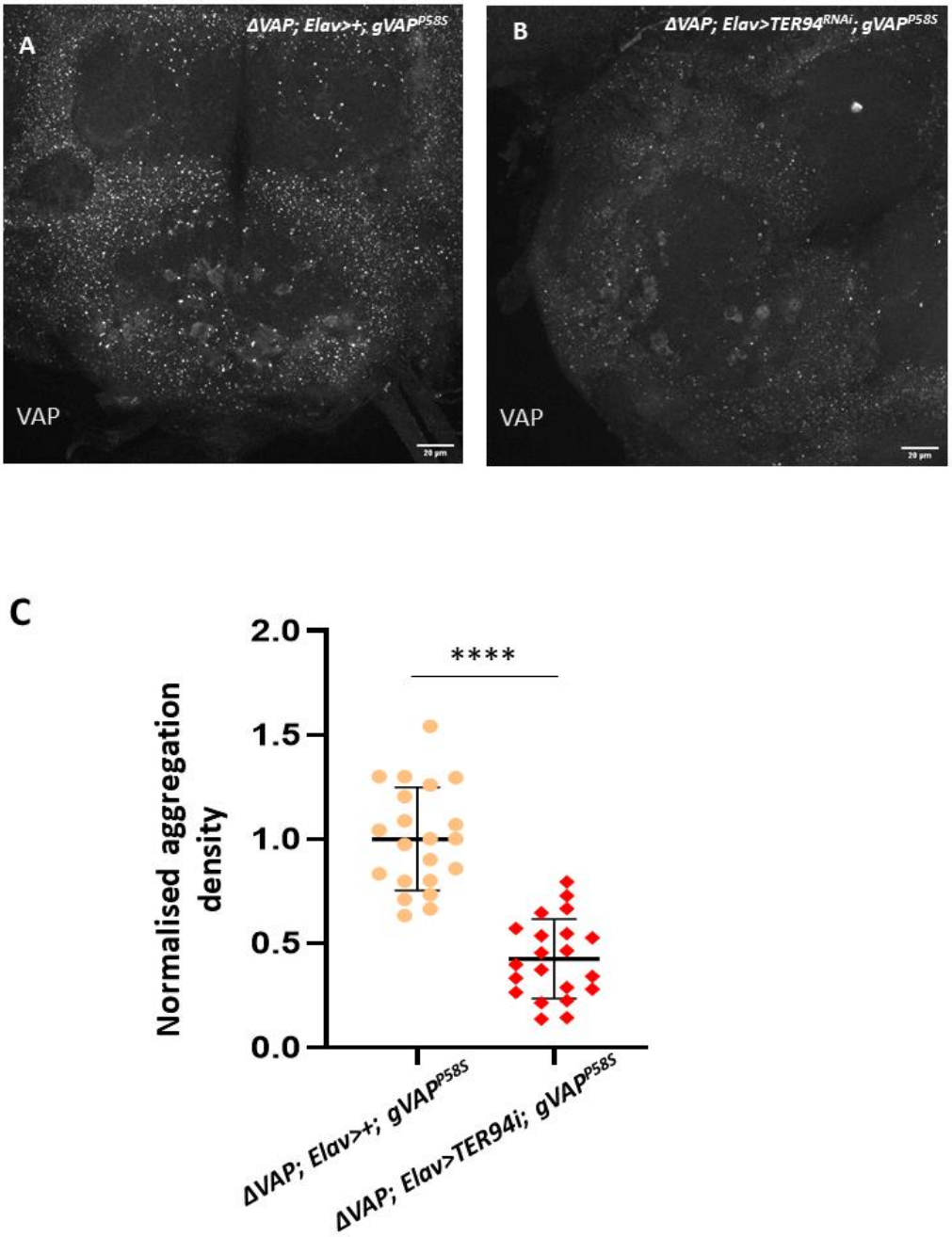


***Figure 3.5: Knocking down dVCP (Ter94) in the neurons reduces VAP aggregation.*** Representative MIP images of the brains of *ΔVAP; Elav/+;gVAP$^{P58S}$/+* (A) and *ΔVAP; Elav>Ter94$^{RNAi}$;gVAP$^{P58S}$/+* (B) stained with VAP antibody. The aggregation density in the *Ter94* neuronal knockdown is significantly reduced (C) (****P< 0.0001, Mann-Whitney Test. Error bars represent SD). Scale bar denotes 20µm.

5) Overexpressing *Ter94$^{R152H}$* neuronally increases VAP aggregation

Knocking down *Ter94* neuronally was seen to reduce VAP aggregation density, indicating that *Ter94* function is needed in some way to regulate VAP aggregation. Following this

observation, it was necessary to understand how overexpression of *Ter94* in the neurons would affect VAP aggregation (Fig 3.6 B). Upon comparing the neuronal overexpression line with the null rescue control (Fig 3.6 A) we see the aggregation appear to increase mildly (Fig 3.6 D, *P=0.0250, Kruskal Wallis Test). From this observation, the wild-type appears to be supporting the aggregation of VAP in some way.

The $VCP^{R155H}$ mutant is a known ALS associated mutation (Johnson et al. 2010) and the $Ter94^{R152H}$ is the homologous mutation in *Drosophila*. A *Drosophila* model developed for studying IBMPFD shows that the $Ter94^{R152H}$ shows degenerative phenotypes that appear to be enhanced in the presence of the wild-type (dominant active) (Chang et al. 2011). We have also observed that overexpressing this mutation in the glia extends the lifespan of the $\Delta VAP;Repo/+;gVAP^{P58S}/+$ line (Tendulkar et al. 2022). To understand the effect this mutation had on VAP aggregation, we overexpressed the mutant neuronally and compared the aggregation with the $\Delta VAP;;gVAP^{P58S}$ control. We observed a significantly higher density of VAP aggregation (Fig 3.6 D, ***P=0.0002).

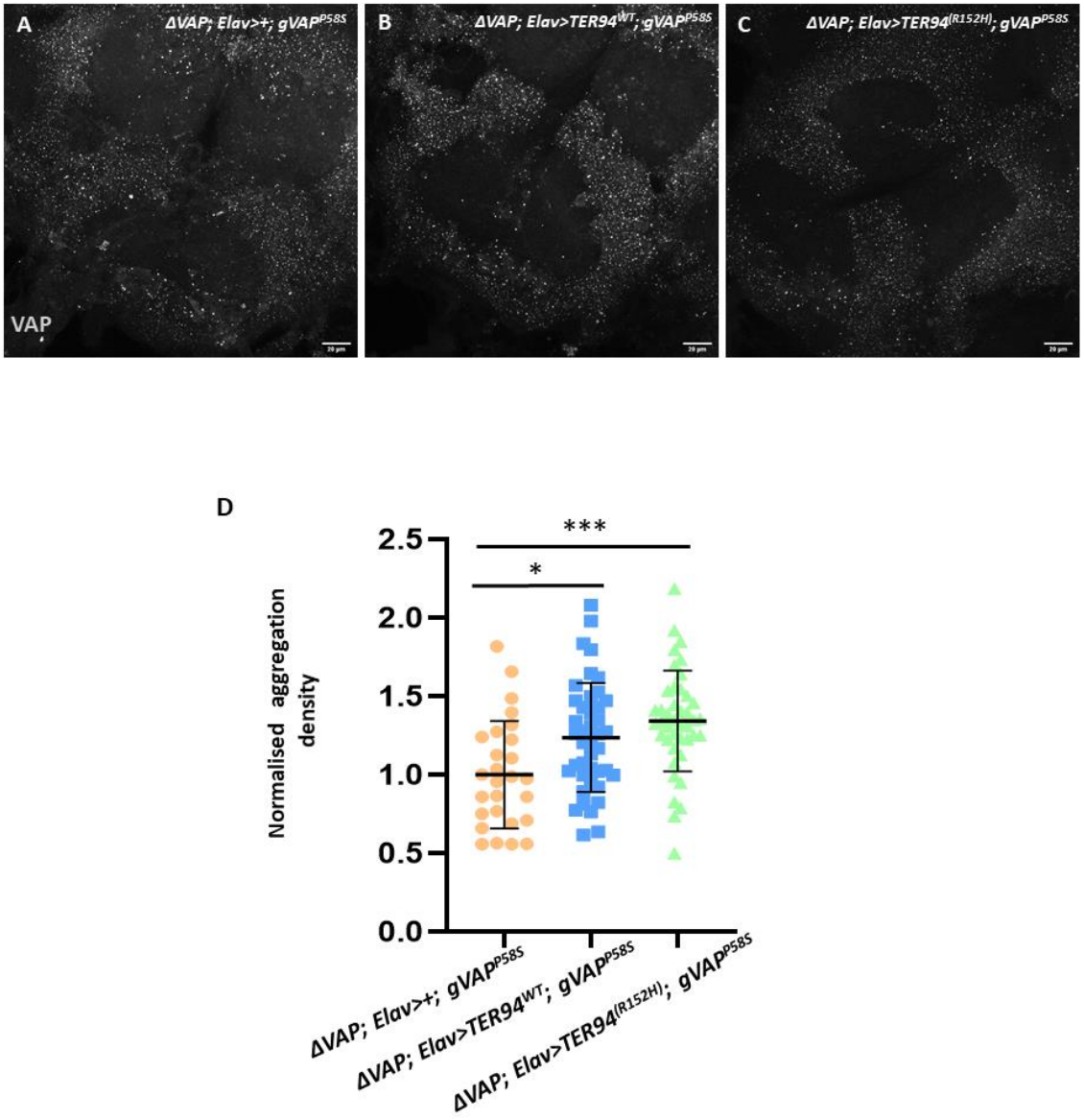


***Figure 3.6: Overexpressing Ter94$^{R152H}$ neuronally increases VAP aggregation.***
Representative MIP images of the brains of 15 day old *ΔVAP;Elav/+;gVAP$^{P58S}$/+* (A), *ΔVAP;Elav>Ter94$^{WT}$;gVAP$^{P58S}$/+* (B) and *ΔVAP;Elav>Ter94$^{R152H}$;gVAP$^{P58S}$/+* (C) fly brains stained with VAP antibody. The aggregation density for both the *Ter94$^{WT}$* and *Ter94$^{R152H}$* neuronal overexpression is higher than that observed in the control (D) (*P=0.0250,***P=0.0002, Kruskal-wallis followed by Dunn's multiple comparisons. Error bars represent SD). Scale bar denotes 20µm.

## Discussion

The UPS has been previously implicated in the clearance of VAP aggregates. VAP aggregates have been found to be ubiquitinated and some studies indicating that the protein clearing pathways are not affected by the VAP (P56S) mutation (Genevini et al. 2014) and that clearance of ER domains restructured by the mutant are removed by the proteasome (Papiani et al. 2012). Our lab has also previously demonstrated the role of the UPS in clearing VAP aggregation via *SOD1* and *TOR* dependent mechanisms (Chaplot et al. 2019). VAP was previously shown to interact with FAF1 through its FFAT motif (Baron et al. 2014) and this interaction was hypothesized to play a role in the clearance of VAP aggregates. Our studies in the null rescue model demonstrated a physical interaction between Caspar and VAP, with glial overexpression of *Caspar* rescuing lifespan defects in the null rescue model (Tendulkar et al. 2022). In order to identify if VAP aggregation was affected by this interaction with Caspar, we stained and analyzed the fly brains for VAP aggregation. We did not observe changes in VAP aggregation density with a variation in *Caspar* levels. The *Caspar* levels also did not appear to affect BiP aggregation density, implying that the rescue was not a result of reduced ER stress either. Taken together, proteasomal clearance and ER stress were understood to not be major reasons behind the observed functional rescues.

FAF1 is capable of interacting with p97 through its UBX domain This interaction opens up the possibility of p97 interacting with VAP through a FAF1-VAP-p97 complex (Baron et al. 2014). p97(or VCP) is also an ALS locus. The ALS associated mutations are known to affect VCP's interaction with the 20S proteasome (Barthelme, Jauregui, and Sauer 2015). Our results with *Ter94* indicate that *Ter94* or *dVCP* is a strong modulator of VAP aggregation. Contrary to what is seen with TDP-43 aggregates (Ritson et al. 2010), knocking down *Ter94* reduces VAP aggregates, while overexpressing either the wild-type or the ALS associated Drosophila mutant R152H increases the VAP aggregation density. This seems to indicate that Ter94 is needed for the maintenance of the VAP aggregate. How this is achieved is not very clear at this point. Ter94 is involved in several regulatory pathways, including the ERAD (Elkabetz et al. 2004), UPS and autophagic pathways (Ju et al. 2009). *VCP* knockdown has been found to induce UPS in mammalian cells (Wójcik et al. 2006) and this might be a possible mechanism for the removal of VAP aggregation. *VCP* is also associated with organization of the ER (Shih and Hsueh 2016), this might also influence VAP aggregation density.

**Future direction**

Our results from the dVCP experiments opens out a wide array of questions to be followed up

1) ERAD and VAP aggregation: Both *VAP* and *VCP* have been implicated in the ERAD. We plan to target the TER94-Npl4-Ufd1 complex and identify if this would affect VAP aggregation.
2) Autophagy and aggregation: VCP has been found to be involved in autophagy and VAP is a known interactor of several components of the pathway. We have also seen possible evidence of VAP aggregation regulation via autophagy in our experiments in Chapter 4, thus we wish to understand this interaction as well.

**Acknowledgements**

Lovleen Garg is thanked for his assistance with the analysis of the glial Caspar overexpression images.

**Materials and methods**

## *Drosophila* maintenance and husbandry

All flies were grown on standard corn meal agar at 25 degrees Celsius. All crosses were set up at 25 degrees Celsius unless specified otherwise.

## *Drosophila* stocks and reagents

The flies expressing genomic $VAP^{WT}$ and genomic $VAP^{P58S}$ were a gift from Hiroshi Tsuda. These lines were balanced with a null line, *Δ166*, as described previously (Tendulkar et al. 2022).

The UAS -$VAP^{P58S}$ line was generated in the Jackson lab (Ratnaparkhi et al 2002). Canton S (0001) lines were procured from Bloomington Drosophila Stock Center (BDSC).

Lines used for Caspar: BL 44027(*UAS-*$Caspar^{RNAi}$) (BDSC), *UAS-*$Caspar^{WT}$ (NCBS)

Lines used for Ter94 experiments: BL 32869 (*UAS-*$dVCP^{RNAi}$) (BDSC), *UAS-*$dVCP^{WT}$*/CyO,* *UAS-*$dVCP^{R152H}$*/CyO* -courtesy J.P. Taylor, University of Pennsylvania (Ritson et al.,2010).

## Larval Ventral Nerve chord preparation

Wandering third-instar larvae were selected and dissected in 1X PBS. They were fixed in 4% PFA with 0.3% PBST for 20 minutes. Post fixation, the samples were washed thrice in 1X PBS and then transferred to a blocking solution (2% BSA in 0.3% PBST) for 1 hour,

followed by incubation in primary antibody for 1 overnight. This was followed by 3 washes with blocking, each lasting 20 minutes and then an overnight incubation with the secondary antibody. Post-secondary, the samples are washed thrice with blocking, each lasting 20 minutes. DAPI is added to the second wash to visualize cell nuclei. Samples are given one final wash in PBS before mounting in anti-fade mounting media.

## Adult brain dissections

Flies of the desired genotype are collected and aged to the requirement. Adult brains are dissected out into cold 1X PBS, followed by a 24-hour fixation in 1.2% PFA at 4 degrees Celsius. This is followed by permeabilization in 5% PBST (2 washes for 20 minutes each) followed by 2 washes in PAT buffer (30 minutes each). Samples were then blocked in 5% BSA in 0.5% PBST for two hours. This was followed by incubation in primary antibodies for 36 hours at 4 degrees Celsius. Post-primary incubation, 4 PAT buffer washes, each lasting 30 minutes, are administered. Samples are then incubated in secondary antibodies for 36 hours. This is followed by another 4 PAT buffer washes (30 minutes each). DAPI (1:1000) is added in the second wash to visualize nuclei. This is followed by a wash in 1X PBS and subsequently stored in PBS with Vectashield mounting media in a 1:1 ratio at 4 degrees Celsius for 12 hours.
For mounting, samples are placed with the antennal lobes facing the coverslip. Samples are bridge-mounted. We have used SlowFade mounting medium (Vectashield, S36937).

Antibodies used: Rabbit Anti-BiP (1:200) (Cell signalling), Rat Anti-ELAV (DSHB; 1:100) and Rabbit Anti-VAP (1:500)(Yadav et al. 2017; Chaplot et al. 2019).

## Microscopy

Mounted samples were imaged using Zeiss LSM710 or Leica SP8 confocal microscopes with 63x objectives. Images were acquired at 16-bit depth as Z stacks. For larval ventral chords, the tip of the ventral cord was imaged at 1X zoom. For the adult brains, the main body of the brain was imaged at 0.75X zoom. Acquisition parameters were kept constant across experimental sets.

## Image analysis

We have used both ImageJ and Huygens Professional software for image segmentation and analysis. The analysis protocol is similar to that used in (Chaplot et al. 2019) with modifications for analysing adult brain images. A threshold is set to segment high intensity punctae from the background signal from the tissue. The threshold is manually adjusted for each genotype in order to segment punctae from the tissue background. Object filters were used to remove objects larger than 200 voxels and smaller than 8 voxels. The punctae were quantified per micrometre of the larval ventral nerve chord or the adult brain and this ratio has been defined as aggregation density. Three 3D ROIs were selected from each brain from the tip of the VNC (larval) or the sub oesophageal zone (SEZ) (adult) and measured. The aggregation density for each ROI was normalized to the mean value for the control group in each experiment. We have used 6 to 12 brains per genotype per experiment. ROI volume has been calculated as the range of the Z- stack of the image. The 3D objects calculator and Visikol plugin has been used in the case of ImageJ to count aggregates and calculate volume.

**References:**

Azuma, Yumiko, Takahiko Tokuda, Mai Shimamura, Akane Kyotani, Hiroshi Sasayama, Tomokatsu Yoshida, Ikuko Mizuta, et al. 2014. "Identification of Ter94, Drosophila VCP, as a Strong Modulator of Motor Neuron Degeneration Induced by Knockdown of Caz, Drosophila FUS." *Human Molecular Genetics* 23 (13): 3467–80. https://doi.org/10.1093/hmg/ddu055.

Baron, Yorann, Patrick G Pedrioli, Kshitiz Tyagi, Clare Johnson, Nicola T Wood, Daniel Fountaine, Melanie Wightman, and Gabriela Alexandru. 2014. "VAPB/ALS8 Interacts with FFAT-like Proteins Including the P97 Cofactor FAF1 and the ASNA1 ATPase." *BMC Biology* 12 (May): 39. https://doi.org/10.1186/1741-7007-12-39.

Barthelme, Dominik, Ruben Jauregui, and Robert T. Sauer. 2015. "An ALS Disease Mutation in Cdc48/P97 Impairs 20S Proteasome Binding and Proteolytic Communication." *Protein Science* 24 (9): 1521–27. https://doi.org/10.1002/pro.2740.

Chang, Ya-Chu, Wan-Tzu Hung, Yun-Chin Chang, Henry C. Chang, Chia-Lin Wu, Ann-Shyn Chiang, George R. Jackson, and Tzu-Kang Sang. 2011. "Pathogenic VCP/TER94 Alleles Are Dominant Actives and Contribute to Neurodegeneration by Altering Cellular ATP Level in a Drosophila IBMPFD Model." *PLoS Genetics* 7 (2): e1001288. https://doi.org/10.1371/journal.pgen.1001288.

Chaplot, Kriti, Lokesh Pimpale, Balaji Ramalingam, Senthilkumar Deivasigamani, Siddhesh S Kamat, and Girish S Ratnaparkhi. 2019. "SOD1 Activity Threshold and TOR Signalling Modulate VAP (P58S) Aggregation via Reactive Oxygen Species-Induced Proteasomal Degradation in a Drosophila Model of Amyotrophic Lateral Sclerosis." *Dis. Model. Mech.* 12 (2): dmm033803.

Costantini, Susan, Francesca Capone, Andrea Polo, Palmina Bagnara, and Alfredo Budillon. 2021. "Valosin-Containing Protein (VCP)/P97: A Prognostic Biomarker and Therapeutic Target in Cancer." *International Journal of Molecular Sciences* 22 (18): 10177. https://doi.org/10.3390/ijms221810177.

Elkabetz, Yechiel, Ilana Shapira, Efrat Rabinovich, and Shoshana Bar-Nun. 2004. "Distinct Steps in Dislocation of Luminal Endoplasmic Reticulum-Associated Degradation Substrates: ROLES OF ENDOPLASMIC RETICULUM-BOUND P97/Cdc48p AND PROTEASOME

*.” *Journal of Biological Chemistry* 279 (6): 3980–89. https://doi.org/10.1074/jbc.M309938200.

Ewens, Caroline A., Silvia Panico, Patrik Kloppsteck, Ciaran McKeown, Ima-Obong Ebong, Carol Robinson, Xiaodong Zhang, and Paul S. Freemont. 2014. “The P97-FAF1 Protein Complex Reveals a Common Mode of P97 Adaptor Binding *.” *Journal of Biological Chemistry* 289 (17): 12077–84. https://doi.org/10.1074/jbc.M114.559591.

Fessart, Delphine, Esther Marza, Saïd Taouji, Frédéric Delom, and Eric Chevet. 2013. “P97/CDC-48: Proteostasis Control in Tumor Cell Biology.” *Cancer Letters* 337 (1): 26–34. https://doi.org/10.1016/j.canlet.2013.05.030.

Genevini, Paola, Giulia Papiani, Annamaria Ruggiano, Lavinia Cantoni, Francesca Navone, and Nica Borgese. 2014. “Amyotrophic Lateral Sclerosis-Linked Mutant VAPB Inclusions Do Not Interfere with Protein Degradation Pathways or Intracellular Transport in a Cultured Cell Model.” *PLOS ONE* 9 (11): e113416. https://doi.org/10.1371/journal.pone.0113416.

Higashiyama, H., F. Hirose, M. Yamaguchi, Y. H. Inoue, N. Fujikake, A. Matsukage, and A. Kakizuka. 2002. “Identification of Ter94, Drosophila VCP, as a Modulator of Polyglutamine-Induced Neurodegeneration.” *Cell Death & Differentiation* 9 (3): 264–73. https://doi.org/10.1038/sj.cdd.4400955.

Hill, Sandra M., Lidia Wrobel, Avraham Ashkenazi, Marian Fernandez-Estevez, Keith Tan, Roland W. Bürli, and David C. Rubinsztein. 2021. “VCP/P97 Regulates Beclin-1-Dependent Autophagy Initiation.” *Nature Chemical Biology* 17 (4): 448–55. https://doi.org/10.1038/s41589-020-00726-x.

Johnson, Janel O., Jessica Mandrioli, Michael Benatar, Yevgeniya Abramzon, Vivianna M. Van Deerlin, John Q. Trojanowski, J. Raphael Gibbs, et al. 2010. “Exome Sequencing Reveals VCP Mutations as a Cause of Familial ALS.” *Neuron* 68 (5): 857–64. https://doi.org/10.1016/j.neuron.2010.11.036.

Ju, Jeong-Sun, Rodrigo A. Fuentealba, Sara E. Miller, Erin Jackson, David Piwnica-Worms, Robert H. Baloh, and Conrad C. Weihl. 2009. “Valosin-Containing Protein (VCP) Is Required for Autophagy and Is Disrupted in VCP Disease.” *The Journal of Cell Biology* 187 (6): 875–88. https://doi.org/10.1083/jcb.200908115.

Kim, Myungjin, Jun Hee Lee, Soo Young Lee, Eunhee Kim, and Jongkyeong Chung. 2006. "Caspar, a Suppressor of Antibacterial Immunity in Drosophila." *Proceedings of the National Academy of Sciences* 103 (44): 16358–63. https://doi.org/10.1073/pnas.0603238103.

Koller, Kerry J., and Michael J. Brownstein. 1987. "Use of a CDNA Clone to Identify a Supposed Precursor Protein Containing Valosin." *Nature* 325 (6104): 542–45. https://doi.org/10.1038/325542a0.

Kushimura, Yukie, Takahiko Tokuda, Yumiko Azuma, Itaru Yamamoto, Ikuko Mizuta, Toshiki Mizuno, Masanori Nakagawa, et al. n.d. "Overexpression of Ter94, Drosophila VCP, Improves Motor Neuron Degeneration Induced by Knockdown of TBPH, Drosophila TDP-43."

Latterich, Martin, Kai-Uwe Fröhlich, and Randy Schekman. 1995. "Membrane Fusion and the Cell Cycle: Cdc48p Participates in the Fusion of ER Membranes." *Cell* 82 (6): 885–93. https://doi.org/10.1016/0092-8674(95)90268-6.

Lee, Jae-Jin, Joon Kyu Park, Jaeho Jeong, Hyesung Jeon, Jong-Bok Yoon, Eunice EunKyeong Kim, and Kong-Joo Lee. 2013. "Complex of Fas-Associated Factor 1 (FAF1) with Valosin-Containing Protein (VCP)-Npl4-Ufd1 and Polyubiquitinated Proteins Promotes Endoplasmic Reticulum-Associated Degradation (ERAD)." *The Journal of Biological Chemistry* 288 (10): 6998–7011. https://doi.org/10.1074/jbc.m112.417576.

Moustaqim-Barrette, Amina, Yong Q Lin, Sreeparna Pradhan, Gregory G Neely, Hugo J Bellen, and Hiroshi Tsuda. 2014. "The Amyotrophic Lateral Sclerosis 8 Protein, VAP, Is Required for ER Protein Quality Control." *Hum. Mol. Genet.* 23 (8): 1975–89.

Neuwald, Andrew F., L. Aravind, John L. Spouge, and Eugene V. Koonin. 1999. "AAA+: A Class of Chaperone-Like ATPases Associated with the Assembly, Operation, and Disassembly of Protein Complexes." *Genome Research* 9 (1): 27–43. https://doi.org/10.1101/gr.9.1.27.

Papiani, Giulia, Annamaria Ruggiano, Matteo Fossati, Andrea Raimondi, Giovanni Bertoni, Maura Francolini, Roberta Benfante, Francesca Navone, and Nica Borgese. 2012. "Restructured Endoplasmic Reticulum Generated by Mutant Amyotrophic Lateral Sclerosis-Linked VAPB Is Cleared by the Proteasome." *Journal of Cell Science* 125 (15): 3601–11. https://doi.org/10.1242/jcs.102137.

Park, Min-Young, Hyun Duk Jang, Soo Young Lee, Kong-Joo Lee, and Eunhee Kim. 2004. "Fas-Associated Factor-1 Inhibits Nuclear Factor-KB (NF-KB) Activity by Interfering with Nuclear Translocation of the RelA (P65) Subunit of NF-KB *." *Journal of Biological Chemistry* 279 (4): 2544–49. https://doi.org/10.1074/jbc.M304565200.

Park, Min-Young, Ji-hyun Moon, Ki-Sung Lee, Hye-In Choi, Jongkyeong Chung, Hyo Jeong Hong, and Eunhee Kim. 2007. "FAF1 Suppresses IκB Kinase (IKK) Activation by Disrupting the IKK Complex Assembly *." *Journal of Biological Chemistry* 282 (38): 27572–77. https://doi.org/10.1074/jbc.C700106200.

Ritson, Gillian P., Sara K. Custer, Brian D. Freibaum, Jake B. Guinto, Dyanna Geffel, Jennifer Moore, Waixing Tang, et al. 2010. "TDP-43 Mediates Degeneration in a Novel *Drosophila* Model of Disease Caused by Mutations in VCP/P97." *The Journal of Neuroscience* 30 (22): 7729–39. https://doi.org/10.1523/JNEUROSCI.5894-09.2010.

Shih, Yu-Tzu, and Yi-Ping Hsueh. 2016. "VCP and ATL1 Regulate Endoplasmic Reticulum and Protein Synthesis for Dendritic Spine Formation." *Nature Communications* 7 (1): 1–16. https://doi.org/10.1038/ncomms11020.

Song, Eun Joo, Seung-Hee Yim, Eunhee Kim, Nam-Soon Kim, and Kong-Joo Lee. 2005. "Human Fas-Associated Factor 1, Interacting with Ubiquitinated Proteins and Valosin-Containing Protein, Is Involved in the Ubiquitin-Proteasome Pathway." *Molecular and Cellular Biology* 25 (6): 2511–24. https://doi.org/10.1128/MCB.25.6.2511-2524.2005.

Tendulkar, S, S Hegde, L Garg, and others. 2022. "Caspar, an Adapter for VAPB and TER94, Modulates the Progression of ALS8 by Regulating IMD/NFκB Mediated Glial Inflammation in a Drosophila Model of Human …." *Hum. Mol. Genet.*

Watts, Giles D. J., Jill Wymer, Margaret J. Kovach, Sarju G. Mehta, Steven Mumm, Daniel Darvish, Alan Pestronk, Michael P. Whyte, and Virginia E. Kimonis. 2004. "Inclusion Body Myopathy Associated with Paget Disease of Bone and Frontotemporal Dementia Is Caused by Mutant Valosin-Containing Protein." *Nature Genetics* 36 (4): 377–81. https://doi.org/10.1038/ng1332.

Wójcik, Cezary, Maga Rowicka, Andrzej Kudlicki, Dominika Nowis, Elizabeth McConnell, Marek Kujawa, and George N. DeMartino. 2006. "Valosin-Containing Protein (P97) Is a Regulator of Endoplasmic Reticulum Stress and of the Degradation of N-End Rule and

Ubiquitin-Fusion Degradation Pathway Substrates in Mammalian Cells." *Molecular Biology of the Cell* 17 (11): 4606–18. https://doi.org/10.1091/mbc.e06-05-0432.

Yadav, Shweta, Rajan Thakur, Plamen Georgiev, Senthilkumar Deivasigamani, Harini K, Girish Ratnaparkhi, and Padinjat Raghu. 2017. "RDGBα Localization and Function at a Membrane Contact Site Is Regulated by FFAT/VAP Interactions." *Journal of Cell Science*, January, jcs.207985. https://doi.org/10.1242/jcs.207985.

# Chapter 4

# *SOD1* as a modulator of VAP aggregation in the null rescue model of *ALS8*

## Introduction

The *SOD1* locus is responsible for encoding a metalloenzyme, called Cu/Zn Superoxide dismutase. It is ubiquitously expressed and highly conserved (Marklund et al. 1982). The protein has been shown to localize in the cytoplasm, nucleus, lysosomes and the mitochondrial intermembrane space (Chang et al. 1988; Keller et al. 1991; Crapo et al. 1992; Sturtz et al. 2001). The enzyme has been thought to be primarily involved in the conversion of superoxide into molecular oxygen and hydrogen peroxide molecules, thus acting as a mitochondrial and cytosolic antioxidant (Reddi and Culotta 2013).

The *SOD1* locus was the first to be identified as an ALS causative locus in 1993 (Rosen et al. 1993). Currently, around 20% of the cases of familial ALS are linked to *SOD1* mutations (Kiernan et al. 2011). Up to 180 mutations have been discovered, of which the most common mutations are the D90A, the A4V and the G93A. De novo mutations in the *SOD1* locus is also associated with cases of sporadic ALS (Müller et al. 2022). *SOD1* mutations were initially thought of being a loss of function mutations, leading to compromised enzyme activity which resulted in oxidative stress and death of neurons. However, later studies in mice showed that neither *SOD1* knockdown, nor overexpression had an effect on mutant SOD1's presence, indicating an alternative mechanism for the mutation (Bruijn et al. 1998). SOD1 aggregates have been detected in the CNS of familial ALS patients post-mortem (Shibata et al. 1996). These aggregates are thought to lead to increased loss of function, though the exact mechanisms behind this are not known. SOD1 aggregates are known to contain other proteins such as Bcl2 which could play a role in triggering cell death (Pasinelli et al. 2004).

We decided to look at *SOD1* as a possible modifier of VAP aggregation and function. Both *SOD1* and *VAPB* are known ALS loci. Mice expressing mutant *SOD1* have been found to express lower levels of VAPB (Teuling et al. 2007). *SOD1* has also been identified as a genetic interactor of VAP in a *Drosophila* model (Deivasigamani et al. 2014). *SOD1*

expression was shown to affect VAP aggregation in an overexpression model (Chaplot et al. 2019).

**SOD1, ROS and the proteasomal machinery**

From previous work done in the lab (Chaplot et al. 2019), *SOD1* was seen to be a strong modulator of VAP aggregation. Neuronal knockdown of *SOD1* resulted in a decrease of aggregation density in the larval VNC of a *VAP (P58S)* neuronal overexpression model. The clearance of aggregates was identified to occur as a result of ROS generated as a result of the *SOD1* knockdown. Through a series of genetic and biochemical experiments, the removal of aggregates was identified to occur through the UPS and this was in turn regulated by TOR signaling. Autophagy was also tested as a likely candidate for the clearance mechanism, however, it did not appear to be changing aggregation density in the context.

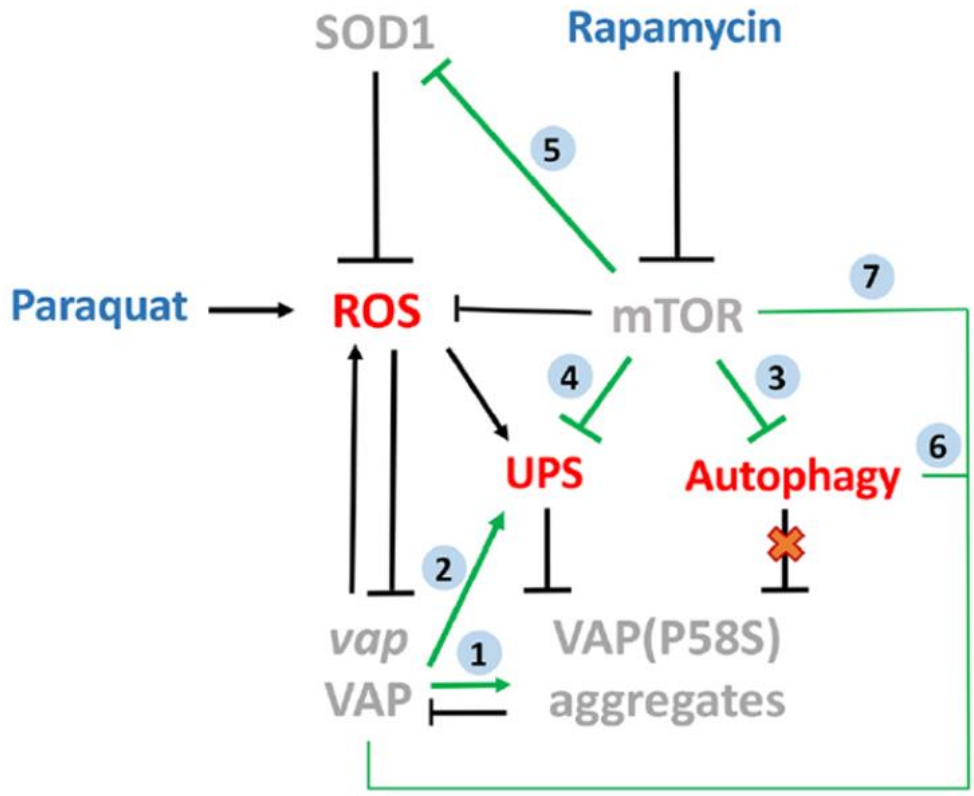


***Figure 4.1: VAP aggregation is modulated by SOD1.***

Model depicting novel relationships of SOD1- and mTOR-induced ROS with VAP and VAP(P58S) aggregates. Clearance of VAP(P58S) protein/aggregates appears to be primarily via the UPS, triggered by ROS, which are, in turn, regulated by cellular pathways such as the mTOR pathway, SOD1 and VAP activity. Autophagy does not appear to be a major contributor to aggregate clearance, under the conditions of this experiment. (Figure taken from Chaplot et al 2019.)

This study identified the involvement of proteasomal machinery in the regulation of VAP aggregates in the larval ventral nerve chord, without the involvement of the autophagic machinery. Our goal of this set of experiments was to validate the presence of similar mechanisms of aggregation regulation in the null rescue model, both larval and adult and observe if there were variations or alternate mechanisms in a background devoid of endogenous VAP.

**Results**

1) Pan-neuronal *SOD1* knockdown results in reduction of larval aggregates in the *ΔVAP;;gVAP$^{P58S}$*/+.

As performed previously, we looked at the larval ventral nerve chords of the *ΔVAP;Elav>+;gVAP$^{P58S}$*/+ and the *ΔVAP;Elav>SOD1$^{RNAi}$;gVAP$^{P58S}$*/+ flies (Fig 4.2 A and B) for the presence of VAP aggregates and quantified them. In this experiment we knocked

down *SOD1* pan neuronally to check if we would observe a change in aggregation density from the ΔVAP;;gVAP$^{P58S}$/+ line. We saw a decrease in aggregation density when comparing both (Fig 4.2 C,**P=0.001, Mann-Whitney Test). This result in the null rescue shows similar behavior to the previously observed clearance of VAP aggregation in the overexpression system used previously (Chaplot et al. 2019).

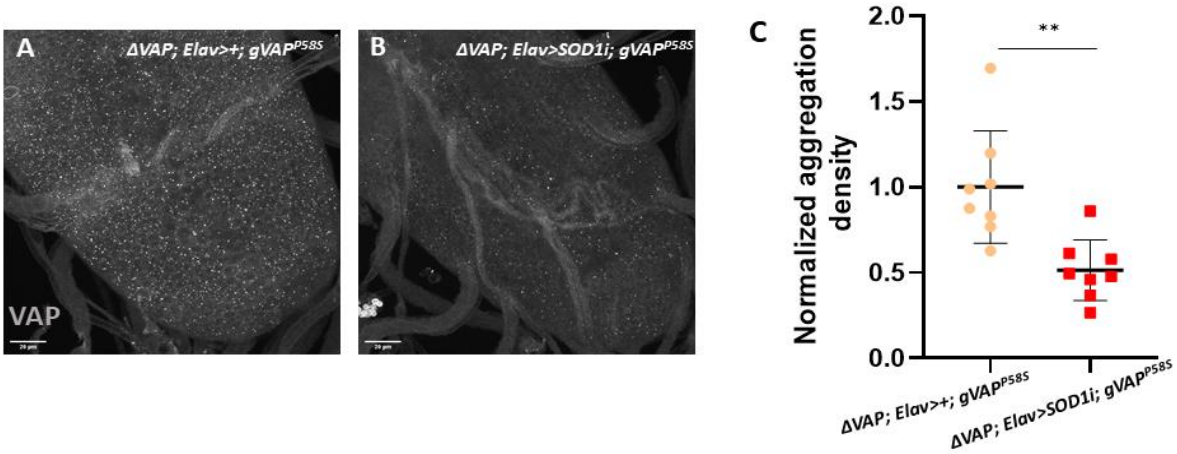


***Figure 4.2: Knocking down SOD1 neuronally reduces VAP aggregation density in the larval Ventral Nerve cord.***

Shown in (A) and (B) are the representative MIPs of larval Ventral nerve chords stained with VAP antibody. In (B) SOD1 is knocked down neuronally using the Elav driver. A reduction in VAP aggregation density is observed when SOD1 is knocked down neuronally (C). Each point represents an average value of aggregation density derived from three ROIs per VNC. (**P= 0.001, Mann-Whitney Test. Error bars represent SD.) Scale bars denote 20µm.

2) *SOD1* knockdown in the adult brain does not affect aggregation density.

Following the observation in the larval VNC, we decided to check adult brains and see if we observed a similar phenotype. We do not see a change after comparing *ΔVAP;Elav>+;gVAP$^{P58S}$*/+ and *ΔVAP; Elav>SOD1$^{RNAi}$; gVAP$^{P58S}$*/+ fly lines in aggregation density between the two genotypes (Fig 4.3 A and B , C, ns, Mann-Whitney Test). We also tried neuronally overexpressing *SOD1$^{WT}$* in the *ΔVAP;Elav;gVAP$^{P58S}$*/+ background (Fig 4.3 D and E) which too did not appear to significantly affect the VAP aggregation (Fig 4.3 F, ns, Mann Whitney Test). This is an interesting observation, considering *SOD1* knockdown affects aggregation in the larval VNC. From this observation, it may be possible that the adult and larval mechanisms of regulation are different and may constitute the activation of different clearance pathways.

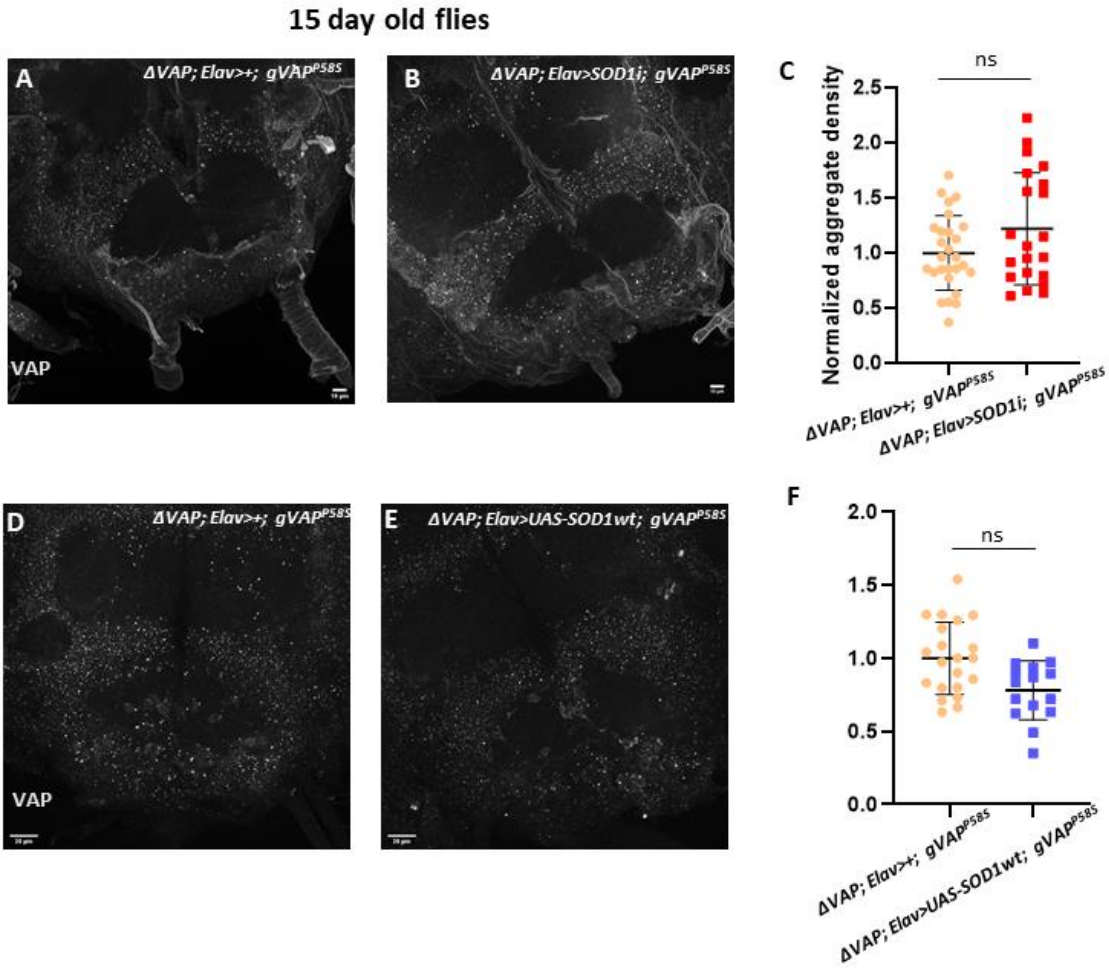


***Figure 4.3: Modulation of SOD1 levels does not affect VAP aggregation in the adult fly brain SOD1.***

Representative MIP images of the brains of *ΔVAP; Elav/+; gVAP$^{P58S}$/+* (A) and *ΔVAP; Elav>SOD1i;gVAP$^{P58S}$/+* (B) stained with VAP antibody. The aggregate density does not change between the two genotypes (C) (ns, Mann Whitney Test).

(D) and (E )are representative MIP images of *ΔVAP;Elav/+;gVAP$^{P58S}$/+*(D) and *ΔVAP;Elav> UAS-SOD1 $^{WT}$;gVAP$^{P58S}$/+* (E). The aggregate density does not change between the two genotypes (F). (ns, Mann-Whitney test). Error bars represent SD. Scale bar denotes 20µm.

3) Autophagy facilitates the clearance of VAP aggregates in a VAP heterozygous background.

The mechanism behind the clearance of aggregation in the case of *SOD1* knockdowns was found to be via the UPS (Chaplot et al. 2019). From our previous observations, we saw a difference in *SOD1*- mediated regulation of VAP aggregation between the larvae and the adult. Larval clearance of VAP aggregation was seen to be a result of ROS mediated

proteasomal clearance, where the clearance was a result of UPS activity. This led us to check for alternative strategies for clearance and test them. One such pathway we tested was the autophagic clearance pathway. Loss of VAP has been shown to affect autophagy through Beclin-1 (Wu et al. 2018). Usually employed for the removal of large substrates in the system, the autophagic clearance pathway involves the coordinated working of several cellular components. We hypothesized that there is a failure of the autophagic pathway in the $VAP^{P58S}$ flies.

Our previous observations in the Tsuda model indicated that VAP aggregation gets cleared with age in the presence of $VAP^{WT}$. If our observation was the result of a rescue in VAP function through a particular pathway, knocking down those suspected pathways should restore the aggregation phenotype. In order to test this, we used female null rescue flies. These flies would have a copy of $VAP^{WT}$ in the background, which would effectively rescue VAP aggregation at day 15 (Fig 4.4 A). We confirmed this and used the line in combination with an *ATG1* knockdown to observe aggregation (Fig 4.4 B). *ATG1* is necessary for the initiation of autophagosomes and its removal would suppress autophagy (Chen and Klionsky 2011). We saw an increase in aggregate density post knockdown of *ATG1* (Fig 4.4 C, ****P< 0.0001, Mann-Whitney Test). This result implicates a role for autophagy in the regulation of VAP aggregation in the adult brain.

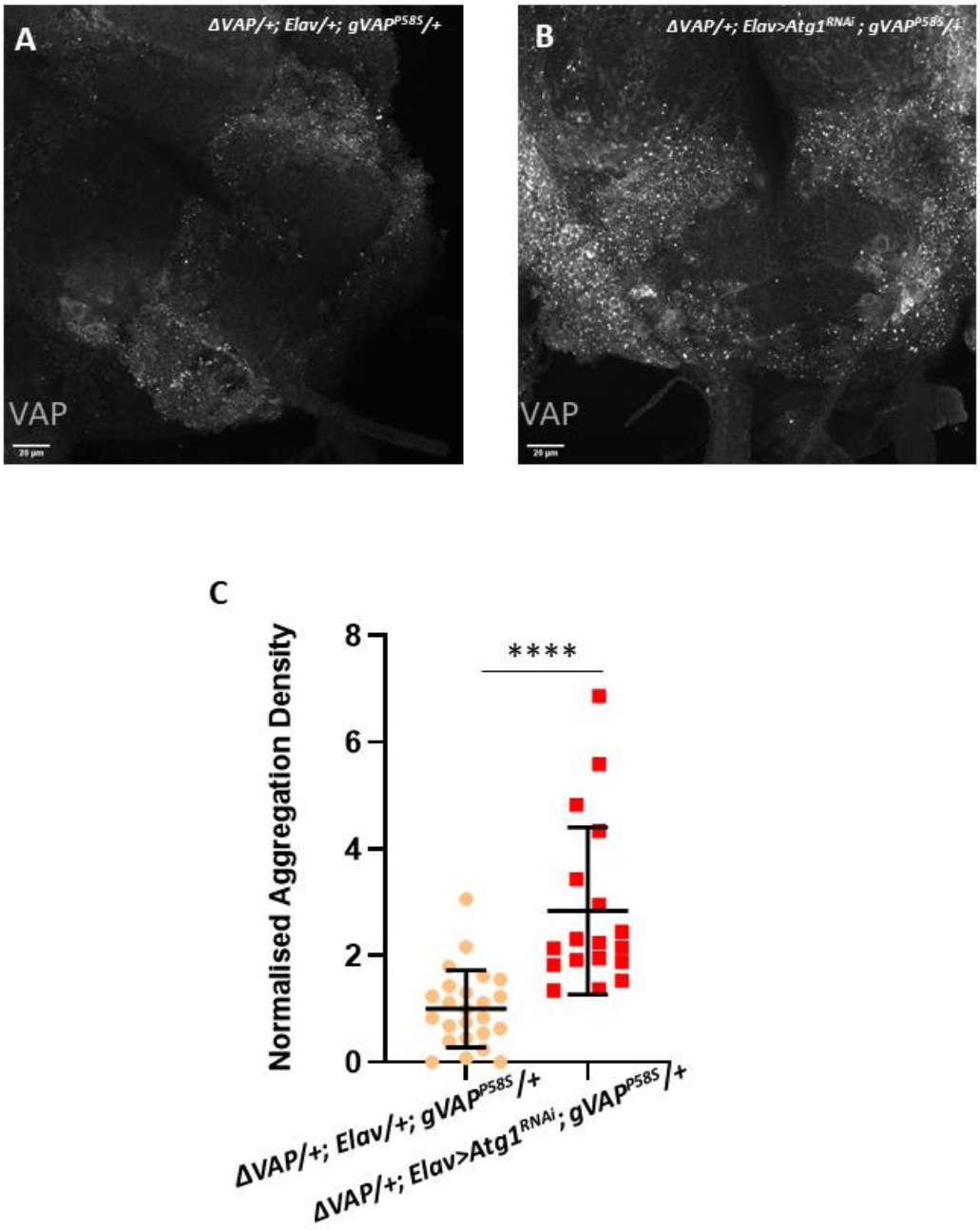


***Figure 4.4 Autophagic inhibition inhibits clearance of VAP aggregates in a VAP heterozygous background.***

Representative MIP images of the brains of *ΔVAP/+;Elav/+;gVAP$^{P58S}$/+* (A) and *ΔVAP/+;Elav>Atg1$^{RNAi}$;gVAP$^{P58S}$/+* (B) stained with VAP antibody. There is an increase in aggregate density upon neuronal knockdown of *Atg1* (C) (****P<0.0001, Mann-Whitney test Error bars represent SD). Scale bar denotes 20µm.

## Discussion

Reactive Oxidative Species (ROS) is a common feature in neurodegenerative disorders. In ALS, SOD1 mutants have been associated with causing high levels of ROS in the system,

which could lead to defects in the nervous system. Defects in NMJ have been identified before symptom onset in SOD1-G93A mutant mice (Rocha et al. 2013). Increased ROS has been shown to increase presynaptic inhibition and reduced neurotransmitter release in a mouse model of SOD1 ALS (Naumenko et al. 2011). *SOD1* has been previously demonstrated to be a genetic interactor of VAP as well as a modifier of VAP aggregation in larval VNC. The mechanism for the regulation of VAP aggregation occurs via the generation of ROS, caused by the knockdown of *SOD1*, which triggers clearance of aggregation via the UPS (Chaplot et al. 2019). We demonstrated the clearance in VAP aggregation in a SOD1 knockdown background in the null rescue larvae, re-affirming the presence of this mechanism in the null rescue system.

Our experiments with SOD1 in larval VNC identified SOD1 as a modulator of VAP aggregation, with the UPS being the primary agent for regulation. We wanted to recapitulate this in the adult brain, but surprisingly, pan-neuronal *SOD1* knockdown did not affect VAP aggregation in the adult brain. Over expression of the wild-type *SOD1* had also not shown an effect on VAP aggregation. Following these observations, we decided to look at alternative mechanisms that could influence aggregation in the adult brain. The larval and adult brain systems for removal of aggregates could vary as the developmental contexts are vastly different. Proteostatic activity and protein turnover is known to decline with age in flies (Tsakiri et al. 2013; Vincow et al. 2021) and this might represent a need for employing alternative mechanisms for aggregate clearance.

Autophagy is an important clearance pathway, especially for the fully differentiated neuronal cells, where removal of insoluble substances by cell division is not possible. Inhibiting basal autophagy has been demonstrated to lead to neuronal aggregates and neurodegeneration in mouse models (Hara et al. 2006; Komatsu et al. 2006). Autophagic clearance of VAP aggregates could be an alternative to proteasomal clearance in the adult brain. We wished to understand if autophagic clearance was indeed used in the adult brain to remove VAP aggregation. *VAP* could play roles in autophagy through its interaction with beclin,(Wu et al. 2018). VAP aggregation could also be a sign of compromised *VAP* function. In order to test this, we, we employed the use of the $VAP^{WT}$ rescue line, where we saw the clearance of VAP aggregates with age. We blocked autophagy in this background and saw an increase in aggregates, implying a role for autophagy in the clearance of VAP aggregates.

Our findings point us to more questions regarding the role of ROS in the adult CNS. We are currently trying to understand the status of ROS in the adult fly brain and its relationship to disease onset and progression. The status of ROS is an important factor for understanding VAP aggregation, as both ROS and Autophagy are known to affect each other. ROS is capable of both inducing, as well as suppressing autophagy (Filomeni et al. 2010; Aucello, Dobrowolny, and Musarò 2009; Chang et al. 2022). Autophagy is also capable of regulating ROS. Autophagy can reduce ROS through mitophagy of damaged mitochondria (Youle and Narendra 2011), and also through antioxidant generation mechanisms through Nuclear factor erythroid 2–related factor 2 (Nrf2) mediated pathways (Bae et al. 2013). If there are defects in autophagy, they may affect the nervous system's response to ROS detrimentally. This would also have implications for treatment options offered for ALS, like Edaravone, which specifically aim to reduce ROS (Cha and Kim 2022).

## Materials and methods

### *Drosophila* maintenance and husbandry

All flies were grown on standard corn meal agar at 25 degrees C. All crosses were set up at 25 degrees Celsius unless specified otherwise.

### *Drosophila* stocks and reagents

The flies expressing genomic $VAP^{WT}$ and genomic $VAP^{P58S}$ were a gift from Hiroshi Tsuda. These lines were balanced with a null line, *Δ166*, as described previously (Tendulkar et al. 2022).

Canton S (0001) lines were procured from Bloomington Drosophila stock center (BDSC)

Lines used for SOD1: BL 34616 ($UAS\text{-}SOD1^{RNAi}$) (BDSC), CG11793-HA (*UAS-SOD1* overexpression) (DPIM line).

### Larval Ventral Nerve chord preparation

Wandering third-instar larvae were selected and dissected in 1X PBS. They were fixed in 4% PFA with 0.3% PBST for 20 minutes. Post fixation, the samples were washed thrice in 1X PBS and then transferred to blocking solution (2% BSA in 0.3% PBST) for 1 hour, followed by incubation in primary antibody for 1 overnight. This was followed by 3 washes with blocking each lasting 20 minutes and then an overnight incubation with the secondary antibody. Post-secondary, the samples are washed thrice with blocking, each lasting 20

minutes. DAPI is added to the second wash to visualize cell nuclei. Samples are given one final wash in PBS before mounting in antifade mounting media.

## Adult brain dissections

Flies of the desired genotype are collected and aged to the requirement. Adult brains are dissected out into cold 1X PBS, followed by a 24-hour fixation in 1.2% PFA at 4 degrees Celsius. This is followed by permeabilization in 5% PBST (2 washes for 20 minutes each) followed by 2 washes in PAT buffer (30 minutes each). Samples were then blocked in 5% BSA in 0.5% PBST for two hours. This was followed by incubation in primary antibodies for 36 hours at 4 degrees. Post-primary incubation, 4 PAT buffer washes each lasting 30 minutes are administered. Samples are then incubated in secondary antibodies for 36 hours. This is followed by another 4 PAT buffer washes. DAPI (1:1000) is added in the second wash to visualize nuclei. This is followed by a wash in 1X PBS and subsequently stored in PBS with Vectashield SlowFade mounting media in a 1:1 ratio at 4 degrees overnight.
For mounting, samples are placed with the antennal lobes facing the coverslip. Samples are bridge-mounted. We have used SlowFade mounting medium (Vectashield, S36937).
Antibodies used: Rabbit Anti-VAP (1:500) (Yadav et al. 2017; Chaplot et al. 2019)

## Microscopy

Mounted samples were imaged using Zeiss LSM710 or Leica SP8 confocal microscopes with 63x objectives. Images were acquired at 16-bit depth as Z stacks. For larval ventral chords, the tip of the ventral cord was imaged at 1X zoom. For the adult brains, the main body of the brain was imaged at 0.75X zoom. Acquisition parameters were kept constant across experimental sets.

## Image analysis

We have used both ImageJ and Huygens Professional software for image segmentation and analysis. The analysis protocol is similar to that used in (Chaplot et al. 2019) with modifications for analysing adult brain images. Briefly, a threshold is set to segment high intensity punctae from the background signal from the tissue. The threshold is manually adjusted for each genotype in order to segment punctae from the tissue background. Object filters were used to remove objects larger than 200 voxels and smaller than 8 voxels. The

punctae were quantified per cubic micrometre of the larval ventral nerve chord or the adult brain and has been defined as aggregation density. Three 3D ROIs were selected from each brain from the tip of the VNC (larval) or the sub oesophageal zone (SEZ) (adult) and measured. The aggregation density for each ROI was normalized to the mean value for the control group in each experiment. We have used 6 to 12 brains per genotype per experiment. ROI volume has been calculated using the the range of the z stack of the image.

**References:**

Aucello, Michela, Gabriella Dobrowolny, and Antonio Musarò. 2009. "Localized Accumulation of Oxidative Stress Causes Muscle Atrophy through Activation of an Autophagic Pathway." *Autophagy* 5 (4): 527–29. https://doi.org/10.4161/auto.5.4.7962.

Bae, Soo Han, Su Haeng Sung, Sue Young Oh, Jung Mi Lim, Se Kyoung Lee, Young Nyun Park, Hye Eun Lee, Dongmin Kang, and Sue Goo Rhee. 2013. "Sestrins Activate Nrf2 by Promoting P62-Dependent Autophagic Degradation of Keap1 and Prevent Oxidative Liver Damage." *Cell Metabolism* 17 (1): 73–84.

Bruijn, L. I., M. K. Houseweart, S. Kato, K. L. Anderson, S. D. Anderson, E. Ohama, A. G. Reaume, R. W. Scott, and D. W. Cleveland. 1998. "Aggregation and Motor Neuron Toxicity of an ALS-Linked SOD1 Mutant Independent from Wild-Type SOD1." *Science (New York, N.Y.)* 281 (5384): 1851–54. https://doi.org/10.1126/science.281.5384.1851.

Chang, L. Y., J. W. Slot, H. J. Geuze, and J. D. Crapo. 1988. "Molecular Immunocytochemistry of the CuZn Superoxide Dismutase in Rat Hepatocytes." *The Journal of Cell Biology* 107 (6 Pt 1): 2169–79. https://doi.org/10.1083/jcb.107.6.2169.

Chaplot, Kriti, Lokesh Pimpale, Balaji Ramalingam, Senthilkumar Deivasigamani, Siddhesh S Kamat, and Girish S Ratnaparkhi. 2019. "SOD1 Activity Threshold and TOR Signalling Modulate VAP (P58S) Aggregation via Reactive Oxygen Species-Induced Proteasomal Degradation in a Drosophila Model of Amyotrophic Lateral Sclerosis." *Dis. Model. Mech.* 12 (2): dmm033803.

Cha, Sun Joo, and Kiyoung Kim. 2022. "Effects of the Edaravone, a Drug Approved for the Treatment of Amyotrophic Lateral Sclerosis, on Mitochondrial Function and Neuroprotection." *Antioxidants* 11 (2): 195. https://doi.org/10.3390/antiox11020195.

Chang, Kun-Che, Pei-Feng Liu, Chia-Hsuan Chang, Ying-Cheng Lin, Yen-Ju Chen, and Chih-Wen Shu. 2022. "The Interplay of Autophagy and Oxidative Stress in the Pathogenesis and Therapy of Retinal Degenerative Diseases." *Cell & Bioscience* 12 (1): 1. https://doi.org/10.1186/s13578-021-00736-9.

Chen, Yongqiang, and Daniel J. Klionsky. 2011. "The Regulation of Autophagy – Unanswered Questions." *Journal of Cell Science* 124 (2): 161–70. https://doi.org/10.1242/jcs.064576.

Crapo, J. D., T. Oury, C. Rabouille, J. W. Slot, and L. Y. Chang. 1992. “Copper,Zinc Superoxide Dismutase Is Primarily a Cytosolic Protein in Human Cells.” *Proceedings of the National Academy of Sciences of the United States of America* 89 (21): 10405–9. https://doi.org/10.1073/pnas.89.21.10405.

Deivasigamani, Senthilkumar, Hemant Kumar Verma, Ryu Ueda, Anuradha Ratnaparkhi, and Girish S Ratnaparkhi. 2014. “A Genetic Screen Identifies Tor as an Interactor of VAPB in a Drosophila Model of Amyotrophic Lateral Sclerosis.” *Biol. Open* 3 (11): 1127–38.

Filomeni, Giuseppe, Enrico Desideri, Simone Cardaci, Giuseppe Rotilio, and Maria Rosa Ciriolo. 2010. “Under the ROS: Thiol Network Is the Principal Suspect for Autophagy Commitment.” *Autophagy* 6 (7): 999–1005. https://doi.org/10.4161/auto.6.7.12754.

Hara, Taichi, Kenji Nakamura, Makoto Matsui, Akitsugu Yamamoto, Yohko Nakahara, Rika Suzuki-Migishima, Minesuke Yokoyama, et al. 2006. “Suppression of Basal Autophagy in Neural Cells Causes Neurodegenerative Disease in Mice.” *Nature* 441 (7095): 885–89. https://doi.org/10.1038/nature04724.

Komatsu, Masaaki, Satoshi Waguri, Tomoki Chiba, Shigeo Murata, Jun-ichi Iwata, Isei Tanida, Takashi Ueno, et al. 2006. “Loss of Autophagy in the Central Nervous System Causes Neurodegeneration in Mice.” *Nature* 441 (7095): 880–84. https://doi.org/10.1038/nature04723.

Keller, G. A., T. G. Warner, K. S. Steimer, and R. A. Hallewell. 1991. “Cu,Zn Superoxide Dismutase Is a Peroxisomal Enzyme in Human Fibroblasts and Hepatoma Cells.” *Proceedings of the National Academy of Sciences of the United States of America* 88 (16): 7381–85. https://doi.org/10.1073/pnas.88.16.7381.

Kiernan, Matthew C, Steve Vucic, Benjamin C Cheah, Martin R Turner, Andrew Eisen, Orla Hardiman, James R Burrell, and Margaret C Zoing. 2011. “Amyotrophic Lateral Sclerosis.” *The Lancet* 377 (9769): 942–55. https://doi.org/10.1016/S0140-6736(10)61156-7.

Marklund, S. L., N. G. Westman, E. Lundgren, and G. Roos. 1982. “Copper- and Zinc-Containing Superoxide Dismutase, Manganese-Containing Superoxide Dismutase, Catalase, and Glutathione Peroxidase in Normal and Neoplastic Human Cell Lines and Normal Human Tissues.” *Cancer Research* 42 (5): 1955–61.

Müller, Kathrin, Ki-Wook Oh, Angelica Nordin, Sudhan Panthi, Seung Hyun Kim, Frida Nordin, Axel Freischmidt, et al. 2022. “De Novo Mutations in SOD1 Are a Cause of ALS.” *Journal of Neurology, Neurosurgery & Psychiatry* 93 (2): 201–6. https://doi.org/10.1136/jnnp-2021-327520.

Naumenko, Nikolay, Eveliina Pollari, Antti Kurronen, Raisa Giniatullina, Anastasia Shakirzyanova, Johanna Magga, Jari Koistinaho, and Rashid Giniatullin. 2011. “Gender-Specific Mechanism of Synaptic Impairment and Its Prevention by GCSF in a Mouse Model of ALS.” *Frontiers in Cellular Neuroscience* 5. https://www.frontiersin.org/articles/10.3389/fncel.2011.00026.

Pasinelli, Piera, Mary Elizabeth Belford, Niall Lennon, Brian J. Bacskai, Bradley T. Hyman, Davide Trotti, and Robert H. Brown. 2004. “Amyotrophic Lateral Sclerosis-Associated SOD1 Mutant Proteins Bind and Aggregate with Bcl-2 in Spinal Cord Mitochondria.” *Neuron* 43 (1): 19–30. https://doi.org/10.1016/j.neuron.2004.06.021.

Reddi, Amit R., and Valeria C. Culotta. 2013. “SOD1 Integrates Signals from Oxygen and Glucose to Repress Respiration.” *Cell* 152 (1–2): 224–35. https://doi.org/10.1016/j.cell.2012.11.046.

Rocha, Mariana C., Paula A. Pousinha, Alexandra M. Correia, Ana M. Sebastião, and Joaquim A. Ribeiro. 2013. “Early Changes of Neuromuscular Transmission in the SOD1(G93A) Mice Model of ALS Start Long before Motor Symptoms Onset.” *PLOS ONE* 8 (9): e73846. https://doi.org/10.1371/journal.pone.0073846.

Rosen, D. R., T. Siddique, D. Patterson, D. A. Figlewicz, P. Sapp, A. Hentati, D. Donaldson, J. Goto, J. P. O’Regan, and H. X. Deng. 1993. “Mutations in Cu/Zn Superoxide Dismutase Gene Are Associated with Familial Amyotrophic Lateral Sclerosis.” *Nature* 362 (6415): 59–62. https://doi.org/10.1038/362059a0.

Shibata, Noriyuki, Kohtaro Asayama, Asao Hirano, and Makio Kobayashi. 1996. “Immunohistochemical Study on Superoxide Dismutases in Spinal Cords from Autopsied Patients with Amyotrophic Lateral Sclerosis.” *Developmental Neuroscience* 18 (5–6): 492–98. https://doi.org/10.1159/000111445.

Sturtz, L. A., K. Diekert, L. T. Jensen, R. Lill, and V. C. Culotta. 2001. “A Fraction of Yeast Cu,Zn-Superoxide Dismutase and Its Metallochaperone, CCS, Localize to the Intermembrane Space of Mitochondria. A Physiological Role for SOD1 in Guarding against Mitochondrial

Oxidative Damage." *The Journal of Biological Chemistry* 276 (41): 38084–89. https://doi.org/10.1074/jbc.M105296200.

Tendulkar, S, S Hegde, L Garg, and others. 2022. "Caspar, an Adapter for VAPB and TER94, Modulates the Progression of ALS8 by Regulating IMD/NFκB Mediated Glial Inflammation in a Drosophila Model of Human …." *Hum. Mol. Genet.*

Teuling, Eva, Suaad Ahmed, Elize Haasdijk, Jeroen Demmers, Michel O Steinmetz, Anna Akhmanova, Dick Jaarsma, and Casper C Hoogenraad. 2007. "Motor Neuron Disease-Associated Mutant Vesicle-Associated Membrane Protein-Associated Protein (VAP) B Recruits Wild-Type VAPs into Endoplasmic Reticulum-Derived Tubular Aggregates." *Journal of Neuroscience* 27 (36): 9801–15.

Tsakiri, Eleni N., Gerasimos P. Sykiotis, Issidora S. Papassideri, Vassilis G. Gorgoulis, Dirk Bohmann, and Ioannis P. Trougakos. 2013. "Differential Regulation of Proteasome Functionality in Reproductive vs. Somatic Tissues of Drosophila during Aging or Oxidative Stress." *The FASEB Journal* 27 (6): 2407–20. https://doi.org/10.1096/fj.12-221408.

Vincow, Evelyn S, Ruth E Thomas, Gennifer E Merrihew, Michael J MacCoss, and Leo J Pallanck. 2021. "Slowed Protein Turnover in Aging Drosophila Reflects a Shift in Cellular Priorities." *The Journals of Gerontology Series A: Biological Sciences and Medical Sciences* 76 (10): 1734–39. https://doi.org/10.1093/gerona/glab015.

Wu, Dan, Zongbing Hao, Haigang Ren, and Guanghui Wang. 2018. "Loss of VAPB Regulates Autophagy in a Beclin 1-Dependent Manner." *Neuroscience Bulletin* 34 (6): 1037–46. https://doi.org/10.1007/s12264-018-0276-9.

Yadav, Shweta, Rajan Thakur, Plamen Georgiev, Senthilkumar Deivasigamani, Harini K, Girish Ratnaparkhi, and Padinjat Raghu. 2017. "RDGBα Localization and Function at a Membrane Contact Site Is Regulated by FFAT/VAP Interactions." *Journal of Cell Science*, January, jcs.207985. https://doi.org/10.1242/jcs.207985.

Youle, Richard J., and Derek P. Narendra. 2011. "Mechanisms of Mitophagy." *Nature Reviews Molecular Cell Biology* 12 (1): 9–14. https://doi.org/10.1038/nrm3028

# Chapter 5

# Generation of CRISPR-Cas9 *ALS8 Drosophila* mutant

## Introduction

Previously, fly models were developed with the *ALS8* mutation. Initial studies for identification of functionally critical *VAP* interactions were carried out using the UAS-Gal4 system to drive expression of mutant $VAP^{P58S}$ protein in a tissue-specific manner (Deivasigamani et al. 2014; Chaplot et al. 2019). These studies furthered our understanding of the cellular functioning and interactions of *VAP* in ALS, however, these systems did not show defects in motor function or lifespan. To better understand the mechanisms involved in the development of these disease phenotypes, we moved on to work on a model first established in the lab of Hiroshi Tsuda (Moustaqim-Barrette et al. 2014). This line was previously discussed in Chapter 2. Briefly, the Tsuda line was a *VAP* null mutant line that has been rescued by the addition of a genomically driven *VAP* allele. When the allele added is $VAP^{P58S}$, one observes a decrease in the lifespan of the emergent fly along with the occurrence of progressive motor defects. We further adapted the fly line in our course of the study to identify genetic and physical regulators of life span, motor defects and $VAP^{P58S}$ aggregation. (Tendulkar et al. 2022). While this set of fly lines proved indispensable for our goal of characterising aggregation and defects, we were limited by the genetic background of this set of null rescue lines. To overcome these limitations, we planned to generate a genomic $VAP^{P58S}$ mutant using CRISPR-Cas9 genome editing. Our success in this project would not only widen our available tool kit for genetic studies but also serve as a strong validation of phenotypes seen previously with null rescue systems.

## CRISPR-Cas9 genome editing

The CRISPR-Cas9 enzyme system was first observed in bacteria. In one study which aimed to study the *iap* gene, the scientists observed the presence of a series of small, repeating and regularly spaced nucleotide sequences (Ishino et al. 1987). The significance of this observation was not realised for another 25 years till the advent of robust genome sequencing techniques. This event led to the discovery of similar clustered repeats in other members of the Archaea group microorganisms and was even declared as a characteristic feature of the group. The term CRISPR (Clustered Regularly Interspaced Short Palindromic Repeats) was coined to describe the clustered repeats (Jansen et al. 2002). The presence of these repeats

across several bacterial species led to the idea of CRISPR being physiologically relevant to their survival (Terns and Terns 2011). The interest in understanding the CRISPR sequences led to a lot of people studying the molecular mechanisms behind it. The CRISPR-Cas (Clustered Regularly Interspaced Short Palindromic Repeats-CRISPR associated protein) system was realised to be an RNA mediated adaptive immune system which makes use of small RNA molecules to selectively target or silence invading viruses, plasmids or foreign nucleic acids. The system is made up of an arrangement of Cas genes in an operon along with a CRISPR array, consisting of unique sequences which are used to target genomic regions specific to invaders. These regions are called spacers and they are interspersed with repeats (Wiedenheft, Sternberg, and Doudna 2012). The CRISPR response to foreign invaders has three major phases: an adaptive phase, an expression phase and an interference phase. In the adaptive phase, the host organism, which harbours a CRISPR array, begins mounting an immune response by adding short sequences of the foreign genome to the end of its array. In the expression and interference phases, the incorporated repeat spacer sequence is transcribed into pre-CRISPR RNA (pre-crRNA), then cleaved to form short crRNA (Deltcheva et al. 2011). The crRNA is assembled into a complex along with Cas proteins and used to target and silence the foreign DNA (Brouns et al. 2008; Sashital, Jinek, and Doudna 2011).

There are three major types of CRISPR-Cas systems (Makarova et al. 2011) (Deltcheva et al. 2011). In all three systems, the presence of a Protospacer Adjacent Motif (PAM) sequence, on the non- target DNA strand, is required for both acquisition of the repeat sequence as well as for cleavage (Garneau et al. 2010; Horvath et al. 2008). In type I and type III systems, the Cas endonucleases are known to process the pre-crRNA, which when mature, organises into a large, multi Cas protein complex, capable of recognising and cleaving the complementary nucleotide sequence. The type II system is a simpler system, consisting of the repeat spacer array, 3-4 Cas genes, in combination with a trans-activating crRNA (tracr RNA) and RNAse III as the major components. Cas9 is a signature of the type II systems (Makarova et al. 2011). It is a large, multidomain protein capable of carrying out the targeting and cleavage of foreign DNA (Jinek et al. 2012).

Because of the compact nature and relative simplicity of the system, the type II system has been adapted for carrying out genetic engineering. The dual tracrRNA:crRNA system has been successfully modified into a single guide RNA (gRNA) further simplifying the system (Jinek et al. 2012). Following this, a variety of applications could be developed using this system. The guide RNA could be designed to target a specific genetic locus, while the Cas9

could be modified and used to generate double stranded breaks (DSBs), made enzymatically inactive and promote DNA silencing, transcriptional regulation and so on. The versatility and fidelity of the system has led to it being used successfully in several model organisms, including mice (Shen et al. 2013), human cell lines (Jinek et al. 2013; Cho et al. 2013) and *Drosophila* (Gratz et al. 2013; Kondo and Ueda 2013).

We decided to use the CRISPR-Cas9 system to generate a genomic $VAP^{P58S}$ mutant for a few reasons. With this strategy, we would be able to create a mutation at the *VAP* locus itself, which would ensure that the expression levels of the mutant were similar to that of wild type. Any positional effects would also be removed in the CRISPR background. If the generation of a mutant was successful, we could also have a lot more options for working with other genetic tools, as the CRISPR mutant would only need a single chromosome available for maintenance.

**Results**

1) Generation of a $VAP^{P58S}$ mutant using CRISPR-Cas9 strategy

## The strategy

With the Tsuda model, we were able to identify and characterise aggregation density along with the relationship between age and aggregation density (refer Chapter 2). We were also able to study VAP aggregation in the context of other ALS associated loci (*SOD1*, *Ter94* and *Caspar*). In order to broaden our scope of genetic experiments for understanding the aggregation process better, we decided to create a genomic *VAP* mutant and for this we employed the CRISPR-Cas9 ssODN based strategy. As the mutation for the disease was a point mutation converting Proline to Serine at the $58^{th}$ position in the protein, we decided to carry out the editing using a Double Strand Break (DSB) at the target locus, followed by repair of the DSB using a single oligodeoxynucleotide (ssODN) template containing the mutation in its sequence. To generate this DSB at the VAP locus, we designed and cloned VAP guide RNA, with which a transgenic VAP gRNA line was generated (Fig 5.1A). For expression of the Cas9, we tested 3 different promoters driving cas9 (Actin-5C, Vasa, Nanos). We settled on using Nanos-cas9 (nos-cas9) as we observed lethality in pupal stages when we used the other promoter driven Cas9s. Following this, we would cross the guide RNA transgenic line with the Cas9 line to give embryos which would be injected with the ssODN. Once the embryos develop into adult flies, they would be crossed to balancers to preserve the genetic mutation and then stabilised, before they are screened. In this case we

have chosen to screen using restriction digestion, wherein the mutation would introduce a site for restriction digestion by a restriction enzyme. Positives would be further tested by genetic sequencing. The strategy has been outlined in (Fig 5.1B).

The design for VAP guide RNA and cloning and injections was carried out by Sushmitha Hegde and Deepti Trivedi (NCBS fly facility).

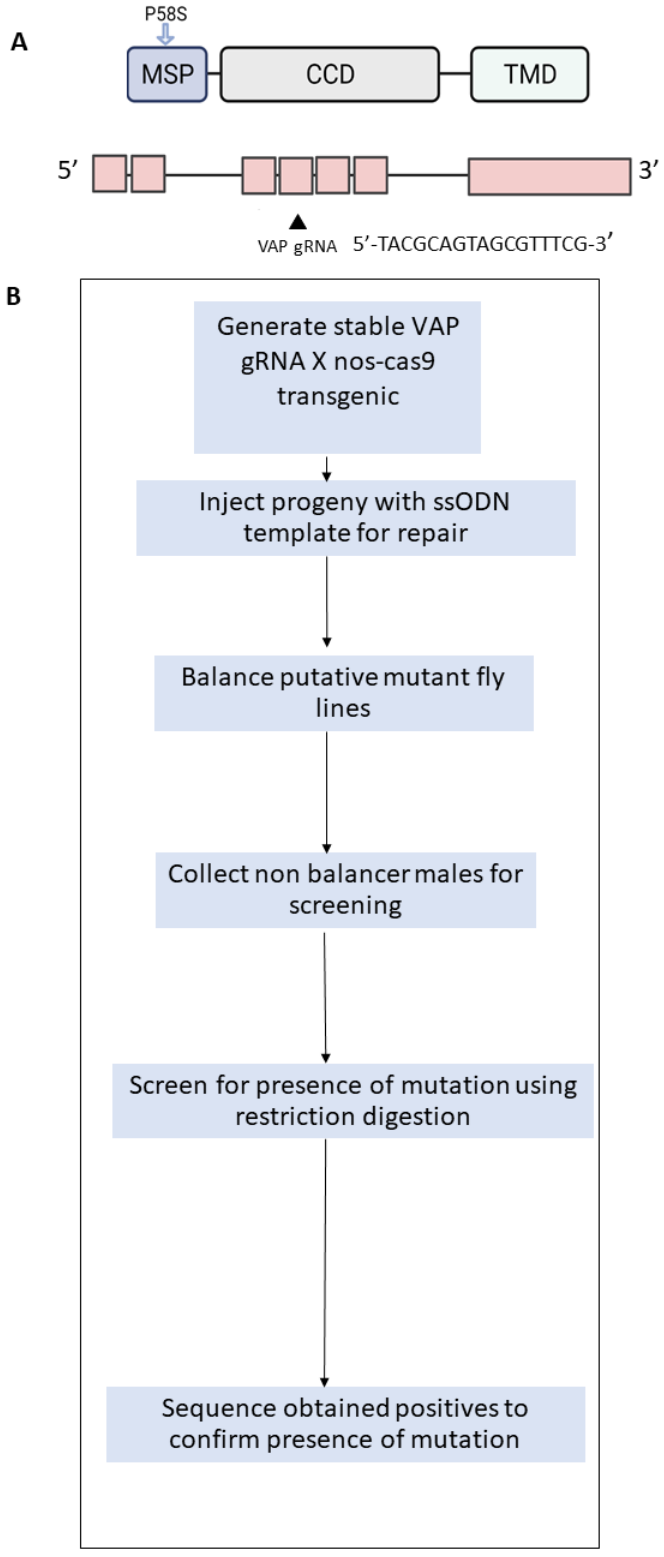


***Figure 5.1: The strategy used to generate a VAP$^{P58S}$ CRISPR-cas9 mutant.***

Schematics for the VAP Protein (blue) and *VAP* genetic locus (pink) are shown in (A). The *VAP$^{P58S}$* mutation is found in the MSP domain of the protein. A single guide RNA was designed to target the genomic region coding for the domain in exon 4. The flow chart of the strategy used for generation and screening is summarised in (B).

**Fly crosses**

The Cas9 required for generating the double stranded break was expressed under the Nanos promoter (nos-cas9). Flies with nos-cas9 were crossed to the generated VAP gRNA transgenic flies. The embryos resulting from the cross were injected with a single stranded oligonucleotide donor (ssODN) containing the mutated template to be used in the repair and generation of the $VAP^{P58S}$ fly. The embryos were then allowed to grow and develop into adult flies before they were crossed to a first chromosome balancer (w- FM7a) to maintain the mutation if it was present. As the Nos-Cas9 used to cross the VAP guide RNA transgenic had a CyO balancer in the background, we ended up getting both straight winged and curly winged flies from the embryos. From the crossing scheme (Fig 5.2) we realised that only straight winged flies would have both the VAP guide RNA and nos-Cas9, thus we selected only straight winged flies out of the emerged flies for further balancing. These flies were crossed once more to the same balancer. Each fly's progeny was collected separately and 3 of the progeny were used to set up stable lines. The lines were stabilised by crossing them with a w-FM7a balancer. After this step, flies showing the absence of the balancer phenotype (kidney shaped eyes) were picked to carry out genomic DNA extraction followed by a restriction digestion based screen to identify putative mutants.

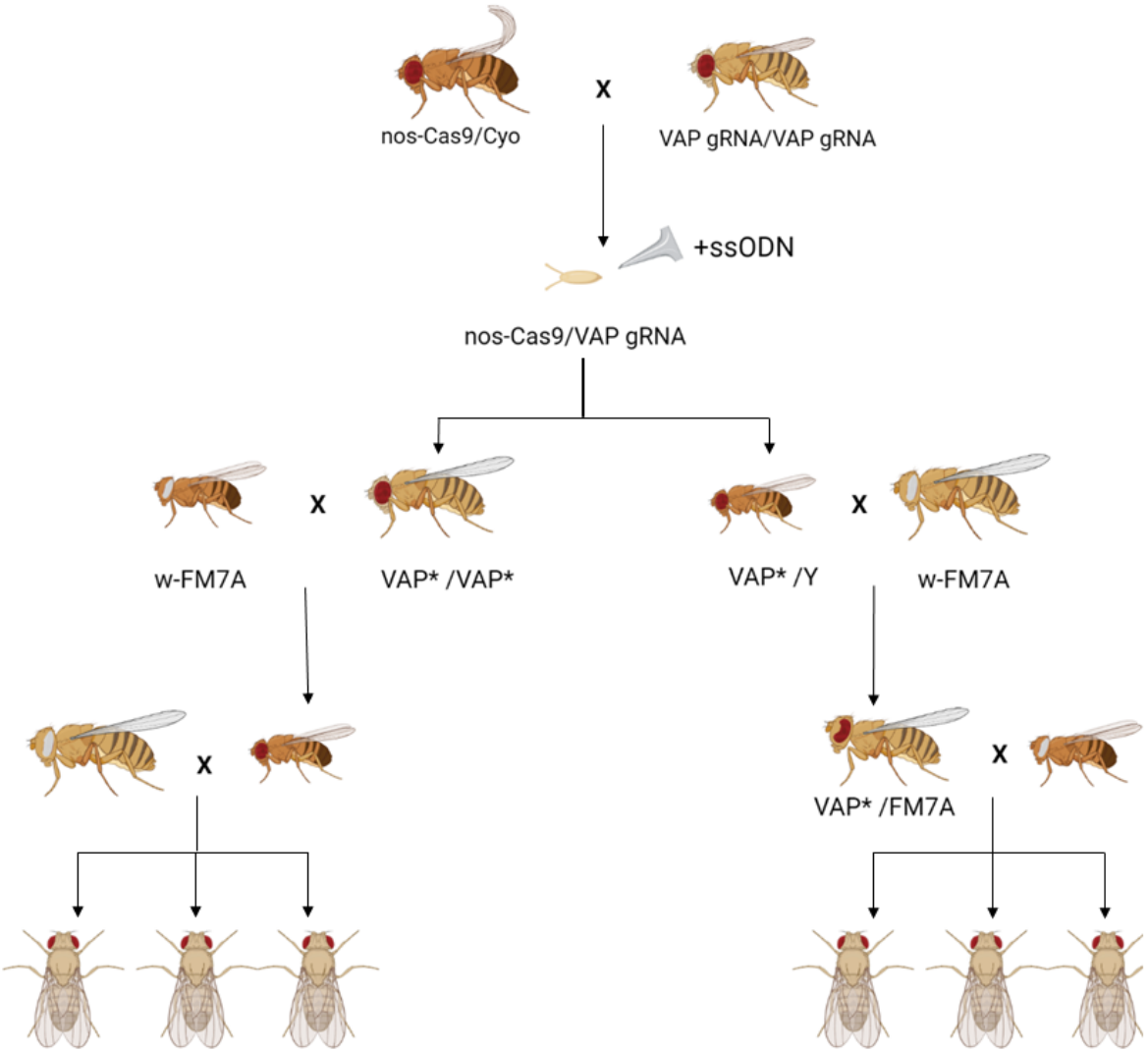


***Figure 5.2: Fly crossing strategy used for generating and identifying VAP CRISPR mutants.*** Stable *VAP* gRNA transgenic flies were crossed with a germline expressing Cas9 (nanos-cas9 or Nos-cas9) to give embryos, which are injected with the ssODN template (containing the P58S mutation) for repair. As the nos-cas9 was balanced over CyO, straight winged flies are selected from the developed embryos for downstream balancing and screening. The balancer phenotypes are depicted in the crosses as white eyes, kidney or bar shaped eyes. Image made on biorender.com.

## Screening for putative lines using Restriction Digestion.

After establishing stable fly lines, we carried out a restriction digestion based screen to identify putative mutants. The ssODN designed for the strategy contains a novel restriction site, which would be introduced into the fly genome upon successful template-based repair. By using the appropriate restriction enzyme on genomic DNA samples isolated from each of

the fly lines (from single flies), we can screen for the presence of the mutation quickly and effectively. In our design and screening, we had incorporated a restriction sequence, 5'-TACGTA-3', at the site of the mutation. This could be accessed and cut by the Eco105I enzyme and generate two fragments, identifiable via gel electrophoresis (Fig 5.3 A).

For screening, we generated 588 stable lines, either by crossing with the balancer or by generating lines homozygous for the mutation. We identified males from each of these lines, as the males would have a single X chromosome with either the mutation or the wild-type, making screening more concise. The males were then prepared individually to obtain genomic DNA (described in the methods) which was further subjected to the restriction digestion. The digested products were then run on an agarose gel to identify the samples which were cleaved. The samples positive for digestion were marked and sent for sequencing to confirm the presence of the mutation.

Post restriction digestion we identified 8 positives. We confirmed the presence of the mutation using genomic sequencing (Fig 5.3 B). We also identified a CRISPR control line, which we sequenced to ensure no mutations in the *VAP* gene. A summary of the number of flies generated, injected, positives has been added in table 2.

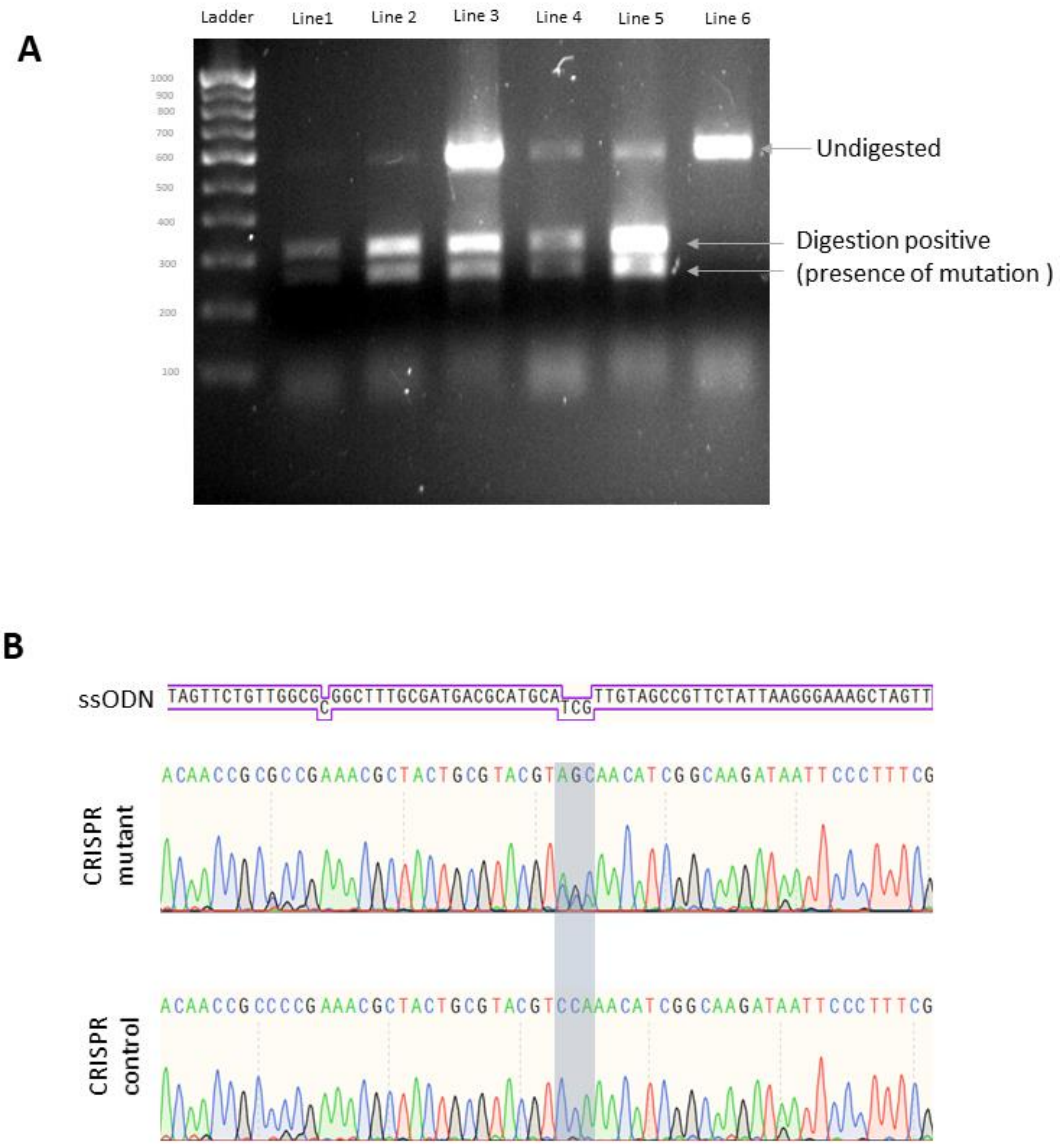


***Figure 5.3: Restriction digestion based screening for putative CRISPR mutants.***
Non-balancer male flies obtained were screened by genomic PCR followed by restriction digestion with SnaB1 (Eco105I) enzyme, as seen in the representative agarose gel image (A). The enzyme recognizes the altered site of mutation due to the appearance of a TACGTA site post-modification, not seen in the case of unmodified flies (A). Genetic sequencing was carried out for identified digestion positives and the presence of the mutation was confirmed as shown in the representative chromatogram (B).

**TABLE 2: SUMMARY OF NUMBERS FOR THE GENERATION OF $VAP^{P58S}$ MUTANT**

| | |
|---|---|
| Injected (Total) | Around 700 |
| CyO flies (cannot be used) | 389 |
| Straight winged flies | 359 |
| Sterile | 163 |
| No of stable lines made | 588 |
| Number of lines screened using restriction digestion | 50 |
| Positives from restriction digestion | 8 |
| $VAP^{P58S}$ mutants identified post sequencing | 7 |

2.) Larval Ventral Nerve Cords of the $VAP^{P58S}$ mutants show the presence of VAP positive punctae.

One of our major reasons for the generation of the mutant was to validate the phenotypes seen in the null rescue model, so we stained larval VNCs with the VAP antibody to observe the localization of VAP protein in the CRISPR mutant lines and the control lines. We observe that the control line, $VAP^{CC}$, shows a diffuse, cytoplasmic staining pattern, typical of VAP protein in a wild type background (Fig 5.4 A-C). In the case of the VAP mutants ($VAP^{279.1}$ and $VAP^{177.1}$), we observe VAP positive punctae, similar to that seen in the $\Delta VAP;;gVAP^{P58S}$ /+ flies (Fig 5.4 D-I). Thus, we were able to show that the CRISPR mutant is similar to the null rescue model in terms of VAP aggregation and localization. As the CRISPR edited mutant is a genomic mutant, with the mutation being made at the genetic locus of VAP itself, this system further serves to validate the aggregation phenotype seen in the null rescue model.

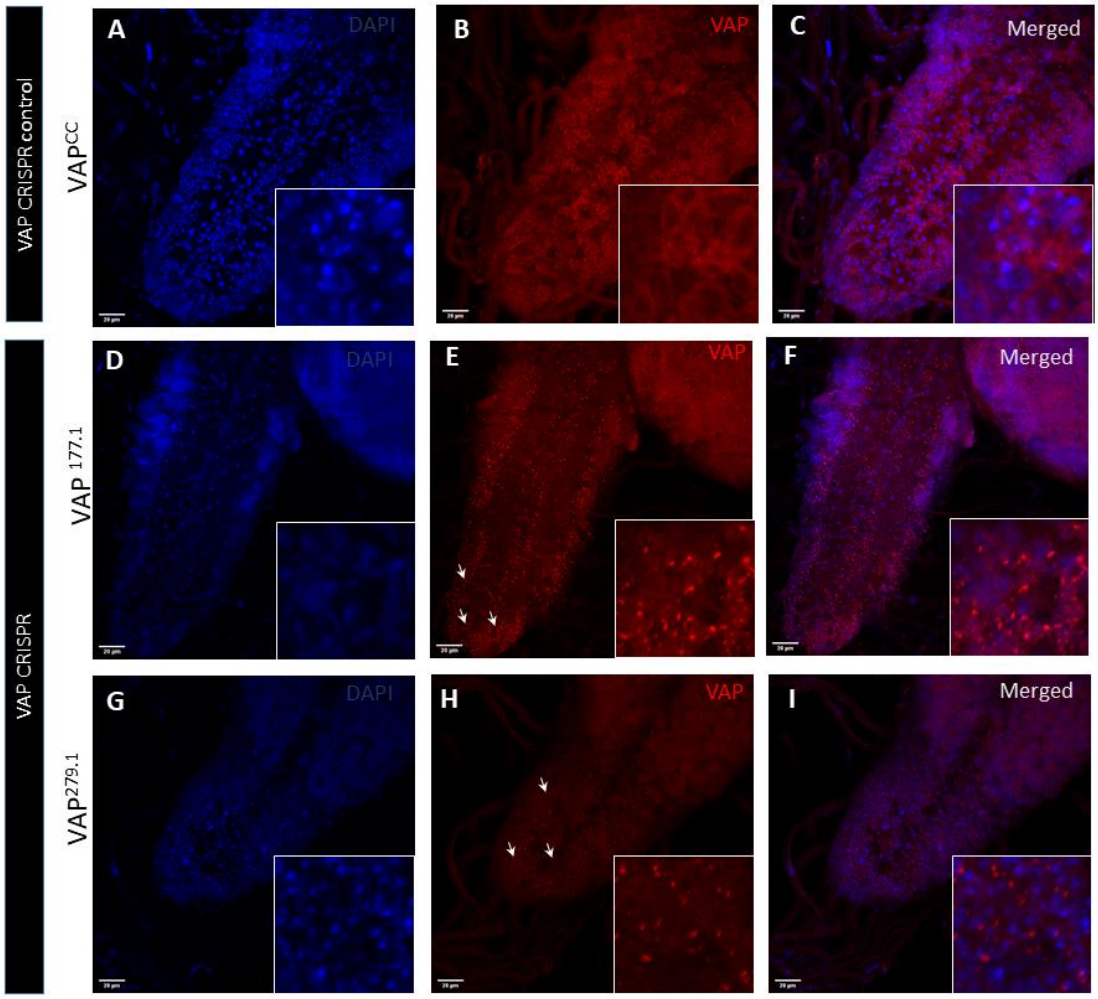


***Figure 5.4: VAP$^{P58S}$ larval Ventral Nerve Cords(VNCs) show punctate localization of VAP.***
VAP localization was marked using anti-VAP antibody in larval ventral nerve cords. Shown here are representative Maximum Intensity Projections (MIP) of Z stacks acquired. The samples were stained with DAPI (A, D and G) and VAP antibody (B, E and H). Insets show a 100% zoomed in view of the shown brain region. Arrows are used to point out punctae seen in the CRISPR-edited *VAP$^{P58S}$* sample (E and H). The DAPI and VAP channels have been merged to create a composite image (C, F and I).

3.) Motor and life span defects are observed in the CRISPR mutants

The Tsuda lines and the null rescue system show both progressive motor degeneration as well as lifespan defects (Refer Chapter 2). These phenotypes mimic the symptoms seen in human ALS, making this set of lines particularly valuable in studies to uncover aetiology. Upon generation of the CRISPR line, we wished to confirm the presence of the motor and lifespan defect associated with the null rescue line. For the validation, we monitored the lifespan of a

set of *VAP* CRISPR mutants and used the CRISPR control to compare it to. The CRISPR mutant lines die off completely by 30 days and shows a reduced lifespan when compared to the CRISPR control line (Fig 5.5 A) We also see a progressive motor degeneration in these flies when they are subjected to climbing assays (Fig 5.5 B). Thus we see similar phenotypes to both the Tsuda model as well as well as the null rescue lines.

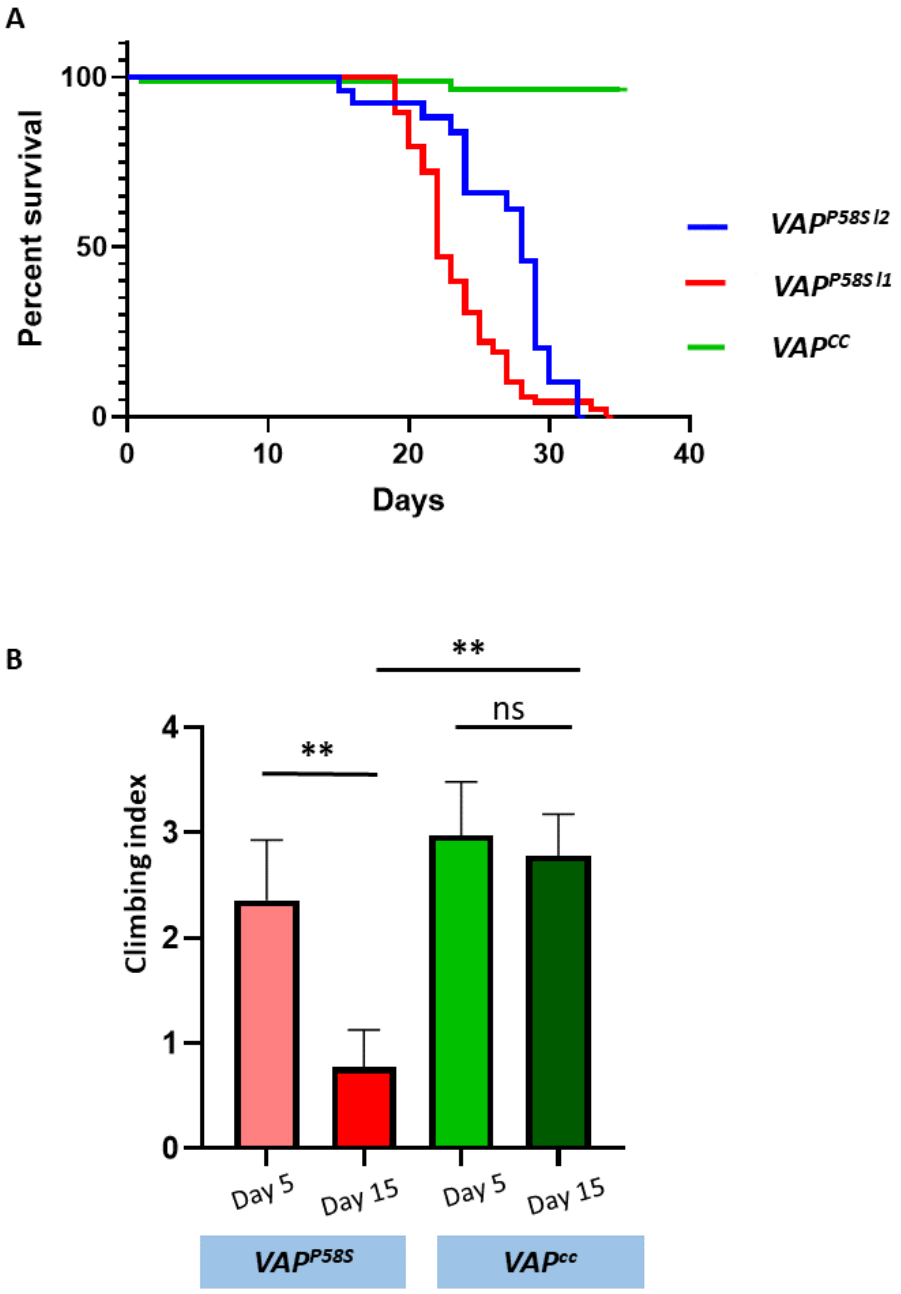


***Figure 5.5: Lifespan and motor defects are seen in VAP mutants.***

(A) The CRISPR mutant show a reduced lifespan compared to the control. The median lifespan of the two lines assayed, $VAP^{P58Sl1}$ and $VAP^{P58Sl2}$ are 22 and 28 respectively. The combined P- value of the curves is P<0.0001. (n=30-40 flies)

(B) The CRISPR mutant $VAP^{P58S}$ line shows a reduction in motor performance with age. The climbing index at day 15 is less than the index on day 5 for the CRISPR $VAP^{P58S}$ (**P= 0.0095, Mann -Whitney test.) The climbing index of the mutant at day 15 is also lesser than the climbing index seen in the control at day 15 (**P=0.0095 , Mann-Whitney test). Motor performance does not decline with age in the control (ns, Mann-Whitney test). Error bars represent SD.

4.) Adult fly brains $VAP^{P58S}$ mutants show the presence of VAP punctae, the density of which do not appear to change with age.

To validate the aggregation behaviour of VAP seen in adult flies we performed a VAP antibody staining of the adult brains as described in materials and methods. We first looked at the brains of adult flies aged 5 days. We observe the diffuse, cytoplasmic staining characteristic of wild type VAP in the control line ($VAP^{CC}$) seen in (Fig. 5.6 A-C). The VAP mutant ($VAP^{279.1}$) shows the presence of VAP positive inclusions (Fig 5.6 D-F). Upon confirming the presence of VAP punctae, we now wanted to see if there was an effect of age on the density of aggregates. For doing this, we stained and imaged 5 and 15 day old mutant fly brains for VAP punctae. As we can see in (Fig 5.6 G-L), there is extensive VAP aggregation observed in the mutant line at these time points. After quantifying the aggregate density for these points we see that there is no real change in the aggregate density between the two day points (Fig 5.6 M). From this, we infer that age may not affect the VAP aggregation density. This was again a result we observed while working with the null rescue line.

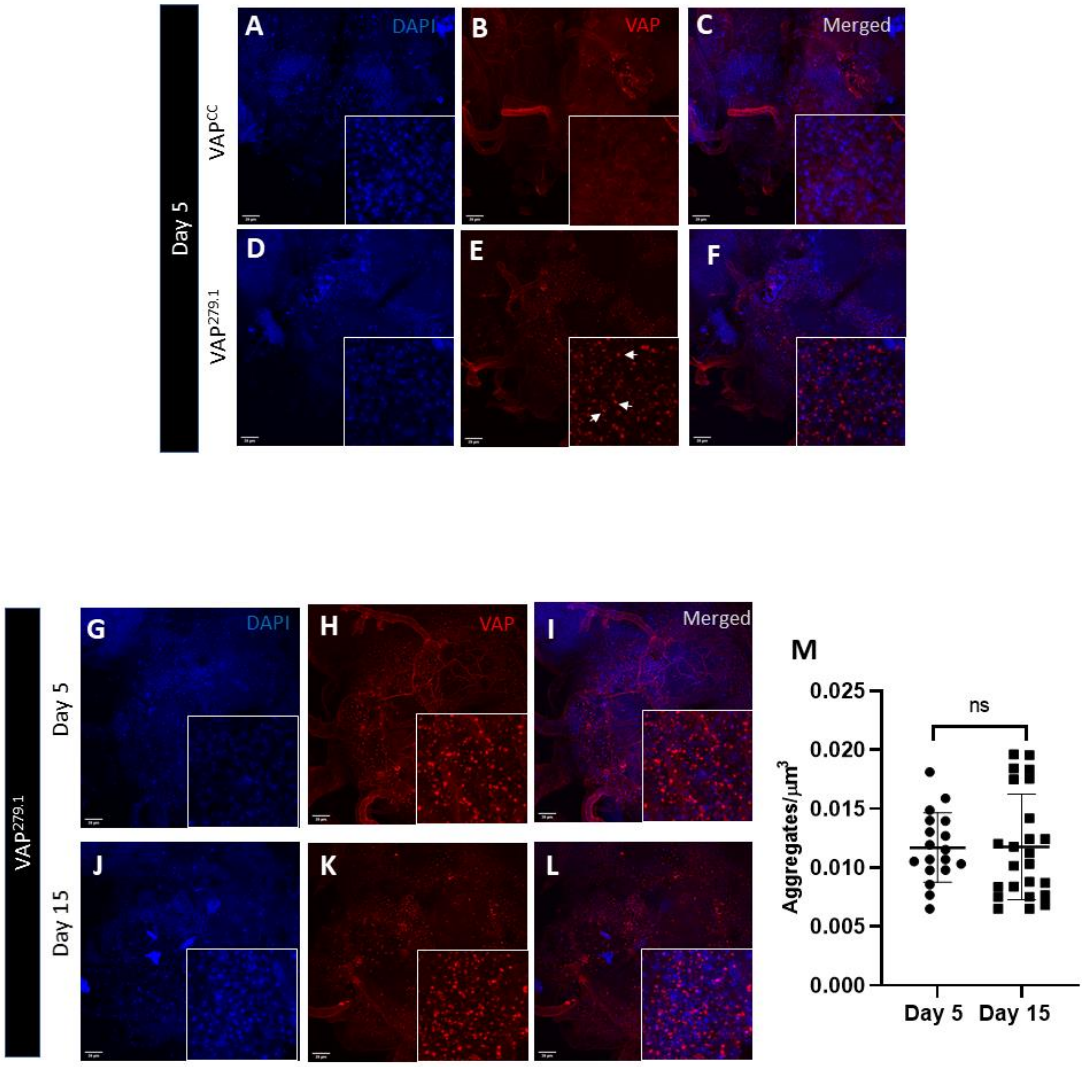


***Figure 5.6: VAP$^{P58S}$ adult flies show punctate localization of VAP.***

VAP localization was marked using anti-VAP antibody in adult drosophila brain samples. Shown here are representative Maximum Intensity Projections (MIP) of Z stacks acquired from *Drosophila* adult brains. The samples were stained with DAPI (A and D) and VAP antibody (B and E). Insets show a 100% zoomed in view of the shown brain region. Arrows are used to point out punctae seen in the CRISPR-edited *VAP$^{P58S}$* sample. The DAPI and VAP channels have been merged to create a composite image (C and F). Representative images of the brains of 5 day old and 15 day old adults stained with DAPI (G and J), anti-VAP (H and K) and composite (I and L). VAP aggregates are seen in both 5 and 15 day old brains (K). When compared to 5 day old brains (H), the density of aggregates does not appear to vary significantly (ns, Mann-Whitney test of significance). Scale bars represent 20 microns.

## Discussion

We have worked previously with the null rescue system, adapted from the line generated in the Hiroshi Tsuda lab. This line has been extremely useful in helping us characterize VAP aggregation behaviour in a *VAP* null background. Studies on this system have also helped us better understand the interaction between VAP and proteins like OSBP (Moustaqim-Barrette et al. 2014) and Caspar (Tendulkar et al. 2022). Nevertheless, the prospect of generating a genomic mutant by modifying the wild type VAP locus had its own appeal. The successful generation of the mutant was an important validation for the functionality of $VAP^{P58S}$ protein. Moreover, the CRISPR mutant also showed motor defects and reduction in lifespan, similar to the null rescue and Tsuda systems discussed in Chapter 2. The larval and adult nervous systems were stained for VAP and they have also shown the presence of VAP aggregates. The aggregation does not seem to be affected with age in the adults, recapitulating the results we saw with the null rescue system.

The generation of this mutant also opens the doors for a wide range of interaction based studies. There is increased freedom to genetically manipulate multiple loci as a result of two free chromosomes in the CRISPR background. ALS has been thought of having oligogenic origins in recent times and our lab's studies with VAP and its interactors (Deivasigamani et al. 2014; Chaplot et al. 2019; Tendulkar et al. 2022) highlight the need for understanding the genetic relationships between ALS loci. We are hopeful that the $VAP^{P58S}$ mutant we have generated may aid more studies in unravelling the roles of VAP and other loci, both in normal physiology and disease.

## Future Directions

With the generation of the CRISPR mutant, we have broadened the scope of genetic experiments that can be achieved. It is now possible to observe the effects of two loci on VAP aggregation simultaneously as we have two chromosomes to work with. With this system we also have the flexibility to recombine it with additional copies of genomic $VAP^{P58S}$, potentially allowing us to look at VAP aggregation in cases where there are three or even 4 copies of $VAP^{P58S}$. We are currently planning to use this system to study the effects of the $VAP^{P58S}$ mutant in several physiological processes including lipid homeostasis, neuroinflammation, circadian rhythm maintenance and flight circuitry development.

With the null rescue model, we had carried out limited studies in the female flies because of the genetic scheme required. The scheme would make it near impossible to have a good

control for studying VAP aggregation in females. The CRISPR mutant allows us to generate females homozygous for the mutation (2 copies), heterozygous (1 mutant copy and 1 wild-type copy) and even a single copy alone (1 copy of mutant over *ΔVAP*). This would allow us to study finer details relating to metabolism and sex dependent differences in aggregation regulation as well.

**Materials and Methods**

## Guide RNA design and cloning:

The VAP guide RNA was designed using the fly CRISPR optimal target finder. Cloning was carried out using the pBFv U6.2 vector according to the standard protocol (Kondo and Ueda 2013).

Forward Primer: 5'-GTACGCAGTAGCGTTTCGGTTTTAGAGCTAGAAATAGC-3'

Reverse Primer: 5'- GAAGTATTGAGGAAAACATA-3'

## Genomic DNA preparation, amplification and restriction digestion

In order to test for the presence of the desired mutation, we employed the use of a restriction digestion based selection using single fly genomic DNA to screen. Single flies were squished in 50 µl of squishing buffer (10mM Tris-Cl pH 8, 1mM EDTA, 25mM NaCl, and 0.2 mg/mL Proteinase K) and incubated with proteinase k at 37 degrees Celsius for 30 minutes, followed by heat inactivation at 85 degrees Celsius. A library of the genomic DNA isolated from the flies was made for screening efficiently. Samples were then selected from this set and the VAP locus was amplified using the following primers-
5'-GCCAAAATAGTGTGACTAATCGGGTGC -3'and
5'-CCATCATTAAGAGTCCTATTCGTTTCCCC-3'.
The PCR product obtained was then subjected to restriction digestion.

For the restriction digestion we employed the use of SnaB1(Eco105I) enzyme (NEB Catalogue no: R0130S). At the time of ssODN design, a novel restriction site for the enzyme was added to the sequence in such a way that the repaired strand with the mutation would be selectively digested. For testing we used the previously amplified gene product and incubated it in SnaB1 in NEB buffer for 1 hour at 37 degrees Celsius, followed by heat inactivation at 85 degrees Celsius. Following Restriction digestion, the products were run and resolved on a 1.2% agarose gel to visualise the digestion.

## Drosophila maintenance and husbandry:

All flies were grown on standard corn meal agar at 25 degrees Celsius. All crosses were set up at 25 degrees Celsius unless specified otherwise.

## Larval Ventral Nerve Cord preparation

Wandering third-instar larvae were selected and dissected in 1X PBS. They were fixed in 4% PFA with 0.3% PBST for 20 minutes. Post fixation, the samples were washed thrice in 1X PBS and then transferred to blocking solution (2% BSA in 0.3% PBST) for 1 hour, followed by incubation in primary antibody for 1 overnight. This was followed by 3 washes with blocking each lasting 20 minutes and then an overnight incubation with the secondary antibody. Post secondary, the samples are washed thrice with blocking, each lasting 20 minutes. DAPI is added to the second wash to visualize cell nuclei. Samples are given one final wash in PBS before mounting in anti-fade mounting media.

## Adult brain dissections

Flies of the desired genotype are collected and aged to the requirement. Adult brains are dissected out into cold 1X PBS, followed by a 24-hour fixation in 1.2% PFA at 4 degrees Celsius with nutation. This is followed by permeabilization in 5% PBST (2 washes for 20 minutes each) followed by 2 washes in PAT buffer (30 minutes each). Samples were then blocked in 5% BSA in 0.5% PBST for two hours. This was followed by incubation in primary antibodies for 36 hours at 4 degrees Celsius. Post primary incubation, 4 PAT buffer washes each lasting 30 minutes are administered. Samples are then incubated in secondary antibodies for 36 hours. This is followed by another 4 PAT buffer washes. DAPI (1:1000) is added in the second wash to visualize nuclei. This is followed by a wash in 1X PBS and subsequently stored in PBS with mounting media in a 1:1 ratio at 4 degrees Celsius overnight. For mounting, samples are placed with the antennal lobes facing the coverslip. Samples are bridge-mounted. We have used SlowFade mounting medium (Vectashield, S36937).

Antibodies used: Rabbit Anti-VAP (1:500) generated in-house, used previously in the following publications: (Yadav et al. 2017; Chaplot et al. 2019; Tendulkar et al. 2022).

## Microscopy

Mounted samples were imaged using Zeiss LSM710 or Leica SP8 confocal microscopes with 63x objectives. Images were acquired at 16-bit depth as Z stacks. For larval ventral cords, the tip of the ventral cord was imaged at 1X zoom. For the adult brains, the main body of the brain was imaged at 0.75X zoom. Acquisition parameters were kept constant across experimental sets.

## Image analysis

We have used Huygens Professional software for image segmentation and analysis. The analysis protocol is similar to that used in (Chaplot et al, 2019) with modifications for analysing adult brain images. Briefly, a threshold is set to segment high intensity punctae from the background signal from the tissue. The threshold is manually adjusted for each genotype in order to segment punctae from the tissue background. Object filters were used to remove objects larger than 200 voxels and smaller than 8 voxels. The punctae were quantified per micrometre of the larval ventral nerve cord or the adult brain and has been defined as aggregation density. Three 3D ROIs were selected from each brain from the tip of the VNC (larval) or the sub oesophageal zone (SEZ) (adult) and measured. The aggregation density for each ROI was normalized to the mean value for the control group in each experiment. We have used 6 to 12 brains per genotype per experiment. ROI volume has been calculated as the range of the Z- stack of the image.

## Lifespan assays

We used around 30-40 male flies for carrying out the lifespan assay. The crosses, as well as the eclosed flies, were maintained at 25 ºC. Each vial had 15 or fewer age-matched flies. The vials were flipped every four days to prevent accidental death due to dry media. The death toll of flies was recorded every day. We followed this assay till 40 days following which all the CRISPR mutants had died, while the control flies were still alive, with few deaths. The data was plotted and analyzed using the log-rank test in Graph Pad Prism8: Survival Assay. Curves were compared to generate an overall p-value of significance. We also added median lifespan data, generated whenever the entire population of a given genotype had died. The median lifespan has been used as a parameter in the following studies (Estes et al. 2011; Piper and Partridge 2016; Moustaqim-Barrette et al. 2014).

## Motor Function

Motor performance of the respective genotype was analyzed using the standard climbing assay (Madabattula et al. 2015; Azuma et al. 2014) with modifications which graded the severity of the defect. Ten flies were taken at a time per genotype in a measuring cylinder, allowed to acclimatise for 10 minutes, and then tapped firmly to induce startling. Following the startle, the flies would attempt to climb and their climbing performance was graded based on how far they climbed in 30 seconds. Flies which could not climb at all were scored 0 (Non-Climbers), flies which climbed till the 100 mL mark were scored 1, till 140 ml were given 2, 160 ml were given a 3 and 200ml and above were given a 4. This was repeated thrice for each set of 10 flies. We have used 30 to 50 flies for our assays. From this information, we would be able to derive a value for the Climbing Index (CI) of the genotype. The Climbing Index is a proxy indicator for the fitness of a particular genotype on a particular day. The formula for climbing index is used in (Azuma et al. 2014).

Climbing Index (CI)=Sum of all three values (Each Score X Number of flies with that score)/ (3 X Total number of flies examined).

**Acknowledgements**

Sushmitha Hegde and Dr.Deepti Trivedi (NCBS fly facility) were involved in the generation of the VAP mutant. Sushmitha designed the VAP guide RNA and Deepti and the NCBS fly facility carried out the cloning and generation of VAP guide RNA transgenic, followed by ssODN injections.

## References


Azuma, Yumiko, Takahiko Tokuda, Mai Shimamura, Akane Kyotani, Hiroshi Sasayama, Tomokatsu Yoshida, Ikuko Mizuta, et al. 2014. "Identification of Ter94, Drosophila VCP, as a Strong Modulator of Motor Neuron Degeneration Induced by Knockdown of Caz, Drosophila FUS." *Human Molecular Genetics* 23 (13): 3467–80. https://doi.org/10.1093/hmg/ddu055.

Brouns, Stan J. J., Matthijs M. Jore, Magnus Lundgren, Edze R. Westra, Rik J. H. Slijkhuis, Ambrosius P. L. Snijders, Mark J. Dickman, Kira S. Makarova, Eugene V. Koonin, and John van der Oost. 2008. "Small CRISPR RNAs Guide Antiviral Defense in Prokaryotes." *Science (New York, N.Y.)* 321 (5891): 960–64. https://doi.org/10.1126/science.1159689.

Chaplot, Kriti, Lokesh Pimpale, Balaji Ramalingam, Senthilkumar Deivasigamani, Siddhesh S Kamat, and Girish S Ratnaparkhi. 2019. "SOD1 Activity Threshold and TOR Signalling Modulate VAP (P58S) Aggregation via Reactive Oxygen Species-Induced Proteasomal Degradation in a Drosophila Model of Amyotrophic Lateral Sclerosis." *Dis. Model. Mech.* 12 (2): dmm033803.

Cho, Seung Woo, Sojung Kim, Jong Min Kim, and Jin-Soo Kim. 2013. "Targeted Genome Engineering in Human Cells with the Cas9 RNA-Guided Endonuclease." *Nature Biotechnology* 31 (3): 230–32. https://doi.org/10.1038/nbt.2507.

Deivasigamani, Senthilkumar, Hemant Kumar Verma, Ryu Ueda, Anuradha Ratnaparkhi, and Girish S Ratnaparkhi. 2014. "A Genetic Screen Identifies Tor as an Interactor of VAPB in a Drosophila Model of Amyotrophic Lateral Sclerosis." *Biol. Open* 3 (11): 1127–38.

Deltcheva, Elitza, Krzysztof Chylinski, Cynthia M. Sharma, Karine Gonzales, Yanjie Chao, Zaid A. Pirzada, Maria R. Eckert, Jörg Vogel, and Emmanuelle Charpentier. 2011. "CRISPR RNA Maturation by Trans-Encoded Small RNA and Host Factor RNase III." *Nature* 471 (7340): 602–7. https://doi.org/10.1038/nature09886.

Estes, Patricia S., Ashley Boehringer, Rebecca Zwick, Jonathan E. Tang, Brianna Grigsby, and Daniela C. Zarnescu. 2011. "Wild-Type and A315T Mutant TDP-43 Exert Differential Neurotoxicity in a Drosophila Model of ALS." *Human Molecular Genetics* 20 (12): 2308–21. https://doi.org/10.1093/hmg/ddr124.

Garneau, Josiane E., Marie-Ève Dupuis, Manuela Villion, Dennis A. Romero, Rodolphe Barrangou, Patrick Boyaval, Christophe Fremaux, Philippe Horvath, Alfonso H. Magadán, and Sylvain Moineau. 2010. "The CRISPR/Cas Bacterial Immune System Cleaves Bacteriophage and Plasmid DNA." *Nature* 468 (7320): 67–71. https://doi.org/10.1038/nature09523.

Gratz, Scott J, Alexander M Cummings, Jennifer N Nguyen, Danielle C Hamm, Laura K Donohue, Melissa M Harrison, Jill Wildonger, and Kate M O'Connor-Giles. 2013. "Genome Engineering of Drosophila with the CRISPR RNA-Guided Cas9 Nuclease." *Genetics* 194 (4): 1029–35. https://doi.org/10.1534/genetics.113.152710.

Horvath, Philippe, Dennis A. Romero, Anne-Claire Coûté-Monvoisin, Melissa Richards, Hélène Deveau, Sylvain Moineau, Patrick Boyaval, Christophe Fremaux, and Rodolphe Barrangou. 2008. "Diversity, Activity, and Evolution of CRISPR Loci in Streptococcus Thermophilus." *Journal of Bacteriology* 190 (4): 1401–12. https://doi.org/10.1128/JB.01415-07.

Ishino, Y, H Shinagawa, K Makino, M Amemura, and A Nakata. 1987. "Nucleotide Sequence of the Iap Gene, Responsible for Alkaline Phosphatase Isozyme Conversion in Escherichia Coli, and Identification of the Gene Product." *Journal of Bacteriology* 169 (12): 5429–33.

Jansen, Ruud., Jan. D. A. van Embden, Wim. Gaastra, and Leo. M. Schouls. 2002. "Identification of Genes That Are Associated with DNA Repeats in Prokaryotes." *Molecular Microbiology* 43 (6): 1565–75. https://doi.org/10.1046/j.1365-2958.2002.02839.x.

Jinek, Martin, Krzysztof Chylinski, Ines Fonfara, Michael Hauer, Jennifer A. Doudna, and Emmanuelle Charpentier. 2012. "A Programmable Dual-RNA-Guided DNA Endonuclease in Adaptive Bacterial Immunity." *Science (New York, N.Y.)* 337 (6096): 816–21. https://doi.org/10.1126/science.1225829.

Jinek, Martin, Alexandra East, Aaron Cheng, Steven Lin, Enbo Ma, and Jennifer Doudna. 2013. "RNA-Programmed Genome Editing in Human Cells." *ELife* 2 (January): e00471. https://doi.org/10.7554/eLife.00471.

Kondo, Shu, and Ryu Ueda. 2013. "Highly Improved Gene Targeting by Germline-Specific Cas9 Expression in Drosophila." *Genetics* 195 (3): 715–21. https://doi.org/10.1534/genetics.113.156737.

Madabattula, Surya T., Joel C. Strautman, Andrew M. Bysice, Julia A. O'Sullivan, Alaura Androschuk, Cory Rosenfelt, Kacy Doucet, Guy Rouleau, and Francois Bolduc. 2015. "Quantitative Analysis of Climbing Defects in a Drosophila Model of Neurodegenerative Disorders." *Journal of Visualized Experiments: JoVE*, no. 100 (June): e52741. https://doi.org/10.3791/52741.

Makarova, Kira S., Daniel H. Haft, Rodolphe Barrangou, Stan J. J. Brouns, Emmanuelle Charpentier, Philippe Horvath, Sylvain Moineau, et al. 2011. "Evolution and Classification of the CRISPR-Cas Systems." *Nature Reviews. Microbiology* 9 (6): 467–77. https://doi.org/10.1038/nrmicro2577.

Moustaqim-Barrette, Amina, Yong Q Lin, Sreeparna Pradhan, Gregory G Neely, Hugo J Bellen, and Hiroshi Tsuda. 2014. "The Amyotrophic Lateral Sclerosis 8 Protein, VAP, Is Required for ER Protein Quality Control." *Hum. Mol. Genet.* 23 (8): 1975–89.

Piper, Matthew D. W., and Linda Partridge. 2016. "Protocols to Study Aging in Drosophila." *Methods in Molecular Biology (Clifton, N.J.)* 1478: 291–302. https://doi.org/10.1007/978-1-4939-6371-3_18.

Sashital, Dipali G., Martin Jinek, and Jennifer A. Doudna. 2011. "An RNA-Induced Conformational Change Required for CRISPR RNA Cleavage by the Endoribonuclease Cse3." *Nature Structural & Molecular Biology* 18 (6): 680–87. https://doi.org/10.1038/nsmb.2043.

Shen, Bin, Jun Zhang, Hongya Wu, Jianying Wang, Ke Ma, Zheng Li, Xueguang Zhang, Pumin Zhang, and Xingxu Huang. 2013. "Generation of Gene-Modified Mice via Cas9/RNA-Mediated Gene Targeting." *Cell Research* 23 (5): 720–23. https://doi.org/10.1038/cr.2013.46.

Tendulkar, S, S Hegde, L Garg, and others. 2022. "Caspar, an Adapter for VAPB and TER94, Modulates the Progression of ALS8 by Regulating IMD/NFκB Mediated Glial Inflammation in a Drosophila Model of Human …." *Hum. Mol. Genet.*

Terns, Michael P., and Rebecca M. Terns. 2011. "CRISPR-Based Adaptive Immune Systems." *Current Opinion in Microbiology* 14 (3): 321–27. https://doi.org/10.1016/j.mib.2011.03.005.

Wiedenheft, Blake, Samuel H. Sternberg, and Jennifer A. Doudna. 2012. “RNA-Guided Genetic Silencing Systems in Bacteria and Archaea.” *Nature* 482 (7385): 331–38. https://doi.org/10.1038/nature10886.

Yadav, Shweta, Rajan Thakur, Plamen Georgiev, Senthilkumar Deivasigamani, Harini K, Girish Ratnaparkhi, and Padinjat Raghu. 2017. “RDGBα Localization and Function at a Membrane Contact Site Is Regulated by FFAT/VAP Interactions.” *Journal of Cell Science*, January, jcs.207985. https://doi.org/10.1242/jcs.207985.

# Appendix I:

# Motor performance and VAP aggregation

The functional implications of VAP aggregation is not clearly understood. While our experiments seem to point towards a loss of VAP function as the major mechanism of pathogenesis, the relation between motor degeneration and VAP aggregation is not very clear. In an attempt to understand this relationship better, we attempted to study aggregation in relation to motor function. For this purpose, we employed the strategy of segregating *ΔVAP ;;gVAP$^{P58S}$/+* flies on the basis of their motor ability and then studying aggregation in the segregated populations. I am presenting the methodology, our observations and conclusions from this particular set of experiments.

**The methodology**

**Motor assays for segregation**

In order to separate out flies with good motor ability and poor motor abilities, we used a modified version of the standard climbing assay (Madabattula et al. 2015), with a modification to segregate flies based on their motor ability. Briefly, flies aged 10 days of the desired genotype were tapped into a 21 cm measuring cylinder and left to acclimatise for 5 minutes. A paper roll is kept on the mouth of the cylinder such that the flies may climb into the roll. The height the flies would have to climb could be adjusted using this setup (Fig I.1). For separating good and poor performers the paper roll was kept at 21 cm height from the base of the cylinder.

Following acclimatisation, flies are tapped in quick succession to the bottom of the cylinder and allowed to climb for 30 seconds. The flies that climb into the roll are then separated out and classified as good performers. The flies which remain in the cylinder are considered poor performers. For wild-type flies, all flies were seen to move into the roll within 30 seconds, hence they do not show segregation on the basis of their climbing at this interval of time. (Fig. I.1)

Following separation, the fly brains were dissected and processed for immunostaining and imaging.

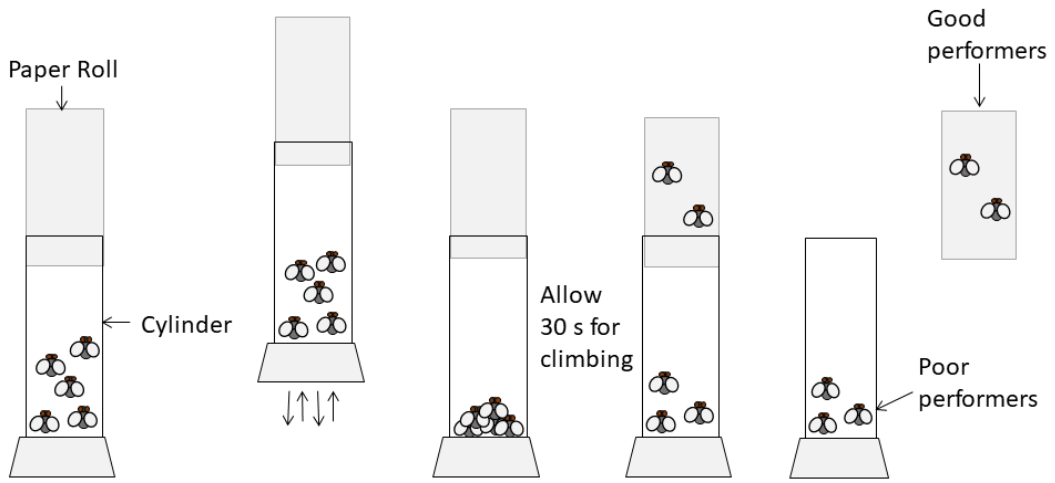


***Figure I.1: A climbing-based segregation methodology.***

The schematic describes the method used for segregating good and poor performers from the fly population. Flies are tapped and allowed to climb for 30 seconds. A paper roll is placed inside the cylinder at a suitable height. After 30 seconds the roll is carefully removed to separate good performers from the remaining flies left in the cylinder (poor performers).

**Dissections, staining, imaging**

Adult flies are anaesthetised using Carbon dioxide and their brains are dissected in 1xPBS (pH-7.4). The brains are fixed in 1.2% PFA for 24 hours, then washed in 5% PBST (2 washes 15 minutes each) followed by washes in PAT buffer (2 washes 20 minutes each). The samples are then blocked in 5% BSA for two hours. The brains are incubated in primary (VAP antibody-1:500) for two overnights and then in secondary (anti rabbit 568 1:1000, Invitrogen) for another two overnights. DAPI was added following secondary antibody wash and was allowed to sit for 30 minutes before proceeding with two more washes in PAT buffer. Samples were then washed with PBS, mounted in glycerol mounting medium and imaged using Zeiss confocal scopes.

Imaging was carried out on a Zeiss 710 confocal and confocal with Anisotropy. 63x oil objective was used to acquire images of 16 bit depth. Images were analysed using ImageJ. For each experiment, imaging parameters are kept constant across the samples.

**Analysis**

There was an amount of variation seen in the VAP staining patterns in the fly brains from the *ΔVAP;;gVAP$^{P58S}$*/+ line . Using a uniform threshold for segmenting images to differentiate aggregates was not working appropriately, with a lot of background VAP intensity also getting picked up in some cases. To represent this better, we used a ratio of the mean aggregate intensity to the mean VAP background intensity. Higher values of aggregate to membrane intensity represented more aggregated VAP than membrane localised diffuse VAP staining.

For calculating this ratio, we would select 15 small ROIs (roughly the size of one cell) each from the top, middle and end plane. The average intensity of the aggregate and the membrane staining around it would be measured and divided to give a value of the ratio. This process was repeated for all the ROIs in the Z stack. The ratios were averaged to give a single value for one VNC.

**Results**

1) An initial experiment demonstrated a stark difference between good and poor performers, subsequent replicates show ambiguous results.

Our initial experiment demonstrated a variation in the background vs aggregate intensity of VAP staining across samples without segregation. We hypothesized that this difference would also be reflected in their motor function. For confirming this, we segregated flies on the basis of their performance, followed by separate staining and imaging of the good and poor performing flies. Post an initial round of segregation as described in the methodology, we saw that this variation was linked to the climbing performance, with poor performers showing more aggregate intensity than background intensity. (Fig I.2 A-C)

Upon following this result up, we performed a few more sets of the experiment. The results from these sets however did not show a significant correlation with the motor defects (Fig I.2 E and F). We also faced problems in collecting adequate number of poor performance for assays as there seemed to be far fewer poor performers that could be segregated successfully with our method.

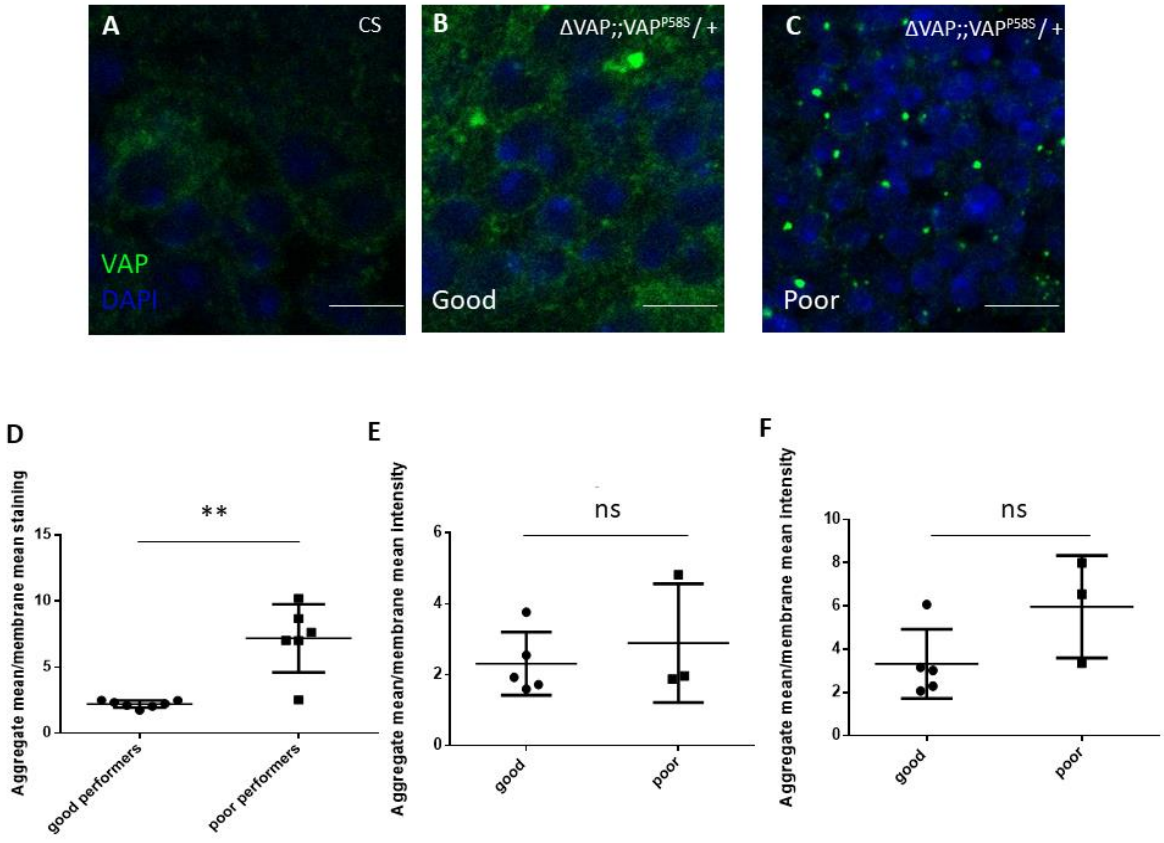


***Figure I.2: Motor function may be correlated with VAP distribution in the adult brain.***
Representative images of the adult brains of 10-day-old CS (A), *ΔVAP;;gVAP$^{P58S}$*/+ good performers (B) and *ΔVAP;;gVAP$^{P58S}$*/+ poor performers (C). There is a distinct difference observed in the VAP staining pattern represented by the aggregate to membrane intensity ratios of good vs poor performers in the first experiment (D, **P= 0.0012, Mann Whitney test). Subsequent tests did not show significant differences between the two populations. (E and F, ns=non-significant, Mann-Whitney Test. Error bars represent SD.)

## Discussion

A variation in motor ability in the population of *ΔVAP;;gVAP$^{P58S}$*/+ had been observed and identified previously (refer chapter 2). The formation of aggregates is a known mechanism to remove misfolded proteins from the cellular ecosystem by converting them into insoluble forms, which are then rendered functionally inactive. In some cases, it removes toxic monomers, such as in Huntington's disease models (Kuemmerle et al. 1999; Arrasate et al. 2004). This could also remove partially functional mutant proteins and cause deterioration in functionality of the organism. We hypothesized that a variation in functionality was represented by the variation in aggregated versus diffuse VAP staining. To test this, we

modified the standard climbing assay to allow us to segregate good climbers from poor climber or non-climbers. While our initial experiment showed us a co-relation between motor function and the aggregate to membrane ratio, we were not able to see a clear and significant difference in successive experiments. Part of this was likely the fewer number of poor performers in each group. This could also be because of the current experimental design. The current methodology works well for segregating non climbers from climbers, but it is not very effective for segregating the poor performers from the good performers. In order to better perform this experiment, we would have to resort to more sensitive assays in the future. Use of a Drosophila Activity Monitor (DAM) where each individual fly can be monitored would be a good option for future studies. Flight assays when performed using specific methods like wing-flap pattern analysis, can also be good methods of finer motor segregation.

**References**

Arrasate, Montserrat, Siddhartha Mitra, Erik S. Schweitzer, Mark R. Segal, and Steven Finkbeiner. 2004. "Inclusion Body Formation Reduces Levels of Mutant Huntingtin and the Risk of Neuronal Death." *Nature* 431 (7010): 805–10. https://doi.org/10.1038/nature02998.

Kuemmerle, S., C. A. Gutekunst, A. M. Klein, X. J. Li, S. H. Li, M. F. Beal, S. M. Hersch, and R. J. Ferrante. 1999. "Huntington Aggregates May Not Predict Neuronal Death in Huntington's Disease." *Annals of Neurology* 46 (6): 842–49.

Madabattula, Surya T., Joel C. Strautman, Andrew M. Bysice, Julia A. O'Sullivan, Alaura Androschuk, Cory Rosenfelt, Kacy Doucet, Guy Rouleau, and Francois Bolduc. 2015. "Quantitative Analysis of Climbing Defects in a Drosophila Model of Neurodegenerative Disorders." *Journal of Visualized Experiments: JoVE*, no. 100 (June): e52741. https://doi.org/10.3791/52741.